AN ANALYSIS OF COMPOUND SPECIFIC CARBON ISOTOPES OF LIPID BIOMARKERS: A PROXY FOR PALEOENVIRONMENTAL CHANGE IN THE MAYA LOWLANDS OF PETEN, GUATEMALA

By

SARAH DAVIDSON NEWELL

A THESIS PRESENTED TO THE GRADUATE SCHOOL
OF THE UNIVERSITY OF FLORIDA IN PARTIAL FULFILLMENT
OF THE REQUIREMENTS FOR THE DEGREE OF
MASTER OF SCIENCE

UNIVERSITY OF FLORIDA

2005

I find the great thing in this world is not so much where we stand, as in what direction we are moving…we must sail sometimes with the wind and sometimes against it, but we must sail, and not drift, nor lie at anchor.

- Oliver Wendell Holmes

ACKNOWLEDGMENTS

First and foremost I would like to thank my advisor, Dr. David A. Hodell, for his constant support, encouragement and inspiration. I appreciate most his faith in my abilities as a research scientist and unspoken prodding to work harder. Over the past two years I have developed a stronger passion for research for which he is unduly responsible.

Perhaps the most influential person through my master's research was Dr. Jason H. Curtis, to whom I now owe my first-born child. Over the past two years, Jason has provided constant and unparalleled support both in the lab and in life. Jason's assistance with all aspects of my lab work and method development is the sole reason why I was able to complete my MS in just two years. Jason provided to me a helping hand in the lab (at the drop of a hat, I should note), an ear for listening to complaints and excitement alike, and a shoulder during stressful times. I would especially like to thank him for the hours spent with our heads buried in the GC oven and for putting up with my spastic personality.

A number of other individuals were instrumental in the completion of my research. I would like to thank Dr. Mark Brenner for constantly reviewing my work and providing additional advisement. Mark's own excitement for this work was an integral part of my completing this project. I would like to thank Dr. Thomas P. Guilderson for allowing me to travel to the CAMS facility at Lawrence Livermore National Laboratory to run my own radiocarbon dates. The experience was incredible and my project has greatly benefited from having the additional radiocarbon dates. I would also like to thank Drs.

Prudence Rice, Katherine Emery and Andrew Zimmerman for the exchange of ideas and thoughtful discussions. I thank Drs. Barbara Leyden, Gerald Haug and Yongsong Huang for sharing their data with me and Drs. Mark Pagani and Yongsong Huang for assistance in the development of my methods. I also thank Jenny Slosek for running all of the bulk isotope data from Lake Sacnab.

There are three individuals to whom sincere thanks are owed for their personal support. Dave Buck, Ellie Harrison-Buck and Michael Hillesheim have provided me with friendship that is unequaled. Each one has supported me in their own individual way and I can not imagine having done any of this without their love and understanding.

Finally, I would like to thank my parents, Michael and Karen Newell, as well as my siblings, Erik and Jessica Sanderson and Jeremy and Erika Newell. Without their unconditional love and support, I never would have made it!

TABLE OF CONTENTS

page

LIST OF TABLES

LIST OF FIGURES

Abstract of Thesis Presented to the Graduate School
of the University of Florida in Partial Fulfillment of the
Requirements for the Degree of Master of Science

AN ANALYSIS OF COMPOUND SPECIFIC CARBON ISOTOPES OF LIPID BIOMARKERS: A PROXY FOR PALEOENVIRONMENTAL CHANGE IN THE MAYA LOWLANDS OF PETEN, GUATEMALA

By

Sarah Davidson Newell

May 2005

Chair: David A. Hodell
Major Department: Geological Sciences

The Petén region of northern Guatemala has been occupied by humans for more than 3000 years. During that time, the lowland tropical environment experienced a prolonged period of anthropogenic disturbance. Forest disturbance in the Petén Lake District of northern Guatemala was associated with Maya agricultural practices as well as clearing for urban development, construction, and fuelwood both for cooking and for lime-plaster production. Expansion of the Maya civilization during the Preclassic (~1000 BC to AD 250) and Classic periods (AD 250 to AD 900) was accompanied by increasing deforestation of Petén watersheds and accelerated rates of soil erosion. Palynological data from the Petén Lake District illustrate the near elimination of high forest taxa and prevalence of disturbance taxa (grasses, weeds) during the height of Classic Maya occupation (~AD 500-800). After flourishing during the Classic period between AD 250

and 800, the Maya civilization in the Petén Lake District experienced a dramatic change between AD 800 and 900 that some have referred to as the "collapse." Population densities declined significantly after AD 900, thereby curtailing human pressures on the landscape. This cycle of population expansion and decline in the Petén Lake District provides a natural historical "experiment" that has been used to study the response of tropical vegetation to long-term changes in land-use by humans. A new line of evidence is used here to complement other archaeological and paleoenvironmental methods: the use of leaf wax biomarkers in palynological inference studies. The molecular and isotopic compositions of leaf waxes have been shown to be reliable indicators of vegetative biomass and are useful for testing palynological inferences. The carbon isotopic composition of long-chain *n*-alkanes of leaf waxes were used as a geochemical proxy for terrestrial vegetation to test palynological inferences of vegetation change in two lake basins (Lakes Sacnab and Salpetén) in the Petén Lake District of the southern Maya Lowlands over the past ~4500 cal yr BP.

Discrepancies between the $\delta^{13}C$ of long-chain *n*-alkanes and vegetation changes inferred from pollen profiles suggest that the two proxies may be recording different characteristics of watershed vegetation as well as different airshed/watershed processes. The data indicate that in the watersheds of Lakes Salpeten and Sacnab, shifts in the proportion of C_3 to C_4 vegetation are most likely controlled by a combination of climate change and human deforestation. The correspondence of $\delta^{13}C$ records to independent proxies for climate change from ~4500 cal yr BP until ~3000 cal yr BP suggest that regional drying and increased climate variability caused an increase in the contribution of C_4 vegetation during that time. Following this period and beginning with the first Maya

occupation in the watersheds, vegetation change was likely a result of human-driven deforestation or perhaps a combination of both climate and human impact.

CHAPTER 1
INTRODUCTION

The Petén region of northern Guatemala (Figure 1) has been occupied by humans for more than 3000 years. During that time, the lowland tropical environment experienced a prolonged period of anthropogenic disturbance. Forest disturbance in the Petén Lake District of northern Guatemala was associated with Maya agricultural practices as well as clearing for urban development, construction, and fuelwood both for cooking and for lime-plaster production. Expansion of the Maya civilization during the Preclassic (~1000 BC to AD 250) and Classic periods (AD 250 to AD 900) was accompanied by increasing deforestation of Petén watersheds and accelerated rates of soil erosion (Brenner, 1983). Palynological data from the Petén Lake District illustrate the near elimination of high forest taxa and prevalence of disturbance taxa (grasses, weeds) during the height of Classic Maya occupation (~AD 500-800) (Islebe *et al.*, 1996; Leyden, 1987, Vaughan *et al.*, 1985, Deevey, 1978).

After flourishing during the Classic period between 250 and 800 AD, the Maya civilization in the Petén Lake District experienced dramatic change between 800 and 900 AD that some have referred to as the "collapse". Population densities declined significantly after 900 AD, thereby curtailing human pressures on the landscape. This cycle of population expansion and decline in the Petén Lake District provides a natural historical "experiment" that can be used to study the response of tropical vegetation to long-term changes in land-use by humans (Deevey, 1969).

Figure 1: Location map showing the approximate location of the Petén Lake District in northern Guatemala. Map adapted from Map #802723 from the Civil Intelligence Agency (http://www.cia.gov/cia/publications/pubs.html).

The exact timing and extent of deforestation during the period of Maya occupation and the reforestation that followed the collapse is debated among archaeologists and paleoecologists. Evidence currently used in the study of ancient human impact on the Maya lowland environments comes from paleobotanical, environmental archaeological and paleolimnological studies. Much of this evidence is derived from palynological research. However, much of this plant-based evidence is biased in one way or another and none can be used in isolation. For example, vegetation "reconstructions" inferred from pollen profiles may be biased because the relative abundance of pollen grains in a sediment profile cannot be directly related to species abundance or biomass (Bradley, 1999). Most pollen in lake sediments represents only the small percentage of tropical vegetation that is pollinated by wind and does not reflect those plants that depend on pollination by insects or self-fertilization. Because certain species produce a disproportionately large number of pollen grains, it is difficult to determine the actual composition of vegetation in the landscape. Furthermore, certain plants may produce pollen under conditions of stress rather than optimum growth (Bradley, 1999). Maize pollen has often been used in Mesoamerican studies as a proxy for agriculture and associated deforestation. One potential concern with traditional palynology, however, is that maize pollen is not typically included in total pollen counts, thus causing an over-representation of other taxa. In addition, maize pollen is large and typically only transported short distances. Alternatively, leaf-waxes derived from maize are probably transported readily and should reflect maize cultivation in the watershed accurately. These shortcomings underscore the need to validate palynological interpretations by independent means.

A new line of evidence is used here to complement other archaeological and paleoenvironmental methods: the use of leaf wax biomarkers in palynological inference studies. The molecular and isotopic composition of leaf waxes have been shown to be reliable indicators of vegetative biomass (Hughen *et al*., 2004; Huang *et al.*, 1999; Huang *et al*., 2001) and are useful for testing palynological inferences (Hughen *et al*., 2004). There are several advantages to using leaf wax biomarkers in conjunction with pollen to assess changes in vegetative biomass. Pollen and leaf waxes are derived from different vegetative sources and thus record different aspects of watershed vegetation (Huang *et al.*, 1999). Whereas pollen reflects only reproductive effort for specific groups of plants, leaf waxes provide a more representative measure of vegetative biomass for various plant types within a watershed. Leaf waxes reflect the contribution of all land plants whereas pollen will disproportionately reflect wind-pollinated species. In addition, plants in the watershed that do not reproduce sexually or are dormant will produce a biomarker signal but yield no pollen.

The isotopic composition of leaf waxes can be used as a geochemical proxy of terrestrial vegetation (Hughen *et al*., 2004; Huang *et al.*, 1999, 2001). Long-chain (C_{27}-C_{33}) *n*-alkanes exhibit a strong odd-over-even carbon-numbered dominance and are produced nearly exclusively by vascular plants as components of epicuticular leaf waxes (Meyers, 1997). The carbon isotopic composition of terrestrial plant biomarkers in lake sediments reflects the relative contribution to the sediments of alkanes coming from plants using the C_3- (tropical trees) versus C_4- (grasses) metabolic pathway. Plants that fix carbon by means of the C_3 pathway include all the high forest trees (Huang *et al.* 2001). C_4 plants include many tropical grasses and maize, which are associated with

cleared land and agriculture in Mesoamerica. The $\delta^{13}C$ values of *n*-alkanes in C_3 plants range from -31‰ to -38‰, whereas *n*-alkanes in leaf waxes of C_4 plants typically range from -19‰ to -25‰ (Freeman, 2001). Stratigraphic variations in the $\delta^{13}C$ ratio of long-chain *n*-alkanes in lake sediment cores should therefore reflect changes in the proportion of C_3 to C_4 vegetation in a lake's watershed (Huang *et al.* 2001; Meyers, 1997).

Here, the carbon isotopic composition of leaf waxes are used as a geochemical proxy for terrestrial vegetation type to test palynological inferences of vegetation change in two lake basins (Lakes Sacnab and Salpetén) in the Petén Lake District of the southern Maya Lowlands. Three specific questions are addressed in this study:

1) Is there a significant relationship between the $\delta^{13}C$ of long-chain *n*-alkanes and vegetation changes inferred from pollen profiles? If the signals are correlated, then both long-chain *n*-alkanes and pollen are most likely recording the same vegetation changes in a watershed. For example, as disturbance taxa (grasses, weeds) replace high forest taxa, one would expect the $\delta^{13}C$ of *n*-alkanes to increase, reflecting a greater proportion of C_4 biomass. Similarly, an increase in the relative proportion of high forest taxa during reforestation should be accompanied by a decrease in the $\delta^{13}C$ of *n*-alkanes. Comparison of pollen taxa and long-chain, *n*-alkane $\delta^{13}C$ records will reveal whether inferred vegetation changes based on the two proxies are in agreement or contradictory. Because pollen and carbon isotopes of leaf waxes may reflect different characteristics of watershed vegetation and different airshed/watershed processes, the two proxies need not necessarily agree.

2) Are $\delta^{13}C$ values of long-chain *n*-alkanes in lake sediments correlated to Maya population density estimates within the same watershed? If agricultural land clearance

was tied to population density, then increased disturbance taxa and maize are expected to increase as populations increased. Because grasses and maize are C_4 plants, one would predict an increase in the $\delta^{13}C$ of *n*-alkanes with population growth. As populations declined and vegetation returned to a C_3-dominated forest, a decrease in the compound-specific carbon isotopic ratios would be recorded. Population density and the $\delta^{13}C$ of long-chain *n*-alkanes may be decoupled if, for example, agricultural practices changed through time from more extensive to intensive methods, or if alternative crops, other than maize, became important in the diet. The relation between population density and $\delta^{13}C$ of long-chain *n*-alkanes can be addressed because population data are available from archaeological transects in the watersheds of both Lakes Sacnab and Salpetén. 3) What was the relative importance of human- and climate-induced changes in vegetation in the Central Petén? It is difficult to assess the effect of climate change during the period of human occupation because it is difficult to tease apart human-induced versus climate-induced changes in vegetation. However, a comparison of the $\delta^{13}C$ of *n*-alkanes with climate proxies that are not confounded by human impact may reveal whether climate played a role in vegetation change at all. If vegetation changes in a watershed were climate-induced, one would predict that long-chain *n*−alkanes would correlate with independent, regional paleoclimate records. For example, a period of increased evaporation/precipitation (E/P) would likely coincide with an increase in the $\delta^{13}C$ of *n*-alkanes, reflecting a greater proportion of C_4 biomass. A period of decreased E/P would likely correspond to a return to a C_3-dominated forest. This question can be answered by comparing proxy records of climate change from Petén and the Caribbean Sea with

compound-specific analyses, and evaluating those data in light of changes in Maya population densities.

CHAPTER 2
BACKGROUND

Modern Setting

The Maya area, located in southeastern Mesoamerica, occupies a broad expanse of land and includes parts of the countries of Mexico, Guatemala, Belize, Honduras and El Salvador. The area has typically been both culturally and geographically divided by scholars into the highlands in the south and the lowlands in the north. The highlands, dominated by a volcanic landscape, refer to the area greater than 1000 ft above sea level (a.s.l.). and spread from southeastern Chiapas toward lower Central America. The lowlands consist of the Yucatan Peninsula in Mexico, Guatemala, and Belize.

The topography of the lowlands is dominated by a limestone platform that has evolved into porous, karst hills with extensive dissolution features. While there are few permanently flowing rivers and lakes are rare in the northern lowlands, there are numerous lake basins in the department of Petén. Soils are relatively thin and vulnerable to rapid erosion with vegetation removal, making agriculture in this region challenging. Today, the lowland Maya practice shifting, slash-and-burn (swidden) agriculture that permits the forest to regenerate at intervals. The poor soils, however, can only be planted for ~2 years; after which, plots are fallowed for 4 to 7 years in the Petén and 15 to 20 years in other parts of the Yucatan (Coe, 1999). These poor soils, in addition to the stress

added by highly seasonal rainfall, make the lowlands a rather harsh place to practice agriculture (Coe, 1999).

The Petén Lake District is located in the Guatemalan Lowlands of the Yucatan Peninsula (Figure 1). The region contains numerous terminal basins that are aligned along a series of east-west aligned *en echelon* faults (Deevey *et al,*. 1979). The bedrock is karst limestone of Cretaceous and Tertiary age with elevations ranging from 100 to 300 m. Most of the lakes have deep troughs at the foot of a steep, north-shore fault scarp which gives rise to their distinctive bathymetry. The water table in the area is deep below the ground surface, making groundwater relatively inaccessible. Perched surface waters often result in seasonally inundated topographic depressions, or *bajos*, that are clay-floored and hold water during the rainy season (Deevey *et al.*, 1979). The major water bodies of the Petén Lake District remain filled throughout the year and extend approximately 100 km from east to west.

Soils in the Petén region are dominated by well-drained, mineral-rich mollisols that support a tropical semi-deciduous and evergreen forest (Lundell, 1937). Modern vegetation is variable throughout the region. The central Petén is mostly semi-deciduous subtropical moist forest while the southwest Petén is dominated by extensive savannas with forested hills that support a diverse, fire-resistant herbaceous flora. The savanna vegetation may have been created during the period of Maya occupation when much of the forest was burned for cultivation (Leyden, 1987). Alternatively, it may be a Pleistocene relict or an edaphic assemblage, the consequence of clayey, hydromorphic soils. The low-lying basins in the northeast Petén are dominated by swamp and

marshland. Vegetation here is dominated by palms, grasses and sedges, but also includes a semi-deciduous higher forest (Lundell, 1937).

Mean modern annual temperature is approximately 25˚C and mean annual precipitation is approximately 1600 mm with a pronounced dry season between January and May (Deevey *et al.*, 1980). There is very little surface drainage in the area and most water that falls as rain is either transpired, evaporated, or directly enters the aquifer (Rosenmeier *et al.,* 2002). The Petén typically receives higher rainfall than the rest of the Yucatan; there is a pronounced decrease in rainfall from south to north on the Yucatan Peninsula. There is also considerable interannual precipitation variability. These inter-annual variations force Maya farmers to practice long-term resource planning. Extensive droughts occur periodically in this area and previous studies have shown that this variability is not solely a modern occurrence (Hodell *et al*., 1995, 2001; Curtis *et al.*, 1998).

Cultural History of the Petén

The ancient Maya civilization of Mesoamerica arose about 2000 B.C. and spanned a period of 3,000 years before undergoing a period of social and political change in the Late and Terminal Classic, between 750 and 1050 AD. These changes resulted in the development of very different Maya political, economic, and ideological systems and were associated with the cessation of construction of major architecture and elite monuments, the reduction of inland trade systems designed for the movement of elite status markers, and the abandonment of some but not all urban centers as populations dispersed into non-urban village settings, and migrated northward into the northern Yucatan and Belizean region. These political and social changes are inferred from the

archaeological record of ancient Maya settlement. Maya civilization was unique in possessing the only written language in the Americas at the time. It also developed the most sophisticated and accurate calendar of the time, monumental architecture, a hierarchical social class system, sophisticated agricultural systems including intensive agriculture, and trade systems extending from northern Mexico to south of Honduras and El Salvador and perhaps as far as South America. The Maya also had a highly developed religious system based, during the Classic period, on semi-divine kingship and a noble class (Sharer, 1994).

The Petén region was continuously occupied by the ancient Maya from the Middle Preclassic (1000 BC) through the Postclassic (AD 900 to 1525), and up to the Spanish conquest in 1697 (Rice and Rice, 1990). The Preclassic period (1000 BC to AD 250) in the Petén region is divided into the Middle Preclassic and Late Preclassic. It is during this period that the Maya are thought to have developed from hunters and gatherers into a complex civilization. This period marked the development of cities, temples and inscribed stone monuments. During the Middle Preclassic, archaeological evidence suggests the presence of social stratification as well as sophisticated religious and economic institutions. The first examples of writing appear in the Late Preclassic (Coe, 1999).

The Classic Period was characterized by remarkable growth of the civilization both in terms of population and social complexity. The Classic Period (AD 300- AD 900) is also subdivided into three periods: the Early Classic, Late Classic and Terminal Classic. During the Early and Late Classic periods, archaeological evidence suggests the development of "states" with centralized political and religious authority in addition to

the erection of carved stone monuments (Coe, 1999). An important change in the political structure occurred at the end of this period, as authority became shared by a council of many instead of one individual (Coe, 1999). Populations grew slowly, but exponentially and in many regions displayed peak population densities between AD 700 and 800 AD (Rice and Rice, 1990).

The Terminal Classic and Post-Classic Periods (AD 900 to AD 1525) are marked by diverse cultural responses throughout Mesoamerica. Much of the southern lowland region experienced the abandonment of Classic cities, temples and religious centers; subsequent political fragmentation resulted in a massive cultural decline that has been referred to as the "collapse" (Coe, 1999). The Maya Terminal Classic, however, is perhaps one of the most important periods in the Petén region. The uniqueness of central Petén lies in the ability to study not only the events leading up to the Maya Terminal Classic period, but the continuity of occupation following the collapse of Classic civilization (Rice and Rice, 2004). This period in the central Petén was both a center and a crossroads for Postclassic Maya civilization. Petén-like architecture and iconographic traits in the northern lowlands are evidence of Late Classic, conflict-driven migration from the Petén region. Throughout the Late Classic and Terminal Classic, the Petén region showed demographic loss, whereas the northern lowlands began to be heavily settled. The lakes region in particular suffered population decline, though the area was never completely abandoned. Archaeological evidence from every major Petén lake basin shows continuous occupation from the Late Classic to the Postclassic, with some indication of population migration between the Rio de Pasión region, the Gulf Coast, and the Petén Lake District during the Postclassic (Rice and Rice, 2004).

The nature of settlements changed from the Late Classic to the Postclassic in the Petén Lakes District. Whereas Classic settlements expanded throughout the watershed, most settlement shifted to small, densely populated areas found primarily on islands and peninsulas in the lakes during the Postclassic. This settlement pattern in itself suggests a "conflict-driven" society. The location of these sites in poor agricultural zones, the presence of defensive structures, as well as the presence of intrusive residential architecture in previously occupied sites, suggests that the Late Classic migration of small groups between the Rio de Pasión and the northern lowlands forced them to settle into an already-established settlement system (Rice and Rice, 2004).

Archaeological evidence overwhelmingly suggests that the Maya population in the Petén Lakes District did not "collapse", but underwent a significant transformation. While there was a pronounced demographic decline, the "collapse" in the Petén did not result in complete depopulation. Instead, intersite conflict led to political restructuring and thus a redistribution of population, especially into fragile lands. The region was one of dynamic and contested lands, and remained so until AD ~1200 (Rice and Rice, 2004).

Interactions among the Ancient Maya, Climate and Environment

The Maya Lowlands have been studied by researchers seeking answers to questions about past human-climate-environment interactions. This research has concentrated on the central Petén, and in particular the Petén Lakes District. In 1972, Edward S. Deevey began a long-term paleoecological project in the Department of Petén, Guatemala. The Central Petén Historical Ecology Project (CPHEP) investigated both the paleolimnology and archaeology of major lake watersheds in the Central Petén (Rice *et al.*, 1985). The objective of the project was to investigate both the social and natural

history of the region through interdisciplinary research, focusing on ecological change as a result of human landscape transformations. One assumption of the CPHEP was that climate change was unimportant during the period of Maya occupation. Recent studies have recognized, however, that climate was not invariant through this period (Hodell *et al.*, 1995; Rosenmeier *et al.*, 2002; Curtis *et al.*, 1998). Research design included paleolimnological studies from other regions that incorporate archaeological perspectives (Dunning *et al*., 1997, 1998; Demarest, 1997). In particular, lake sediment cores were used to develop long-term, high resolution records of environmental change within a watershed and were used in conjunction with archaeological surveys that estimated the timing and density of human occupation.

The impacts of long-term Maya occupation in the Central Petén Lake District on both terrestrial and lacustrine environments were summarized by researchers in the CPHEP (Binford *et al.*, 1987) (Figure 2). The model is generalized and does not necessarily describe the history of human and environmental changes for each and every lake basin.

Archaeological surveys consisted of systematic mapping of settlement remains and test-pit excavations, and provide estimates of settlement patterns and population growth in the central Petén (Rice and Rice, 1990). Surveys were completed in each of three twin-lake basins: Sacnab-Yaxha, Macanche-Salpetén, and Quexil-Peténxil. The trends of population growth are notably similar in each basin surveyed, although the true variation was probably not captured by the coarse chronological framework, which was based on ceramic phases, not radiocarbon. Occupation of the region began at approximately 1000 BC and was followed by a steady increase until the end of the Late

Classic (AD 750-800), when populations reached their peak in most basins (Figure 3). Population growth was exponential in the Yaxha-Sacnab basins but not in the other basins, which experienced a small population decline during the Early Classic.

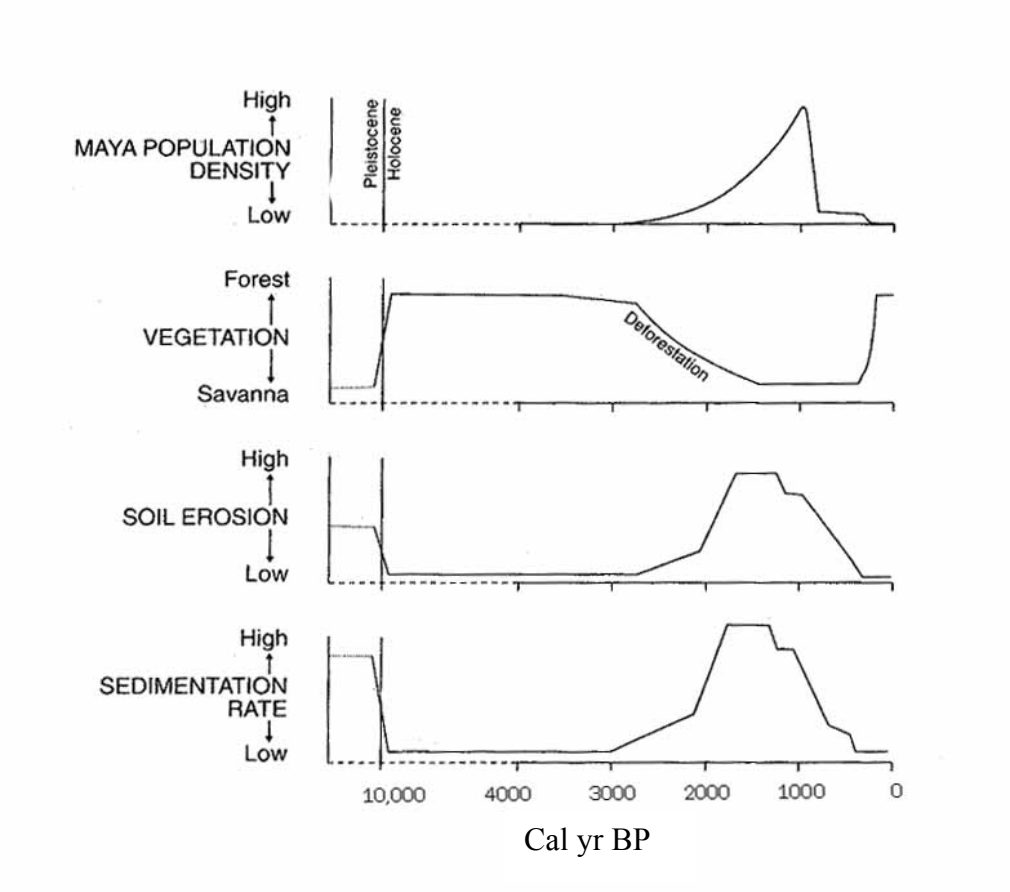

Figure 2: Impact of long-term Maya settlement on the terrestrial and aquatic environments in the Petén, Guatemala. Modified from Rice *et al.* (1985).

Sediment cores from numerous lakes in Petén show similar stratigraphic changes in sediment composition and geochemistry (Figure 2) (Cowgill and Hutchinson, 1966; Deevey *et al.*, 1979; Brenner, 1983; Vaughan *et al.*, 1985; Rice *et al.*, 1985; Binford *et al.*, 1987; Leyden, 1987; Curtis *et al.*, 1998; Islebe *et al.*, 1996). Holocene sediment prior

to Maya occupation is comprised of organic-rich (30-60%) gyttja (Brenner *et al.*, 2002). Overlying the pre-Maya gyttja is a clay-rich horizon known as the "Maya clay." The

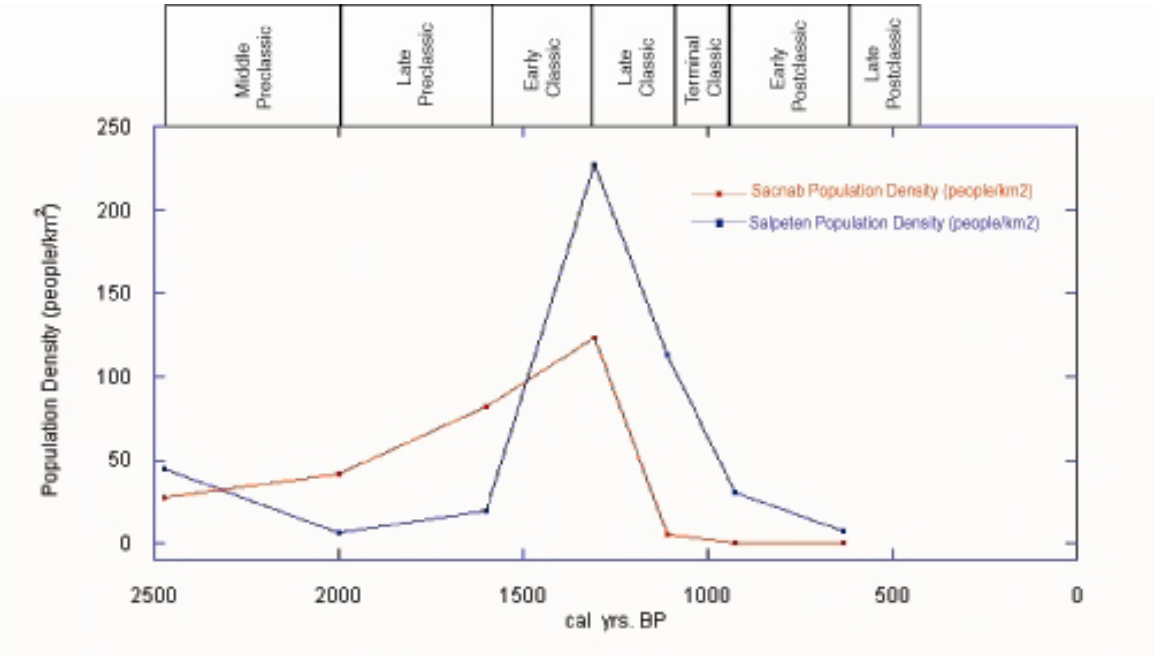

Figure 3: Population density estimates versus time (cal yr BP) and time periods for Lake Sacnab and Lake Salpetén from the Middle Preclassic (cal yr BP) to the Late Postclassic (cal yr BP). Data from Rice and Rice, 1990.

base of the Maya clay has been dated to approximately 3,000 yr BP (Brenner, 1994; Rosenmeier *et al.*, 2002) and reflects accelerated erosion associated with early land clearance by humans (Deevey *et al.*, 1979; Brenner, 1983; Vaughan *et al.*, 1985; Rice *et al.*, 1985; Binford *et al.*, 1987; Leyden, 1987; Curtis *et al.*, 1998; Islebe *et al.*, 1996). Studies outside the region *per se* suggest the increase in colluviation may have been partly related to regional drying (Hodell *et al.*, 1995; Hodell *et al.*, 1996; Curtis *et al.*, 2001). Nutrient-rich soils became unstable as forest cover was removed and replaced by a savanna-like landscape. Increased soil erosion is reflected by high net accumulation rates of lake sediments. As erosion progressed, organic-rich surficial soils were removed

and the underlying bedrock was weathered and transported to the lake basin. This is reflected by the high proportion of inorganic sediments. Overlying the Maya clay unit is another organic-rich layer that is inferred to represent sediments deposited following the Maya collapse (Brenner *et al*., 2002).

Deforestation and environmental disturbance accompanied growth of the Maya population from the Preclassic to the Late Classic (Figure 2). Vaughan *et al.* (1985) developed pollen stratigraphies for Lakes Quexil and Sacnab that indicate changes in vegetation through the period of Maya occupation. The pre-Maya pollen assemblage was dominated by high forest taxa such as *Moraceae*, whereas the early to mid-Preclassic is characterized by an open forest and, probably, culturally-induced savanna. Late Preclassic to Late Classic sediments are dominated by clay-rich sediments and 70% non-arboreal pollen. Vaughan et al. (1985) defined three distinct disturbance pollen zones. The Late Preclassic zone is characterized by savanna trees and shrubs. The landscape transitions to nearly grassland during the Early Classic, with only one type of arboreal pollen present (Ramon). The Late Classic to Postclassic contains only grassland taxa. Some increases in high-forest taxa near the top of this interval show evidence of reforestation, as does the pollen spectrum during the Postclassic period. If we assume an anthropogenic cause for the replacement of arboreal with grassland taxa, a sharp rise in arboreal pollen and a decrease in grassland types imply regional depopulation (Vaughan *et al.*, 1985). Although each study is thought to reflect primarily local vegetation changes, multiple subsequent studies from the Petén and surrounding lowlands, with the exception of the work done by Cowgill *et al*. (1966) and Dunning *et al.* (1997), have all detected a similar decline in high-forest taxa from the Late Preclassic through the

Terminal Classic that is interpreted to reflect human-driven deforestation (Islebe *et al.,* 1996; Leyden, 1987, Vaughan *et al.,* 1985, Deevey, 1978). The pollen zones were assigned ages by "cultural zonation", or the correlation with ages of archaeological periods. Subsequently, they may contain some chronological error. However, these same pollen zones have now been independently dated in other lake cores (Leyden, 1987 and Rosenmeier *et al.*, 2002) and are considered reasonable.

Leyden (1987) used a 15 m sediment core from Lake Salpetén, Guatemala to develop a high-resolution pollen record from the basin to reconstruct Holocene vegetation changes. The sediment record spans from the pre-Maya to the present, and shows distinct evidence of Maya land clearance. While there is an apparent lack of disturbance taxa in the early Preclassic, the pollen zones representing the Late Preclassic through the Postclassic show evidence for abundant terrestrial herbs and strongly suggest Maya land clearance. Leyden attributes the lack of disturbance taxa in the early Preclassic to small local populations in the Salpetén basin at that time. Some discrepancies, however, may lie within the issues of chronological control. Leyden suggests that a few high-forest taxa actually increased initially, and declined later as forest removal was intensified. Presence of oak during the Classic period may suggest a savanna landscape, but this is relatively unclear. Leyden suggests that after the initial deforestation, the forest structure was relatively stable. However, greater proportions of maize pollen during the Late Classic through Postclassic indicate intensified agricultural activities. In the gyttja layer above the Maya clay, the concentration of total pollen grains nearly doubles, suggesting forest regrowth after depopulation of the lake basin (or slowed bulk sedimentation rate). Leyden proposes that these forests regenerated rapidly, but

were more open than pre-Maya forests. This may have been related to climate rather than anthropogenic influences; regional drying may be suggested by the Post-Maya continuation of open forests. This period is dominated by secondary growth, as suggested by the increases in successional shrubs and trees.

While most vegetation studies have focused on forest clearance, a select few have concentrated on revealing the dynamics of afforestation following the Maya collapse in the central Petén region of Guatemala (Wiseman, 1985; Brenner *et al.*, 1990). Wiseman (1985) used pollen in lake sediments to track vegetation changes and the nature of these changes in response to cultural collapse in the Maya Lowlands. Seven cores from Lakes Peténxil and Quexil were collected and sampled for pollen analyses and used in conjunction with modern pollen and fauna studies that examined 0.1 ha plots in various stages of regrowth. This modern analog guided inferences about forest succession based on the fossil pollen record. All cores that penetrated into Late Classic Period deposits showed a subsequent replacement of agricultural weeds by secondary forest growth. The pollen spectrum during the early Classic to Postclassic was similar to samples taken from soils under swidden agriculture. One notable feature of the sediment cores is that each core shows essentially the same pollen spectra, suggesting that the conditions in the basin were in spatial equilibrium. Wiseman cites the decrease in maize pollen and subsequent recolonization by forest as key evidence for depopulation; however, poor chronological control makes it difficult to determine the precise timing of both environmental and demographic changes.

Interpreting vegetation change from palynological data is further complicated by the challenge of obtaining accurate chronological control. Prior to the advent of AMS

dating and the potential to measure ^{14}C in very small (~20µg) samples of organic carbon, many early radiocarbon ages from Petén lakes were based on dating of bulk sediment or carbonate shells. Shells may incorporate carbon derived from the dissolution of ancient limestone and thus appear older than their true age. This problem extends to organic matter that is fixed photosynthetically within the lake, i.e. autochthonous organic matter. Primary producers may incorporate carbon derived from dissolved ancient limestone, and thus display "too-old" ages. This hard-water lake error has compromised the reliability of early chronologies. To further complicate matters, many subsequent studies assigned ages to the pollen stratigraphy by correlation with ages of archaeological periods. Dating error within one pollen record was thus transferred to records from other lake cores. Chronological imprecision in both sediment cores and archaeological studies creates challenges for linking environmental disturbance and human population sizes (Yaeger and Hodell, in press).

Despite the overwhelming evidence for late Holocene vegetation change in the Petén region, it is difficult to distinguish between the impacts of climate and Maya occupation on forest composition. While the CPHEP assumed that climate was relatively constant for the past 10,000 years, recent work has proved otherwise. A sediment core from Lake Chichancanab in northern Yucatan provides evidence for regional drying that occurred beginning approximately 1000 BC with a distinct interval of droughts between AD 800 and AD 1000 that coincided with the Terminal Classic collapse (Hodell *et al.*, 1995, Hodell et al. in press). Another paleoclimate record from Punta Laguna, on the northeastern Yucatan Peninsula, indicates alternating wet-dry shifts in the hydrologic balance through the late Holocene with the driest period lasting from approximately AD

280 to 1080 (Curtis *et al.*, 1998). Four severe drought events were revealed, including one that occurred during the Maya Hiatus (AD 600) and one that occurred concurrently with the Late Classic drought recorded in the Chichancanab record.

A climate record from Lake Salpetén indicates a trend similar to the Chichancanab record (Rosenmeier *et al.*, 2002). Lake levels decreased continuously from approximately 1000 BC, with the lowest lake level occurring between AD 800 and 900. This inferred drought coincides with the Terminal Classic collapse of the Classic Maya. The record also showed reduced soil erosion as well as forest recovery after AD 850, likely associated with Maya population decline (Rosenmeier *et al.*, 2002). Rosenmeier argues, however, that these changes may not be entirely climate-related, but rather due to the effects of human-induced vegetation change on the lake's hydrology.

The impact of humans on regional vegetation and soil stability, as well as the influence of climate change on the Classic Maya, illustrate the complex interplay among climate, humans, and the environment throughout the Late Holocene in the Maya Lowlands. While it is extremely difficult to separate the signals of human versus climate-controlled changes in the environment, further investigations of vegetation change with precise chronological control may provide additional evidence that the Maya had a profound impact on their lowland tropical environment. The "natural experiment" provides an excellent opportunity to study the relationship between changes in human population sizes, land-use activities, climate changes, and vegetation responses. Additionally, such studies can help us understand how ecosystems respond once human and climate pressures are curtailed.

Study Sites

Paleolimnological cores from two lakes in the Central Petén Lake District, one in the east and one in central Petén, were examined for compound-specific carbon isotopes (Figure 4). Comparison of the records from Lake Sacnab and Lake Salpetén permits a regional assessment of vegetation change.

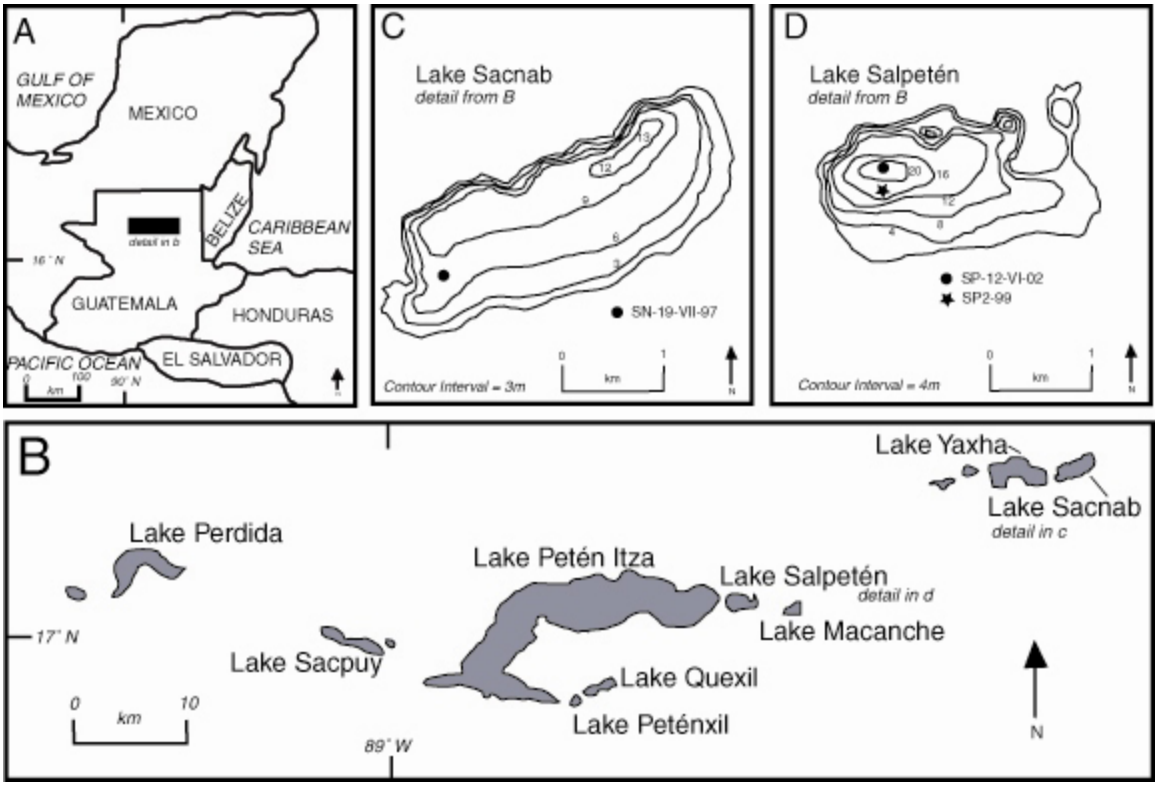

Figure 4: Location map showing: (A) the Yucatan Peninsula and the location of the Petén Lake District within Guatemala, (B) detail of the Petén Lake District, (C) the bathymetry of Lake Sacnab and location of core SN-19-VII-97 and (D) the bathymetry of Lake Salpetén and location of cores SP-12-VI-02 and SP2-99.

Lake Sacnab

Lake Sacnab (17˚03'N and 89˚23'W) is located in the eastern part of the Petén Lake District near the border between Guatemala and Belize (Figure 4c). The lake has a surface area of 3.9 km^2 and is ~3.5 km long by 1.5 km wide (Deevey *et al.*, 1980). The maximum depth is 13 m. The lake is thermally stratified, but occasional mixing is

indicated by the absence of permanent stagnation. Lake waters are relatively poor in nutrients, with the majority of nutrients being supplied by erosion of upland soils (Deevey *et al.*, 1980). Lake Sacnab has no outflow, thus making the sediments the primary sink for dissolved and particulate matter that enters the lake.

Lake Salpetén

Lake Salpetén (16˚58'N and 89˚40'W) is located ~35 km to the WSW of Lake Sacnab and has a surface area of approximately 2.6 km^2 (Rosenmeier *et al.*, 2002) (Figure 4d). The lake has a maximum depth of approximately 32 m (Brezonik and Fox, 1974). Lake waters are sulfate-rich and have high total dissolved solids (4.76 g $L^{-}1$) (Deevey *et al.* 1980). Surface temperatures range from 27˚C to 30˚C throughout the year (Rosenmeier *et al.*, 2002). Lake Salpetén is closed hydrologically and lake-bottom sediments are the primary sink for dissolved and particulate matter that enters the lake.

Compound-Specific Carbon Isotopic Studies

The major source of organic matter in lake sediments is generally derived from phytoplankton living in the water column or aquatic macrophytes. Land plants may also provide an important source of organic matter to lake sediments. The relative contribution of these three sources is influenced by productivity of lacustrine algae, aquatic macrophytes, and terrestrial plants. Transport processes and preservation may also influence the ultimate contribution of organic compounds from various sources (Meyers, 1997). In order to determine relative changes in algal, macrophyte, or terrestrial plant productivity, it is necessary to discriminate between the sources of organic matter sequestered in lake-bottom sediments. Certain compounds in lake

sediments, commonly called biomarkers, are uniquely derived from specific sources of organic matter. Leaf waxes are produced exclusively by vascular plants and serve as a protective coating on leaves and stems (Eglinton and Hamilton, 1967). The abundance and molecular and isotopic composition of leaf waxes reflect vegetative biomass and have been used to discern relative changes in terrestrial vegetation (Figure 5) (Hughen *et al*., 2004; Filley *et al.*, 2001; Huang *et al.*, 1999, 2001). The wax particles, introduced into the atmosphere by wind and dust ablation off live vegetation (Simoneit, 1977), have a molecular composition that is generally similar to that of their source vegetation (Conte and Weber, 2002). Leaf waxes can also be remobilized from soils during exposure (Schefub, 2003). Leaf waxes settle onto lake surfaces from the atmosphere and are incorporated into lake-bottom sediments. Leaf waxes thus have atmospheric residence times on the order of days to weeks, making them especially valuable as tracers of abrupt vegetative change. Leaf waxes record biomass of exposed leaf surface area in the watershed and thus have the capability of resolving rapid responses to climate or other environmental changes.

The isotopic analysis of long-chain *n*-alkanes has proven to be a useful new tool for evaluating qualitative changes in terrestrial vegetation (Hughen *et al*., 2004; Filley *et al.*, 2001; Huang *et al.*, 1999, 2001). Long-chain (C_{29}-C_{33}) *n*-alkanes exhibiting a strong odd-over-even carbon-numbered dominance are produced nearly exclusively by vascular plants as components of epicuticular leaf waxes (Meyers, 1997). In addition, *n*-alkanes are chemically and biologically resistant and are often found in sediments in quantities sufficient for analysis. Preservation of lipids, and in particular *n*-alkanes, is generally good. Studies have shown greater preservation of *n*-alkane terrestrial biomarkers versus

algal biomarkers (Meyers *et al.*, 1984; Meyers and Ishiwatari., 1993; Meyers and Eadie, 1993) suggesting that studies utilizing these biomarkers are more robust.

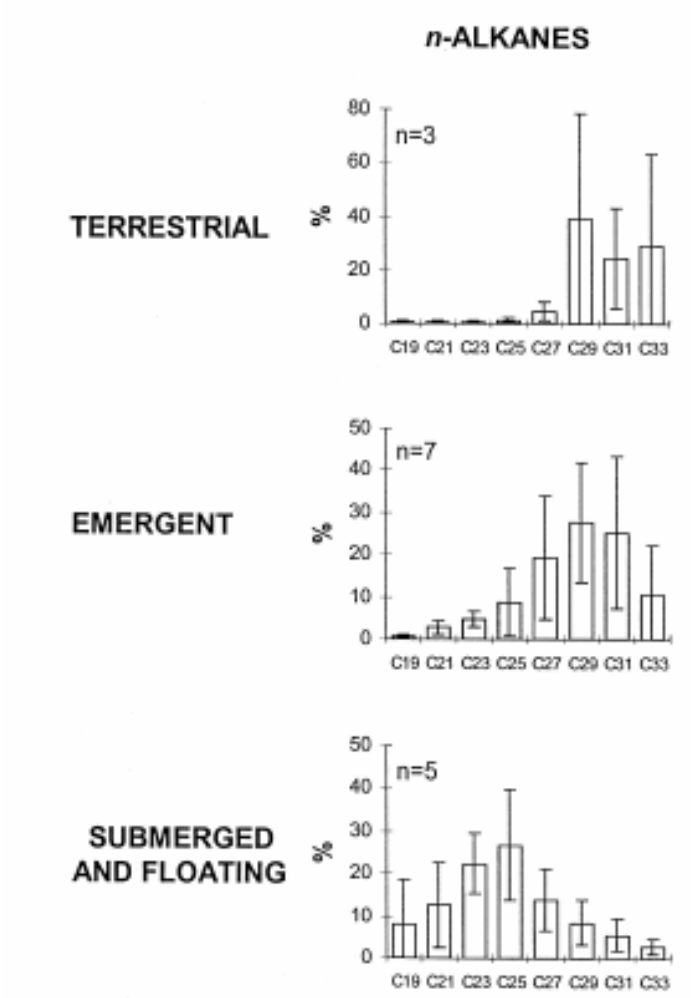

Figure 5: Histograms from Ficken *et al.* (2000) showing the molecular distribution of n-alkanes from the three categories: terrestrial, emergent, and submerged/floating. Only odd carbon number distributions are shown and bars represent 1 standard deviation.

The carbon isotopic composition of long chain *n*-alkanes (>C_{27}) reflects the relative contribution of C_3 and C_4 plants (Hughen *et al*., 2004; Filley *et al.*, 2001; Huang *et al.*, 1999; Huang *et al*., 2001). Plants that fix carbon by means of the C_4 metabolic pathway include the tropical grasses (including maize) and are associated with land

clearance. C_4 plants are more competitive than plants using the C_3 pathway under both high water stress (such as during drought) as well as lower ambient pCO_2 levels. Plants that fix carbon by means of the C_3 pathway include all the high forest trees (Huang *et al.,* 2001). Plants that use the C_3 pathway have bulk $\delta^{13}C$ values in the range of -21‰ to -28‰, whereas C_4 plants display bulk $\delta^{13}C$ values between -11‰ and -15‰ (Lajtha and Marshall, 1994). Stratigraphic variations in the $\delta^{13}C$ ratio of long-chain *n*-alkanes in lake sediment cores will thus reflect the changes in the proportion of C_3 to C_4 vegetation in a lake's watershed (Huang *et al.,* 2001).

Previous studies have shown that it is possible to recognize C_4 plant expansions by examining the carbon isotopic composition of long-chain n-alkanes in sediment cores. Huang, *et al*. (2001) examined leaf wax n-alkanes from two sites in Mesoamerica and found contrasting moisture variations over the last 25,000 years. Data indicate that regional climate plays a large role in the relative abundance of C_3 versus C_4 plants. Enriched $\delta^{13}C$ values during the Last Glacial Maximum (LGM) suggest an expansion of C_4 plants in the sediments of Lake Quexil during the LGM as a result of low partial pressure of atmospheric carbon dioxide (pCO_2) and increased aridity. Results indicate that it is possible to recognize vegetation changes by examining the compound-specific carbon isotopes of preserved organic matter in lake sediments. This study provides information that complements past studies that analyzed only bulk sediment or pollen and thus provide a better record of changes in terrestrial vegetation in the Petén Lake District.

CHAPTER 3
METHODS

Core Collection

Lake Sacnab

On 19 July 1997, two sediment cores were retrieved from Lake Sacnab in 8.0 m of water. A 152-cm-long core (SN-19-VII-97-MWI) was taken using a piston corer designed to recover undisturbed sediment-water interface profiles (Fisher *et al.*, 1992). The sediment core was sampled in the field at 1-cm intervals by vertical extrusion into a sampling tray fitted to the top of the core barrel. A total of 3.7 m of sediment was collected in four additional sections (SN-19-VII-97-LEX) using a piston corer with polycarbonate tubing.

Cores were extruded and sectioned at 1-cm intervals. Magnetic susceptibility was measured for each section using a GEOTEK multi-sensor core logger (MSCL) at Florida State University, Tallahassee. All samples from core SN-19-VII-97 were freeze-dried and ground in preparation for compound-specific carbon isotopic analyses. Magnetic susceptibility data were used to determine that there was a 25.5-cm offset between the mud-water interface core and the piston core. All depths in the deeper core sections were adjusted using the mud-water interface as the 0-cm datum.

Lake Salpeten

On 12 June 2002, two sediment cores were retrieved from 23 meters water depth in Lake Salpeten. A short (93 cm) trigger/gravity core (SP-12-VI-02-1A-MWI) and a longer (550 cm) Kullenberg piston core (SP-12-VI-02-1A) were both collected in polycarbonate liners. The Kullenberg core was cut in the field into approximately 1-m lengths for transport to the University of Florida, where cores were stored in a cooler.

Whole core sections were analyzed for magnetic susceptibility, gamma ray attenuation (GRA) bulk density and ρ-wave velocity using a GEOTEK MSCL at the University of Florida. Each section of the Kullenberg core was split lengthwise into archive and sampling halves and described. The sampling half was U-channeled and taken to the Ocean Drilling Program Core Repository in Bremen, Germany for elemental analysis on the X-Ray Fluorescence (XRF) Core Scanner. Additional samples were taken from the remainder of the sampling half at the University of Florida at 10-20 cm intervals for compound-specific carbon isotopic analyses. The mud-water interface core was sampled at 1 cm intervals at the University of Florida by vertical extrusion into a sampling tray fitted to the top of the core barrel. All samples from core SP-12-VI-02 were freeze-dried and ground in preparation for compound-specific carbon isotopic analyses. Magnetic susceptibility and density data were used to determine the 7-cm offset between the mud-water interface core and the Kullenberg core and depths assigned to deeper sections were adjusted accordingly.

Chronology

Lake Sacnab

Radiocarbon ages for Lake Sacnab sediments were determined by accelerator mass spectrometry (AMS) using terrestrial organic matter (seeds, charcoal and wood) at Lawrence Livermore National Laboratory Center for AMS (LLNL-CAMS) and the National Ocean Science AMS (NOSAMS) facility at Woods Hole Oceanographic Institution. Radiocarbon ages were converted to calendar ages using the program OxCal v 3.9. (Bronk Ramsey, 1995; Bronk Ramsey, 2001) and atmospheric data from Stuiver *et al.* (1998).

The sample that was analyzed at NOSAMS was pretreated on-site whereas the samples analyzed at LLNL-CAMS were pretreated at the University of Florida. For the LLNL-CAMS samples, backgrounds were scaled relative to sample size using UF processed Pliocene wood blanks to determine the modern-C contribution (4±1μg). All radiocarbon ages are adjusted to a $\delta^{13}C$ value of -25 per mil.

Lake Salpeten

Radiocarbon ages for Lake Salpeten sediments were determined by AMS ^{14}C dating of terrestrial organic matter (seeds, charcoal and wood) at LLNL-CAMS. Radiocarbon ages were converted to calendar ages using the program OxCal v 3.9 (Bronk Ramsey, 1995; Bronk Ramsey, 2001) and atmospheric data from Stuiver *et al.* (1998).

Bulk Elemental Geochemical Analyses

Total carbon (TC) and total nitrogen (TN) were measured on all samples from core SN-19-VII-97 using a Carlo Erba NA 1500 CNS elemental analyzer with autosampler. Analytical precision for TC and TN is approximately ± 0.5%. Total

inorganic carbon (TIC) in the sediments was measured by coulometric titration (Engleman *et al.,* 1985) with a UIC (Coulometrics) Model 5011 CO_2 coulometer coupled with a UIC CM5240-TIC inorganic carbon preparation device. Analytical precision is approximately ± 0.5% based on analysis of 16 calcium carbonate internal standards. Organic carbon (OC) was calculated by subtracting TIC from TC. Weight percent calcium carbonate (%$CaCO_3$) was calculated by multiplying IC by 8.33. Weight percent organic matter (%OM) was estimated by multiplying OC by 2.5.

Bulk Carbon and Nitrogen Isotopic Analyses

Bulk organic sediment samples were analyzed on-line for carbon and nitrogen isotopes using a VG PRISM Series II isotope ratio mass spectrometer with a triple trap preparation device linked to a Carlo Erba NA 1500 CNS Elemental. Bulk carbon isotopic results are reported in standard delta (δ) notation relative to the Vienna PeeDee Belemnite (VPDB) standard. Precision for $\delta^{13}C$ samples was approximately ±0.15‰ based on nine analyses of NBS-22. Bulk nitrogen isotopic results are reported in standard delta (δ) notation relative to atmospheric N_2. Precision for $\delta^{15}N$ samples was approximately ±0.20‰ based on nine analyses of peptone.

Compound-Specific Carbon Isotopic Analyses

The extraction and isolation methods used for lipids in this study were patterned after Silliman *et al.* (2000) and M. Pagani (personal communication, 2003). Prior to extraction, approximately 15 µg of C_{34} *n*-alkane was added to each sample as an internal standard for *n*-alkanes. Lipids were extracted from approximately 3-5 g of dry sediment using 2:1 methylene chloride/methanol in a Dionex Accelerated Solvent Extractor (ASE) (for program see Appendix A). Extraction efficiencies averaged approximately 89% for

all samples. The samples were then evaporated and solvent exchanged to hexane using a hot water bath while adding a stream of dinitrogen gas (N_2). Samples were dissolved in 1 mL of hexane and added to a 1 cm x 29 cm glass column filled with 2.5 g of 5% deactivated silica gel. 15 mL of hexane was used to elute the *n*-alkanes. Full isolation scheme procedures are outlined in Appendix B. Samples were urea adducted to obtain clean *n*-alkanes for gas chromatography as outlined in Appendix C. After urea adduction, samples were concentrated in 200 µL of hexane in preparation for analysis on a Perkin Elmer 8500 Gas Chromatograph (GC) to determine purity and appropriate concentrations for GC-IRMS analyses. Samples of 4 µL were injected into the GC with a 30 m DB-1 column (0.25 mm ID). The gas chromatograph was used in split injection mode with a ratio of 20:1 and equipped with a FID detector. The GC oven temperature was programmed to maximize alkane separation (Table 1). The necessary dilution for GC-IRMS analysis was calculated and samples were transferred to a glass auto-sampler vial and sealed with a Teflon crimp cap. Samples were typically dissolved in 20-100 µL hexane. Carbon isotopic analyses were performed using a Hewlett Packard 6890 GC connected to a Finnigan MAT Delta$^+$ XL Mass Spectrometer via a GC-C III interface.

Table 1: Perkin Elmer 8500 Gas Chromatograph oven program for sample analyses.

Rate °C/min	Temperature °C	Time (min)
	50	1
6	300	20

The n-alkanes were separated on a fused silica capillary column (30 m x .32 mm i.d.; .25µm film thickness) using helium as the carrier gas. The GC oven temperature was programmed to maximize alkane separation (Table 2). Alkanes were combusted into CO_2 in a ceramic oxidation reactor containing three braided NiO/CuO/Pt wires. Three

pulses of a standard, calibrated CO_2 reference gas were injected via the GC-C II interface to the IRMS for the measurement of $\delta^{13}C$ values of individual alkanes. A laboratory working standard (UFIS) consisting of three n-alkane chains (C_{19}, C_{25} and C_{30}) was measured along with unknowns at the beginning and end of each run, as well as after every fourth sample analysis within a run. UFIS was calibrated to a set of standard *n*-alkanes (Mix A) from Indiana University with known $\delta^{13}C$ values. Long-term analytical precision, based on repeated analysis of *n*-alkanes in UFIS, was ±0.4‰. Data were acquired and processed using ISODAT NT 2.0 software. All reported carbon isotopic compositions for samples represent averaged values for duplicate analyses. Duplicate analyses had a standard deviation of approximately ±0.5‰. Long-term analytical precision based on analysis of the internal standard C_{34} was ±0.4‰.

Table 2: Hewlett Packard 6890 GC oven program for sample analyses.

Rate ˚C/min	Temperature ˚C	Time (min)
	50	2
6	299	0
10	300	4

CHAPTER 4
RESULTS

Chronology

Lake Sacnab

Twelve AMS ^{14}C dates were obtained from core SN-19-VII-97 and yielded a maximum age of 4580 ^{14}C yr BP on a sample at 439.5 cm (Table 3). The core chronology was established by converting sediment depths to age using three linear regression equations (Figure 6):

196.5-0 cm: age (cal yr BP) = 11.863 x depth, $r^2 = 0.9628$;

369.5-196.5 cm: age (cal yr BP) = 4.6821 x depth + 1495, $r^2 = 1$;

439.5-369.5 cm: age (cal yr BP) = 17.683 x depth - 3293.2, $r^2 = 0.9317$.

The age of the base of the core (445 cm) is estimated to be ~4650 cal yr BP based on extrapolation of the linear regression from 369.5 to 439.5. Sedimentation rates for the three intervals are:

196.5-0 cm = 0.081 cm/yr;

369.5-196.5 cm = 0.214 cm/yr;

439.5-369.5 cm = 0.052 cm/yr.

The wood date at 363.5 cm had a large error because of its small size and was not used to establish the chronology.

Lake Salpeten

Two AMS ^{14}C dates were obtained from core SP-12-VI-02-1A and yielded a maximum age of 3985 ^{14}C yr BP (Table 4). Additional chronological control was

obtained by correlating the $\%CaCO_3$ record from core SP2-19-VII-99 (Rosenmeier *et al.,* 2002b) and the scanning XRF Ca concentration data from core SP-12-VI-02-1A (correlation coefficient = 0.505) using AnalySeries v. 1.0 (Paillard *et al*., 1996). Ten tie points were used to correlate the records (Figure 7, Table 5).

Table 3: AMS ^{14}C dates for samples from sediment core SN-19-VII-97 from Lake Sacnab. For the LLNL-CAMS samples, backgrounds were scaled relative to sample size using Pliocene wood blanks prepared at UF (4±1µg). All radiocarbon ages are adjusted to a $\delta^{13}C$ value of -25 **‰**. Radiocarbon ages were converted to calendar ages using the program OxCal v 3.9 (Bronk Ramsey, 1995; Bronk Ramsey, 2001) and the atmospheric data set of Stuiver *et al.* (1998). All ages reported in this thesis are in calendar years before present (relative to AD 1950).

Sample ID	Composite Depth (cm)	Accession Number	Sample Material	Age ± 1 σ (^{14}C yr BP)	Calibrated Age (cal yr BP)	Calibrated Age ± 95.4% Probability (AD/BC)
SN-19-VII-97-MWI_45.5	45	CAMS 58754		280 ± 60	390	AD 1600 ± 115
SN-19-VII-97-LEX1_109.5	84	CAMS 58755		1210 ± 50	1165	AD 800 ± 110
SN19VII97MWI_97-98	97.5	CAMS 106265	seed charcoal, leaf	990 ± 50	880	AD 1100 ± 115
SN19VII97MWI_121-123	122	CAMS 106266	material	1650 ± 60	1560	AD 400 ± 155
SN-19-VII-97-LEX1_152.5	127	CAMS 58756		1620 ± 50	1515	AD 400 ± 120
SN19VII97MWI_145-147	146	CAMS 106267	charcoal, leaf material	1740 ± 100	1650	AD 300 ± 235
SN19VII97LEX2_221-223	196.5	CAMS 106268	seed, charcoal	2370 ± 40	2415	500 BC ± 90
SN-19-VII-97-LEX4_414.5	363.5	OS 18657	wood	2500 ± 160	2555	600 BC ± 400
SN19VII97LEX4_394-396	369.5	CAMS 106269	charcoal, leaf material	3030 ± 60	3225	1300 BC ± 160
SN19VII97LEX4_404-407	379.5	CAMS 106270	charcoal, leaf material	3300 ± 70	3540	1600 BC ± 155
SN19VII97LEX4_434-436	409.5	CAMS 106271	charcoal, leaf material	3450 ± 40	3740	1800 BC ± 105
SN19VII97LEX4_464-466	439.5	CAMS 106272	charcoal, leaf material	4050 ± 80	4580	2600 BC ± 275

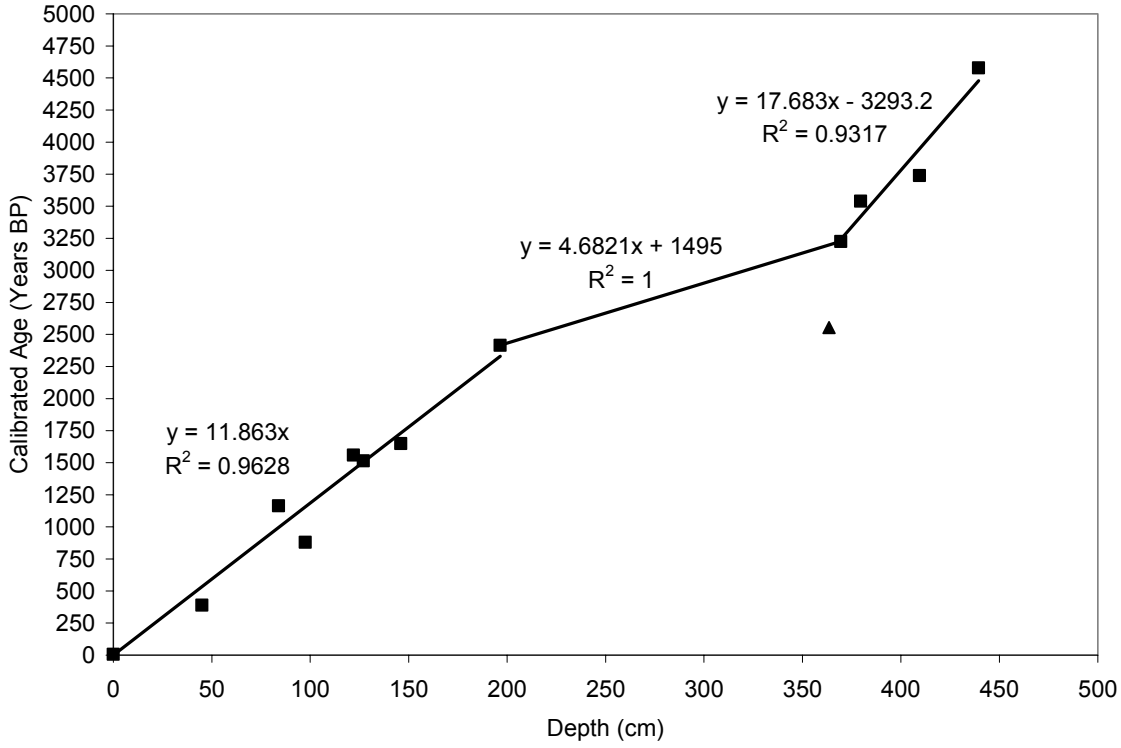

Figure 6: Depth versus calibrated age (yr BP) for terrestrial wood, seed and charcoal samples in Lake Sacnab core SN-19-VII-97. Squares indicate samples analyzed at LLNL-CAMS and the triangle indicates the sample measured at NOSAMS.

Table 4: AMS ^{14}C dates for samples from sediment core SP-12-VI-02-1A from Lake Salpeten.

Sample ID	Sample Material	Composite Depth (cm)	Accession Number	Age ± 1 σ (14C yr BP)	Calibrated Age (cal yr BP)	Calibrated Age ± 95.4% Probability (AD/BC)
SP12VI02 ST1A_110-111	charcoal	110.5	CAMS 106273	210 ± 60	165	1790 AD ± 170
SP12VI02 ST1A_442-445	charcoal	443.5	CAMS 106274	3985 ± 50	4455	2500 BC ± 200

Table 5: Tie points used to correlate the %$CaCO_3$ record from core SP2-19-VII-99 (Rosenmeier *et al.,* 2002b) and the scanning XRF Ca concentration data from core SP-12-VI-02-1A (correlation coefficient = 0.505) using AnalySeries v. 1.0 (Paillard *et al*., 1996). Included are the respective ages for each set of correlated depths. Ages for depths in core SP2-19-VII-99 were determined using the chronology outlined in Rosenmeier *et al*. (2002) while ages for depths in SP-12-VI-02-1A were determined using the correlation (Figure 4).

Depth in SP-12-VI-02-1A	Depth in SP2-19-VII-99	Age (cal yr BP)
152	151	1660
201.5	201	2030
215	213	2090
236.5	236	2210
246	248	2270
265.5	266	2390
293.5	289	2590
310.5	301	2730
330	309.5	2860
376	331	3250

The core chronology was established by converting sediment depths to age with two equations derived by linear regression for two intervals (Figure 8). The top of the core was assumed to be modern.

152-0 cm: age (cal yr BP) = 10.976 x depth, $r^2 = 1$;

376-152 cm: age (cal yr BP) = 6.8806 x depth + 599.66, $r^2 = 0.9947$.

The age of the base of the core (563.5 cm) was estimated to be ~4500 Cal yr BP based on extrapolation of the linear regression from 152 to 376 cm. The radiocarbon date at 110.5 cm was not used to construct the chronology because of its small sample size and suspicion that the charcoal fragments may have been displaced down core. Based on a comparison between magnetic susceptibility records from SP-12-VI-02-1A and SP2-19-VII-99, the radiocarbon date at 443.5 cm was not used to construct the chronology

because it caused deeper sediments to appear too old based on a comparison with core SP-80-1. Sedimentation rates for the two intervals are as follows:

196.5-0 cm = 0.091 cm/yr;

563.5-196.5 cm = 0.142 cm/yr.

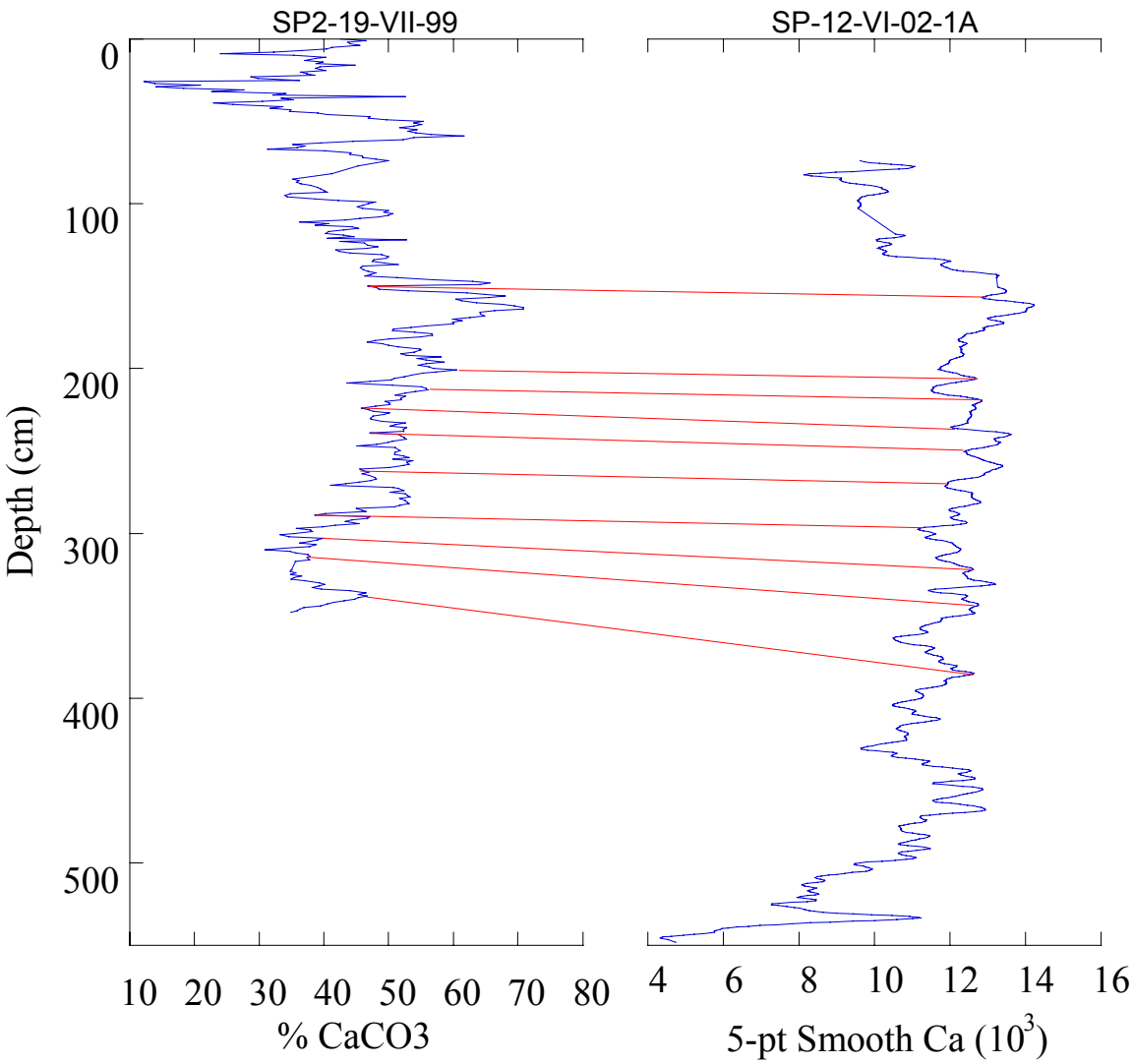

Figure 7: Correlation of SP2-19-VII-99 and SP-12-VII-02-1A using $\%CaCO_3$ in the SP2-19-VII-99 core and the scanning XRF Ca concentration data from the SP-12-VII-02-1A core.

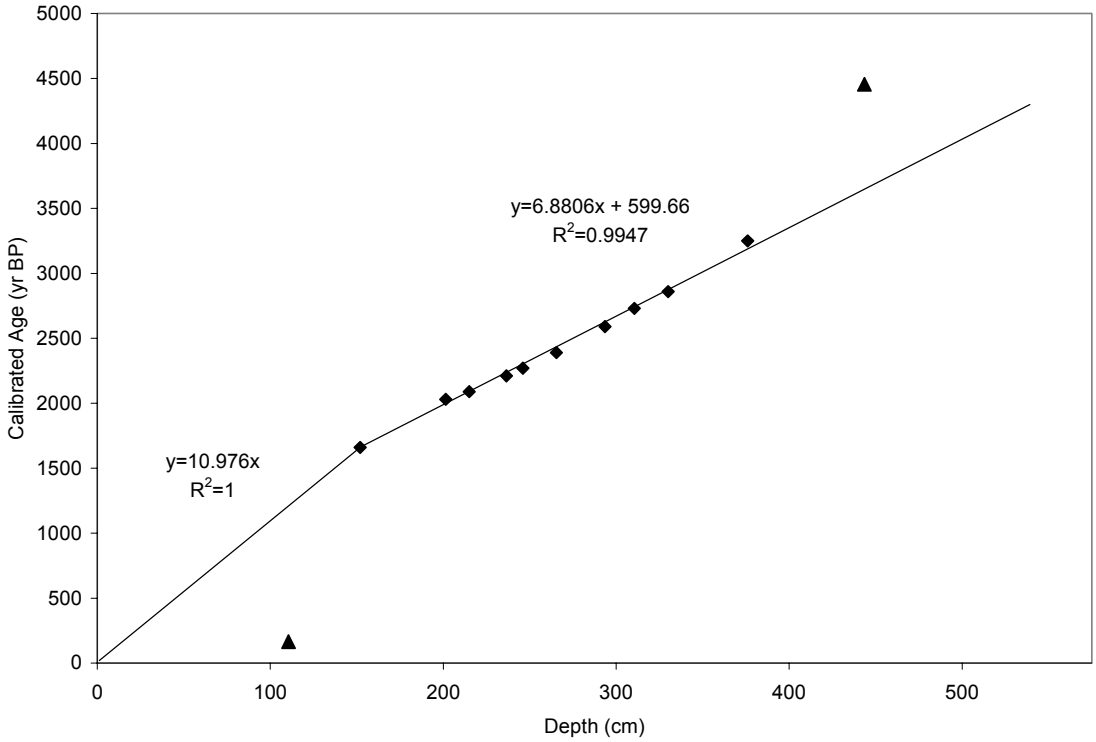

Figure 8: Calibrated ages (yr BP) versus depth for correlated tie points in core SP-12-VII-02-1A as well as radiocarbon dates of terrestrial samples in Lake Salpeten core SP-12-VII-02-1A. Triangles indicate dates analyzed at LLNL-CAMS while the diamonds represent tie points.

Elemental Geochemical Analyses

Lake Sacnab

From 4500 cal yr BP to ~3300 cal yr BP, sediments are dominated by organic matter as reflected by high %OM and %N concentrations and low magnetic susceptibility and $\%CaCO_3$ (Figure 9). The %Other is low (~20%) at 4500 cal yr BP, and increases continuously to the base of the Maya clay at 3300 cal yr BP. Beginning at the base of the Maya clay unit at ~3300 cal yr BP, magnetic susceptibility and $\%CaCO_3$ begin to increase and %OM and %N decrease abruptly. Sediment composition between ~3300 and 1200 cal yr BP is dominated by inorganic sediment (clay and detrital carbonate) as

reflected by relatively high values of magnetic susceptibility, %$CaCO_3$ and %Other. While the %OM and %N are relatively constant during this time, the magnetic susceptibility, %$CaCO_3$ and %Other show some variation. %Other remains relatively unchanged from 3300 to 2600 cal yr BP, reaching maximum values of 90% during this time before decreasing to 50% between 2700 and 2400 cal yr BP. %Other remains relatively constant from 2400 cal yr BP to 1600 cal yr BP, when values begin to increase and reach 60% at 1200 cal yr BP. Following this maximum, %Other decreases continuously from 1200 cal yr BP to the present. At ~3300 cal yr BP, magnetic susceptibility increases, rising to a maximum of ~20 SI at 2700 cal yr BP before decreasing to an average of 10 SI for the remainder of the Maya clay unit. %$CaCO_3$ increases from 3300 cal yr BP to 2400 cal yr BP, reaching a maximum of ~45%. %$CaCO_3$ then decreases to ~4% at 1200 cal yr BP and remains low until the present. At the top of the Maya clay unit, %OM and %N begin to increase and do so continuously from 1200 cal yr BP to present.

Lake Salpeten

Magnetic susceptibility increases from the base of the core to ~4100 cal yr BP (Figure 10). Values remain high from 4100 to ~2000 cal yr BP reflecting the high clay content of the sediment. Beginning at ~2000 cal yr BP, magnetic susceptibility begins to decline with two distinct steps centered at 1700 and 1300 cal yr BP. From 800 cal yr BP to the present, magnetic susceptibility values remain low and relatively unchanged.

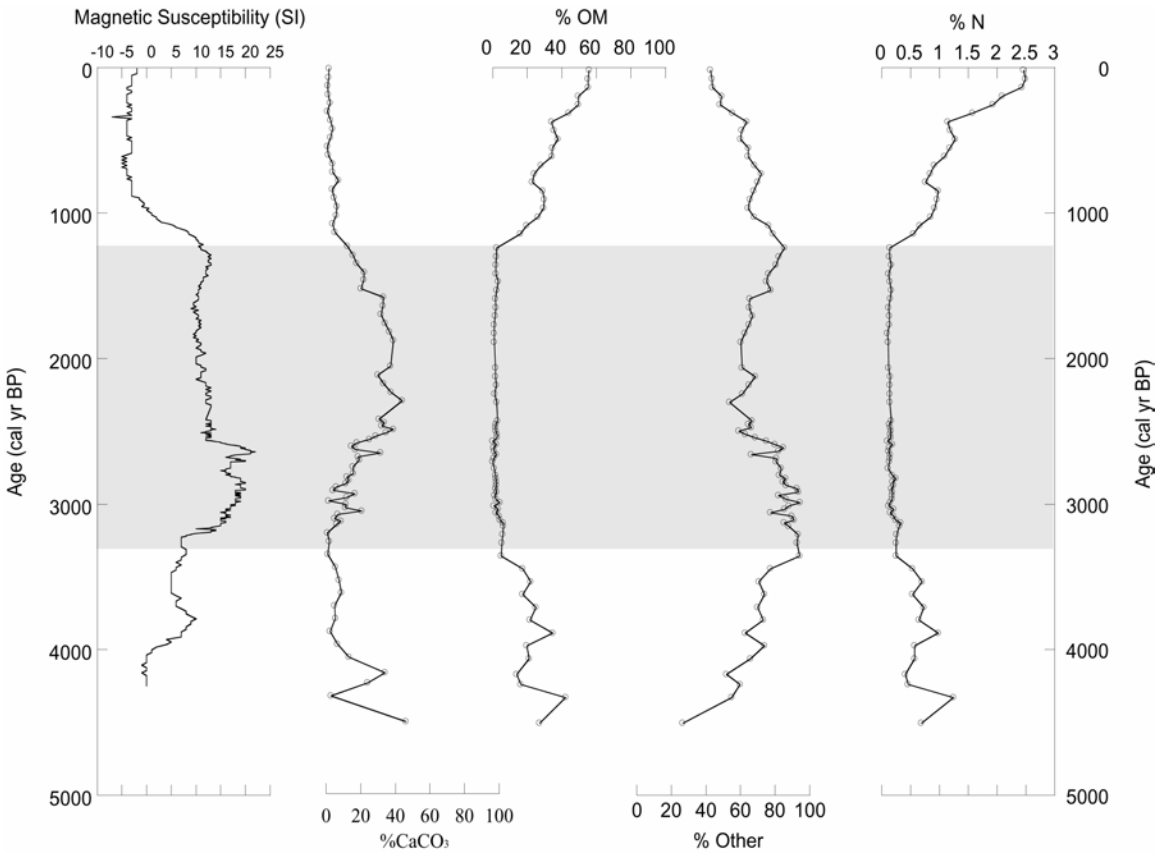

Figure 9: Magnetic susceptibility, percent calcium carbonate (%CaCO3), percent organic matter (% OM), percent other (%Other) and percent nitrogen (%N) versus age in calibrated years before present (cal yr BP) from Lake Sacnab. The gray highlighted area represents the "Maya clay" unit.

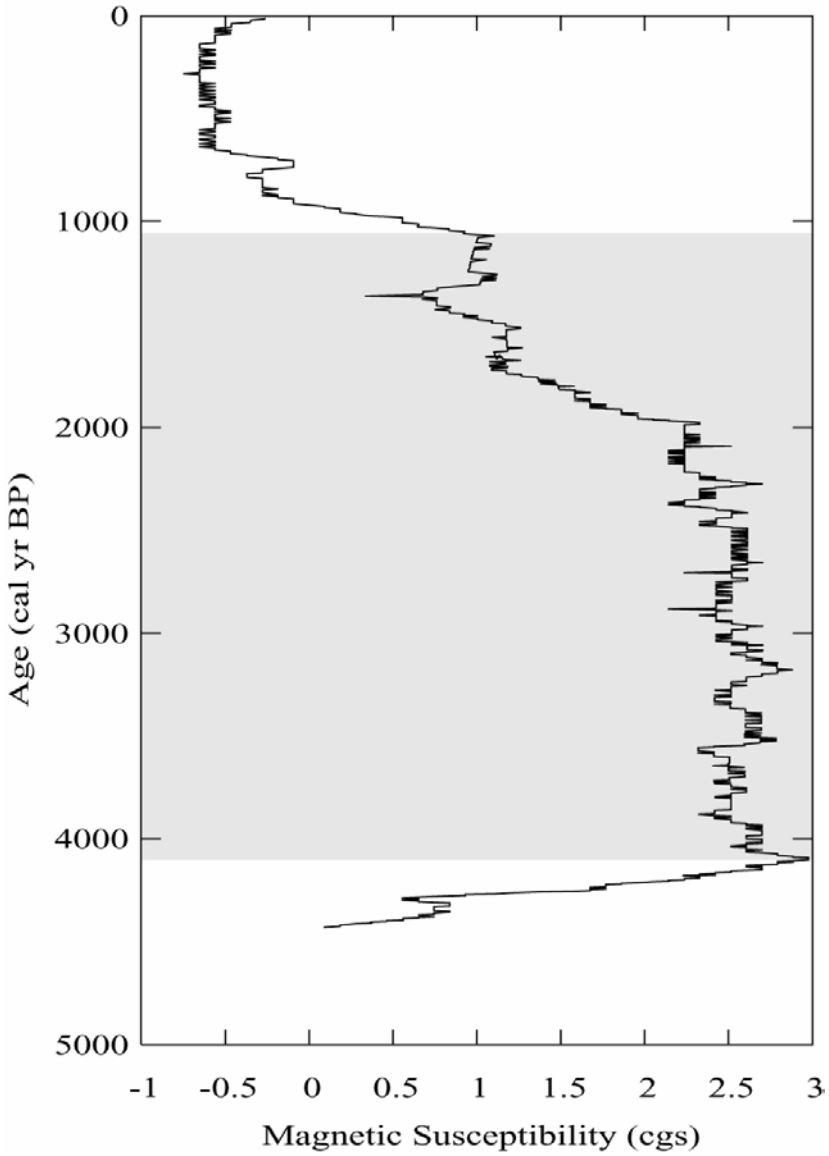

Figure 10: Magnetic susceptibility versus age in calibrated years before present (cal yr BP) for core SP-12-VII-02-1A from Lake Salpeten. The gray highlighted area represents the "Maya clay" unit.

Bulk Carbon and Nitrogen Isotopes

The carbon and nitrogen isotopic records of bulk organic matter show similar patterns during the last 4650 years (Figure 11). Bulk $\delta^{13}C$ values range from -21‰ to -28‰ throughout the core, whereas bulk $\delta^{15}N$ values vary between 0‰ and 5‰. Carbon isotopic values generally increase from -27‰ at the base of the core to -23‰ at ~3300 cal yr BP. The $\delta^{13}C$ values of bulk organic matter average -23‰ from 3300 to 2500 cal

yr BP, and then decrease between 2500 and 2000 cal yr BP. Bulk organic $\delta^{13}C$ remains unchanged and averages -25‰ from 2000 to 1300 cal yr BP. A sharp 2.5‰ decrease in $\delta^{13}C$ occurs at 1250 cal yr BP, followed by a slight trend toward increasing values toward present.

The $\delta^{15}N$ of bulk organic matter averages ~2‰ from 4500 cal yr BP to 3500 cal yr BP. From 3500 cal yr BP to 3300 cal yr BP, $\delta^{15}N$ values increase by 2‰ and remain high from 3300 cal yr BP to 1200 cal yr BP, averaging 3‰. The nitrogen isotopic composition then decreases abruptly by 3.5‰ at 1200 cal yr BP, and averages 1‰ from 1200 cal yr BP to present.

Compound-Specific Carbon Isotopes

Lake Sacnab

Samples were analyzed for the $\delta^{13}C$ of long-chain n-alkanes (C_{29}, C_{31}, and C_{33}) in Lake Sacnab sediments at approximately centennial resolution since 4650 cal yr BP (Figure 12). The $\delta^{13}C$ signals for C_{31} and C_{33} show similar trends and will be described in unison, whereas the $\delta^{13}C$ of C_{29} differs somewhat and will be described separately.

The $\delta^{13}C$ of C_{31} and C_{33} averaged -33‰ at the base of the core and gradually increased to -29‰ at ~3300 cal yr BP. Values generally remain high from ~3300 cal yr BP to ~2500 cal yr BP and averaged -28‰. From 2500 to 2100 cal yr BP, $\delta^{13}C$ decreases from -28‰ to -32‰ and values remain unchanged from 2100 to 1300 cal yr BP. At 1300 cal yr BP, the carbon isotopes of C_{31} and C_{33} record a rapid decrease with values reaching -39‰ and -37‰, respectively. Following this excursion, the $\delta^{13}C$ of *n*-

alkane chains C_{31} and C_{33} increases at 1100 cal yr BP and averages -32‰ to the top of the core.

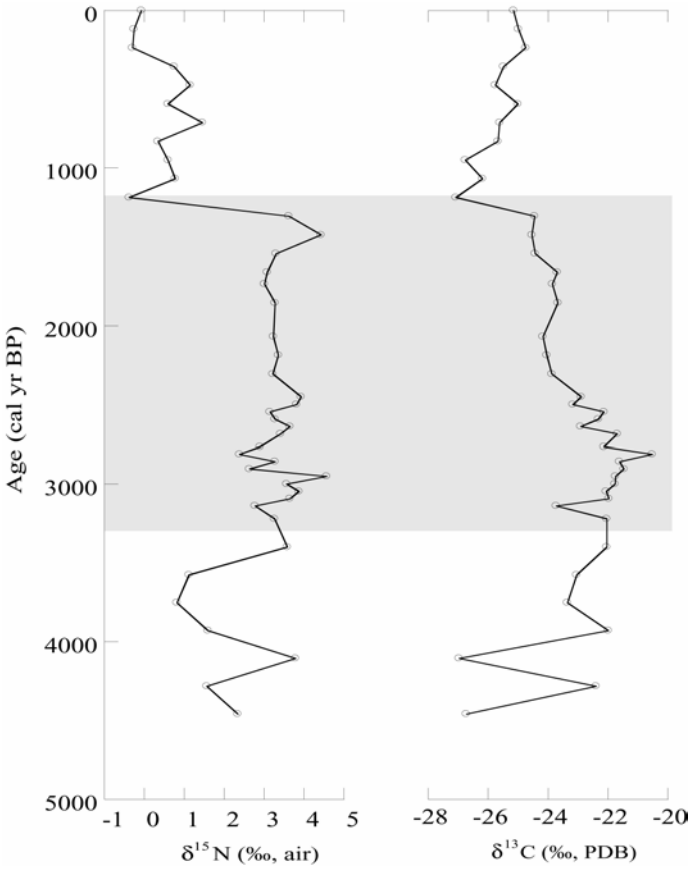

Figure 11: Bulk carbon and nitrogen isotopes for core SN-19-VII-97 from Lake Sacnab. The gray highlighted area represents the "Maya clay" unit.

The $\delta^{13}C$ of C_{29} at the base of the core is -32‰ and generally remains unchanged from ~4500 cal yr BP to ~2500 cal yr BP, with an average ratio of approximately -29‰. From 2500 cal yr BP to 2100 cal yr BP, $\delta^{13}C$ decreases from -29‰ to -33‰ and values remain unchanged from 2100 cal yr BP and 1300 cal yr BP. At 1300 cal yr BP, the carbon isotopes of C_{29} record a rapid decrease, reaching a value of -35‰. Following this excursion, the $\delta^{13}C$ of C_{29} is highly variable, with values ranging from -24‰ to -33‰ during the period from 1100 cal yr BP to the present.

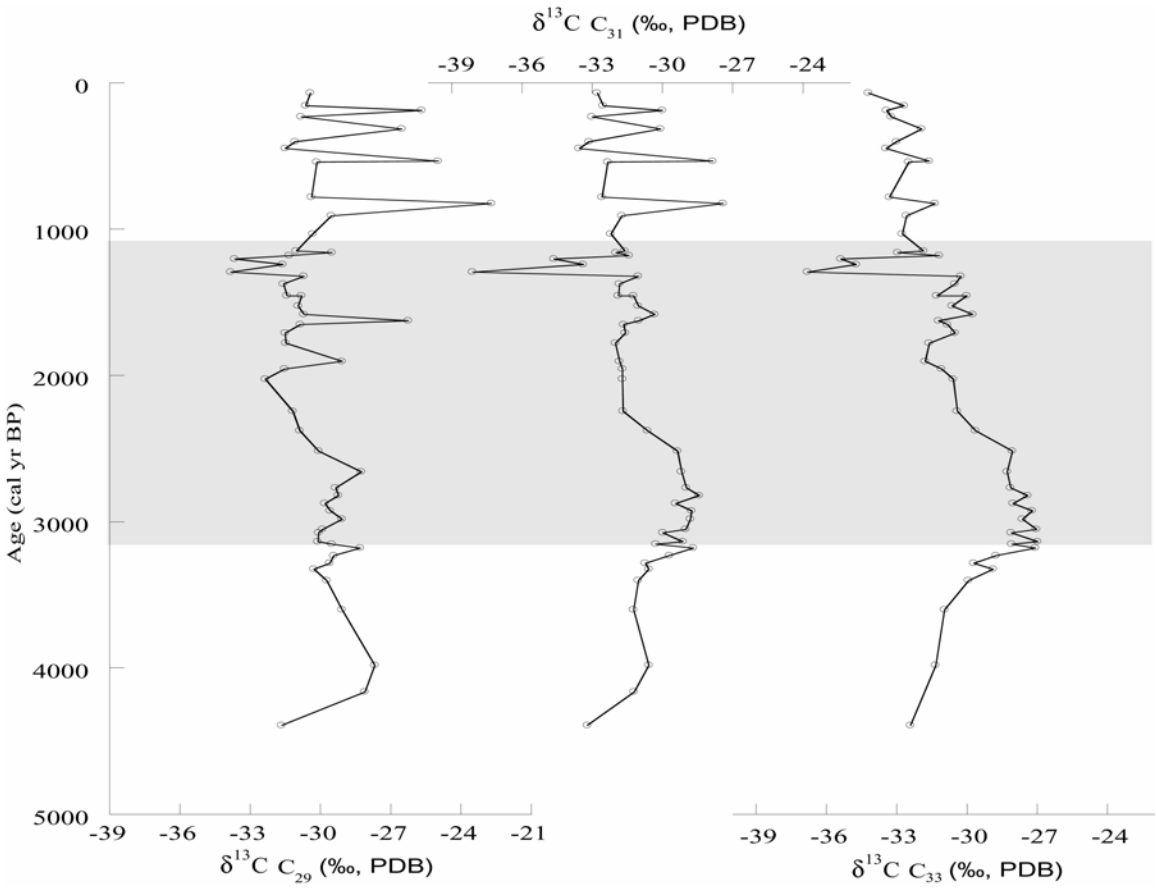

Figure 12: Compound-specific $\delta^{13}C$ results of long chain *n*-alkanes (C_{29}, C_{31}, and C_{33}) from Lake Sacnab, Guatemala versus age in calibrated years before present (cal yr BP).

Lake Salpeten

Samples were analyzed for the $\delta^{13}C$ of long-chain n-alkanes (C_{29}, C_{31}, and C_{33}) in Lake Salpeten sediments at an approximate resolution of 200 years for the past 6000 cal yr BP (Figure 13). The $\delta^{13}C$ signals for C_{29}, C_{31}, and C_{33} show similar trends and will be described in unison; variations in $\delta^{13}C$ of C_{29}, however, are muted relative to C_{31} and C_{33}.

The $\delta^{13}C$ of long-chain *n*-alkanes averaged -32‰ at the base of the core and gradually increased to -28‰ at ~5200 cal yr BP. Values generally remained unchanged from ~5200 cal yr BP to ~3300 cal yr BP and averaged -30‰. From 3300 to 2500 cal yr

BP, $\delta^{13}C$ increased from -30‰ to -27‰. The isotopic ratio decreased from 2500 cal yr BP to the present, reaching minimum values that range from -33‰ to -36‰.

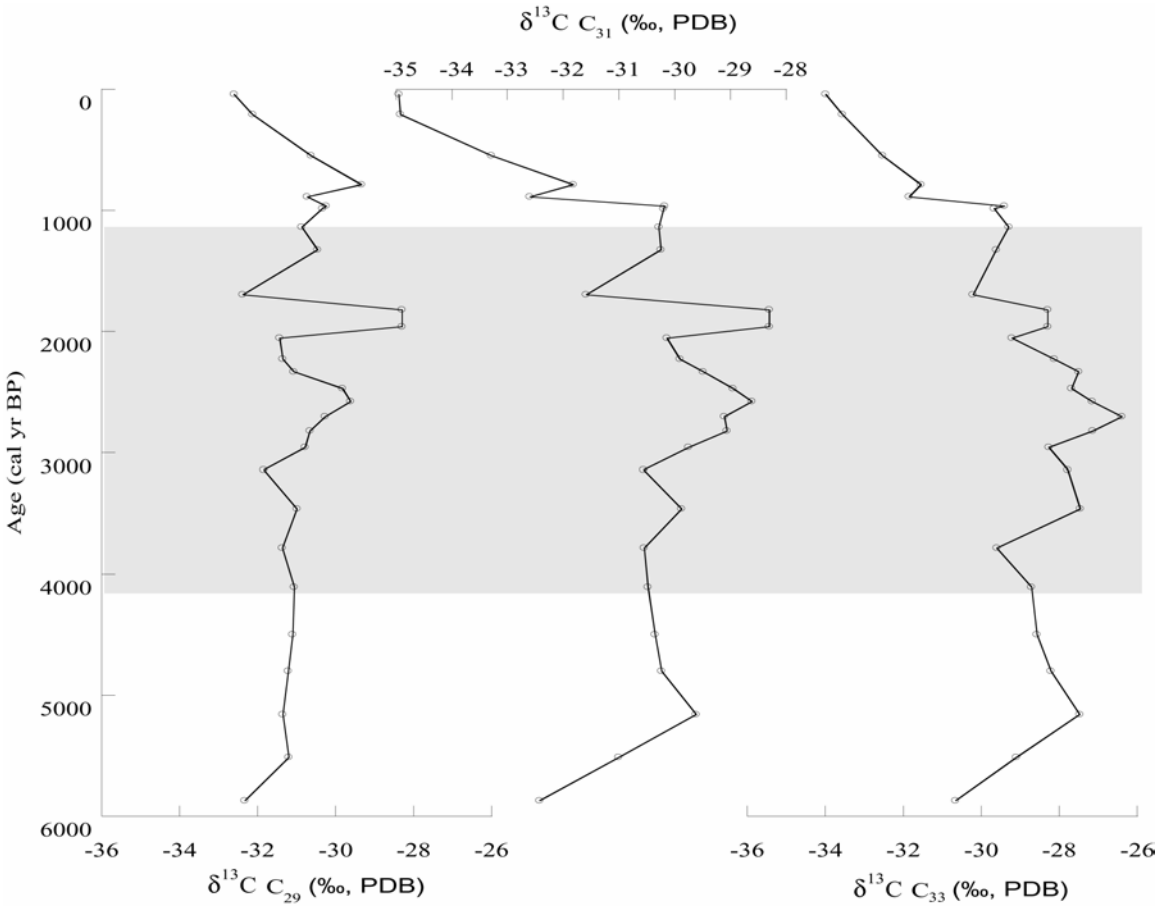

Figure 13: Compound-specific $\delta^{13}C$ results of long chain *n*-alkanes (C_{29}, C_{31}, and C_{33}) from Lake Salpeten, Guatemala versus age in calibrated years before present (cal yr BP).

CHAPTER 5
DISCUSSION

Implications for Changes in Land-use

Changes in land-use can be inferred from the lithological composition of lacustrine sediments, which reflect changes in material transfer from the watershed to the lake. With increased land clearance, the detrital load to a lake basin will increase. Sediment cores taken from Lakes Sacnab and Salpetén show similar changes in sediment composition. This common pattern has been documented throughout the central Petén lake district and is interpreted to reflect sediment compositional and rate changes related to the history of Maya settlement and population in the region (Cowgill and Hutchinson, 1966; Deevey *et al*., 1979; Brenner, 1983; Vaughan *et al*., 1985; Rice *et al*., 1985; Binford *et al*., 1987; Leyden, 1987; Curtis *et al*., 1998; Islebe *et al.*, 1996).

The sediment composition and magnetic susceptibility records in Lake Sacnab (Figure 6) document changes in material transfer from the catchment to the lake. Magnetic susceptibility is a proxy for the concentration of magnetic minerals contained within the sediment, which are derived from the erosion of soil and bedrock in the watershed and subsequently transported to the lake. $CaCO_3$ in sediments can be derived from either authigenic precipitation within the lake or by the weathering and transport of detrital carbonate from soils or limestone bedrock. There is little to no observed lacustrine carbonate in the sediments of Lake Sacnab, which may suggest that most of the $CaCO_3$ is detrital. Inorganic carbon and oxygen isotopes measured on bulk material from the lake have values that range from -8‰ to 0‰ and -4‰ to 0‰, respectively. These

values are generally consistent with measured mean values of Petén soils surrounding Lake Quexil ($\delta^{13}C \approx$ -10‰ to -7‰, $\delta^{18}O \approx$ -3‰ to 0‰,) (Leyden *et al.*, 1993) and indicate that the source for sediment $CaCO_3$ is dominantly allochthonous $CaCO_3$ as opposed to diffuse authigenic $CaCO_3$. Thus, relative shifts in $\%CaCO_3$ may serve as an additional indicator of erosion in the catchment. Organic matter in lacustrine sediments is derived from multiple sources including terrestrial vegetation, lacustrine algae and bacteria, and aquatic macrophytes. The %Other may also serve as a proxy indicator of landscape erosion. Because there is relatively little contribution to the sediments other than $CaCO_3$ and organic matter, the %Other is a likely indicator of non-carbonate clastic material (clay) eroded from the watershed. It is important to note the effects of the closed-sum problem inherent in using weight % data. Dilution may play a major role in down-core variations of any of the three components. As the % of any component increases, the other two components will respond by decreasing in % to sum to 100%. Therefore, variation in the delivery of any of the sediment components, especially during the deposition of the Maya clay, would significantly alter the apparent input of the other sediment components. To avoid the "closed-sum" problem, accumulation rates ($g/cm^2/yr$) can be calculated. Accumulation rates of the three individual sediment components provide a better indication of erosion and sediment deposition. Unfortunately, the density data necessary to calculate accumulation rates are not available for Core SN-19-VII-97 from Lake Sacnab. Anselmetti *et al.* (in prep), however, calculated accumulation rates for specific time intervals in Lake Salpetén for the period between 8500 cal yr BP and the present. Data indicate that erosion rates were lowest during the early to mid-Holocene and increased beginning in the Early Preclassic. Erosion rates were highest during the

Late Preclassic period (2200 to 1700 cal yr BP) and subsequently decreased over time even during the height of Maya occupation in the watershed (1700 and 1100 cal yr BP). The sedimentological history and associated watershed erosional characteristics determined by Anselmetti *et al.* (in prep) are consistent with those determined in this study.

In Lake Sacnab, Holocene sediment prior to Maya occupation is classified as gyttja. Overlying the pre-Maya gyttja is a clay-rich horizon known as the "Maya clay", associated with increased sedimentation rates. The onset of Maya clay deposition appears to have begun at 3300 cal yr BP and lasted until ~1200 cal yr BP. This unit is common in all the central Petén lakes and has been interpreted previously to reflect accelerated erosion associated with Maya land clearance (Deevey *et al.*, 1979; Brenner, 1983; Vaughan *et al.*, 1985; Rice *et al.*, 1985; Binford *et al.*, 1987; Leyden, 1987; Curtis *et al.*, 1998; Islebe *et al.*, 1996) and/or possibly regional drying (Hodell *et al.*, 1995; Curtis *et al.*, 1998). In the Lake Sacnab watershed, soils likely became unstable as forest cover was removed at the onset of Maya occupation. The common soil type in the Petén are mollisols, consisting thin (typically <1 m) mineral soils that develop over $CaCO_3$-rich material called *sascab* (Brenner *et al*., 2002).

Down-profile erosion of Petén soils following deforestation is evidenced in the sedimentological history. Changes in the ratio of %Other to %$CaCO_3$ suggest that the organic- and clay-rich surface horizon was eroded between 3300 and 2500 cal yr BP. Once the watershed had been denuded of organic-rich top soils, the weathering and erosion of more carbonate-rich, deep soils (sascab) ensued from 2500 to 1300 cal yr BP, as evidenced by the increase in the influx of $CaCO_3$ and decrease in %Other (Figure 6).

This period (between 3300 and 1200 cal yr BP) was characterized by enhanced delivery of detrital material to the lake and resulted in sediments with a low organic content, which is likely a dilution effect.

Overlying the Maya clay unit is another organic- and clay-rich layer that is inferred to represent decreased erosion following the cessation of agriculture and increased contribution of lacustrine organic matter to the sediment. Stratigraphic changes in sediment composition in Lake Sacnab are similar to those in other lakes in the Petén determined in previous studies (Deevey *et al.*, 1979; Brenner, 1983; Vaughan *et al.*, 1985; Rice *et al.*, 1985; Binford *et al.*, 1987; Leyden, 1987; Curtis *et al.*, 1998; Islebe *et al.*, 1996) and suggests that the history of human and environmental changes is similar throughout the central Petén region.

The magnetic susceptibility record from Lake Salpetén shows a similar trend to Lake Sacnab in the transfer of watershed material to the lake but with a distinct difference in timing (Figure 10). The onset of Maya clay deposition, indicated by the enhanced delivery of watershed-derived detrital material resulting from landscape denudation, appears to have begun at 4100 cal yr BP and lasted until ~1100 cal yr BP. Previous work (Rosenmeier *et al.*, 2002) in Lake Salpetén, however, has indicated that the Maya Clay was deposited between ~3300 and 1100 cal yr BP. The apparent discrepancy between the two cores is most likely related to the chronology of core SP-12-VI-02-1A (this study), which was correlated to core SP2-19-VII-99 (Rosenmeier *et al.*, 2002) using ten tie points (see Chapter 4). In using this method, there is the possibility for miscorrelations that would cause error in the chronology. Core SP-12-VI-02-1A was dated indirectly and ages for the Maya clay from Rosenmeier *et al*. (2002) are probably

more accurate. Archaeological settlements in the Lake Salpetén watershed are documented beginning at ~3000 cal yr BP (Figure 3) (Rice and Rice, 1990) and roughly coincided with the sedimentological evidence for human occupation of Rosenmeier *et al*. (2002).

For the most part, compound-specific carbon isotopes track magnetic susceptibility closely throughout the records for both Lake Sacnab and Lake Salpetén (Figures 14, 15). The magnetic susceptibility record is generally considered a proxy for changes in amount of detrital material transported from the landscape into the lake that, in turn, is affected by the amount of vegetation in a watershed. In both lakes, periods of inferred increased erosion occur simultaneously with periods of higher relative contributions of C_4 vegetation. As vegetation shifts from high-forest taxa to a more savanna-like landscape during forest removal, rapid erosion of watershed soils resulting from soil destabilization ensues. Because both magnetic susceptibility and the compound-specific records are influenced by vegetation cover and type and are indicative of landscape conditions, the correlation of these proxies was not unexpected.

Sources of Organic Matter

Organic matter in lacustrine sediments is derived from multiple sources including terrestrial vegetation, lacustrine algae, and aquatic macrophytes. The C/N ratio can provide information about the proportions of algal versus terrestrial plant contribution to organic matter (Prahl et al., 1980; Meyers, 1994; Kaushal and Bindford, 1999). Organic matter from algae and bacteria has C/N weight ratios ranging between 5 and 12, whereas organic matter from vascular land plants usually has weight ratios of 24 and greater (Meyers, 1994). While C/N ratios between 36 and 48 are generally characteristic of

cellulose-rich vascular plants, weight ratios between ~14 and 20 suggest a mixture of both algal and vascular plant material (Ertel and Hedges, 1985).

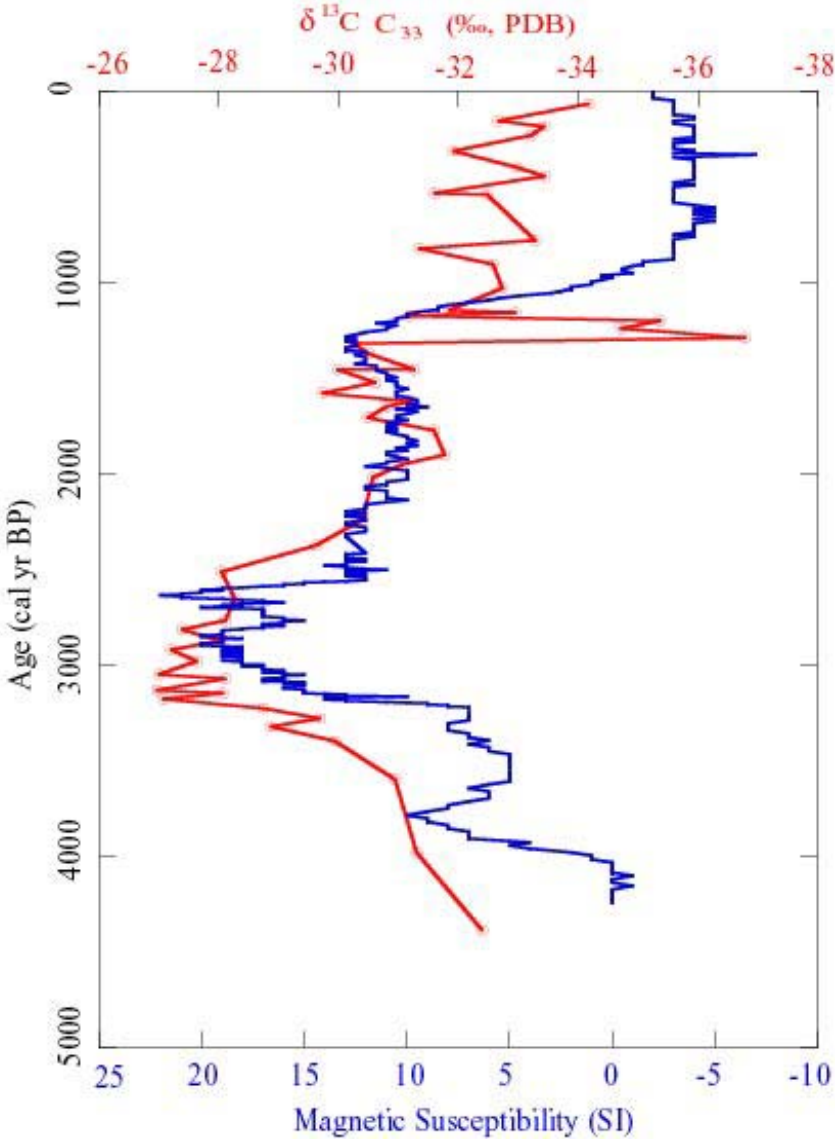

Figure 14: Comparison of $\delta^{13}C$ of C_{33} from Lake Sacnab with magnetic susceptibility.

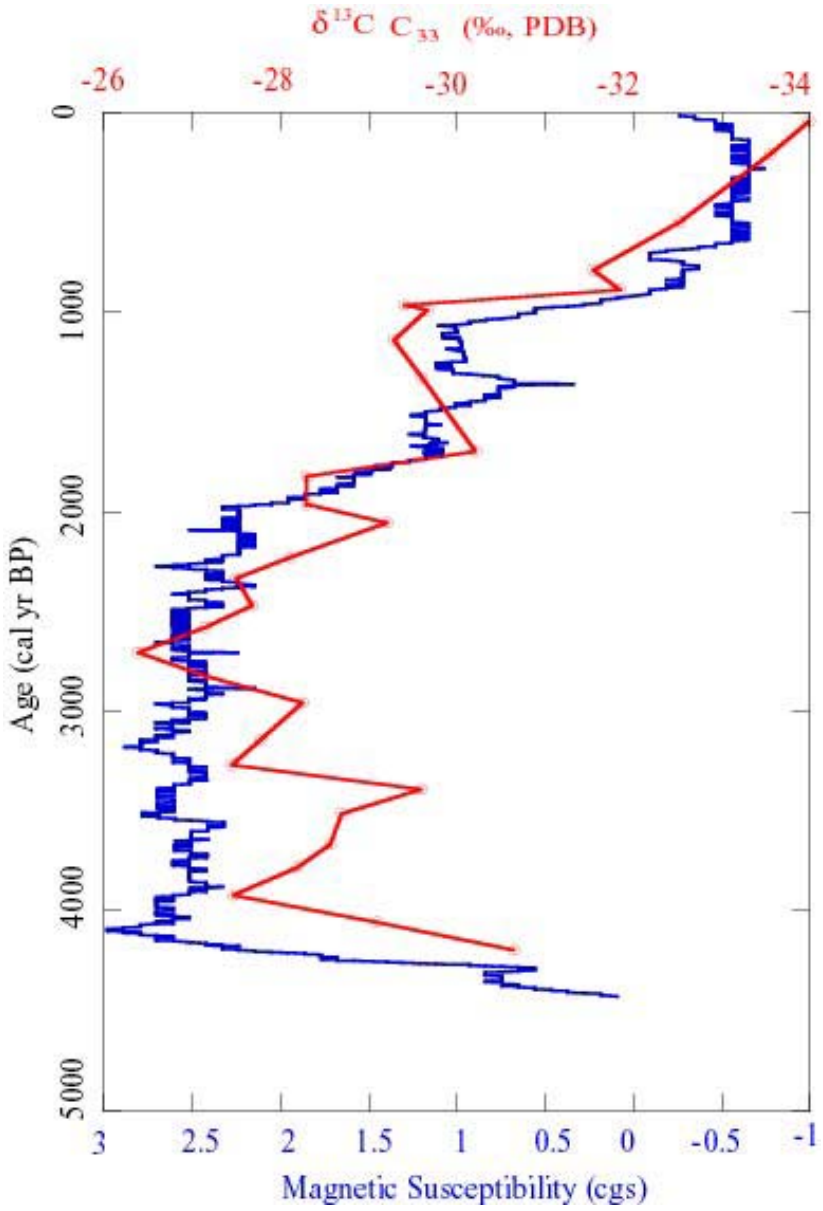

Figure 15: Comparison of $\delta^{13}C$ of C_{33} from Lake Salpetén with magnetic susceptibility.

In Lake Sacnab, the C:N ratio suggests that the source of organic matter to the lake may have changed over the last 4500 years (Figure 16). Values range from 10 to 20 in the earliest part of the record, from 4500 to 2700 cal yr BP, and suggest a mixture of both algal and terrestrial plant material. From 2700 cal yr BP to 1300 cal yr BP, increased ratios of C:N suggest the predominant contribution of terrestrial vegetation to

sediment organic matter. Values are low from 1300 cal yr BP to the present, ranging only between 9 and 13.5, suggesting a return to dominantly aquatic organic matter.

The distinguishing C:N ratios among the different types of organic matter generally survive both sinking and sedimentation in lacustrine environments. However, certain diagenetic processes such as dissolution, oxic/anoxic cycles and bacterial processes may modify the original ratios (Müller and Mathesius, 1999). For this reason, C:N values are often used together with the carbon isotope ratio of bulk organic matter to determine both the source(s) and composition of organic matter.

The period between 4500 and 2700 cal yr BP has bulk isotope values that suggest an increasing contribution of a mix of C_3 and C_4 land plants while the C:N ratio suggests additional contribution from algae. From 2700 to 1300 cal yr BP, both the C:N and the bulk isotopes suggest a dominant contribution from C_4 terrestrial plants and is followed by a period between 1300 cal yr BP and the present in which there is a higher contribution from algae, aquatic macrophytes and C_3 terrestrial vegetation.

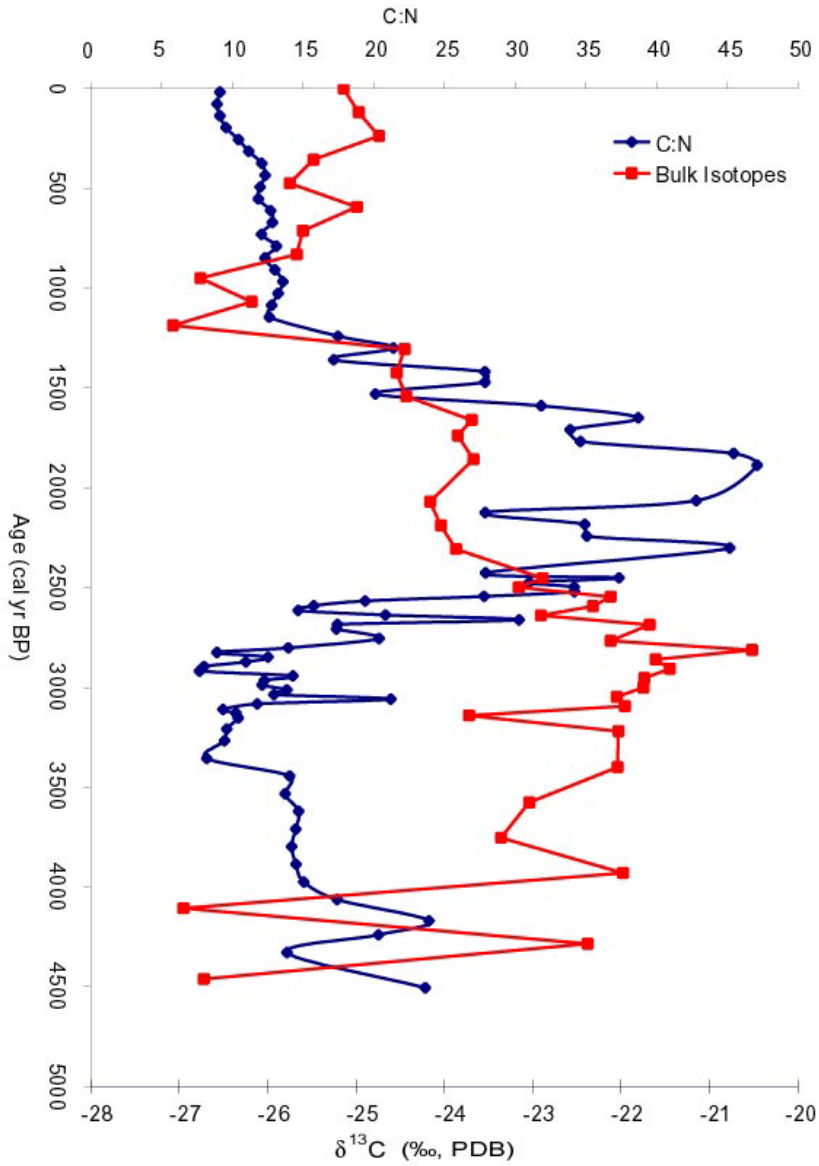

Figure 16: C:N ratios in weight % and bulk organic matter isotopes from Lake Sacnab.

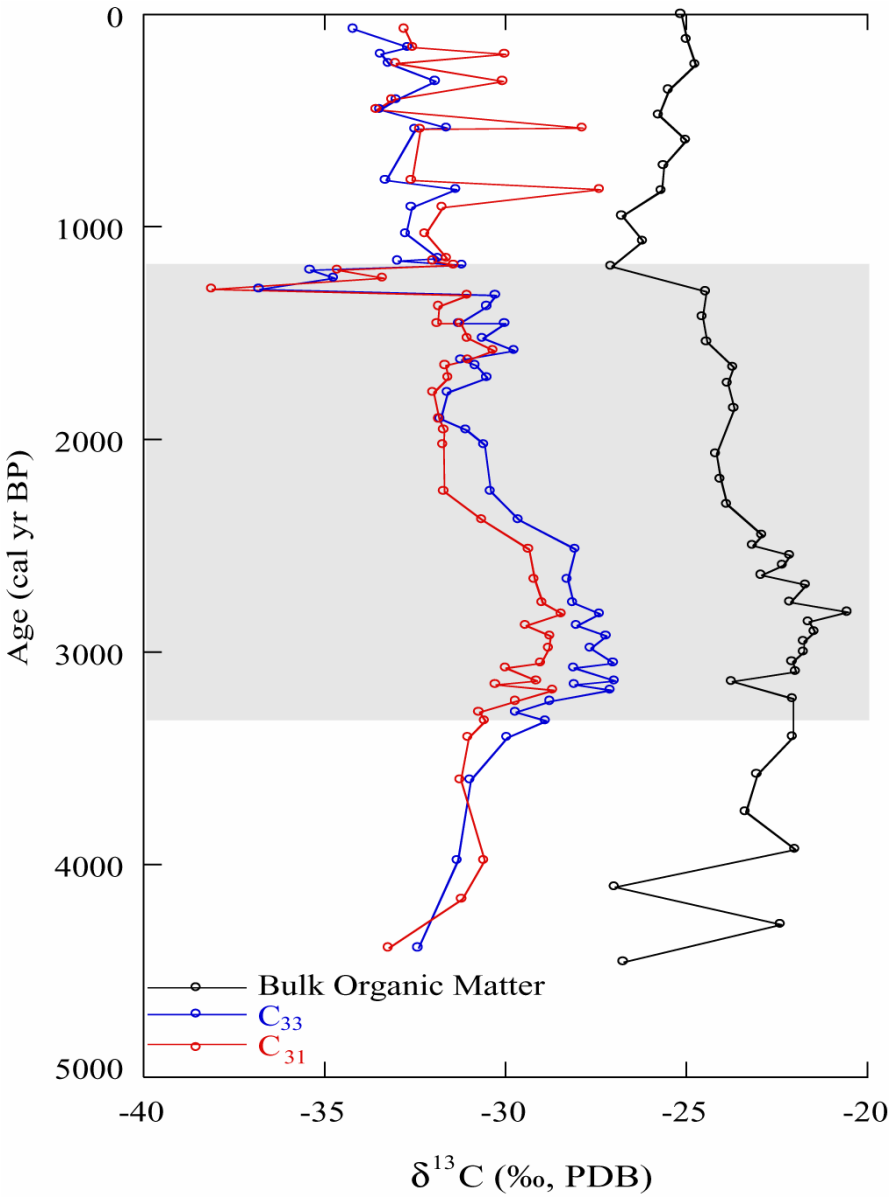

Figure 17: Comparison of $\delta^{13}C$ values for bulk organic matter, C_{31} and C_{33} from Lake Sacnab.

The $\delta^{13}C$ of bulk organic matter in Lake Sacnab sediments shows similar trends as the compound-specific record which might indicate that the bulk organic matter within the lake sediment is dominated by terrestrial organic matter with only a small contribution from aquatic macrophytes and algae (Figure 17). However, the C:N ratios

suggest that the source(s) of organic matter changed over time and is likely a better proxy for the source(s) of organic matter. The bulk and compound-specific isotopes show the most distinct variation in trend in the latest part of the record, from ~1200 cal yr BP to the present and may be explained by the increased contribution from aquatic macrophytes and lacustrine algae as demonstrated by the C:N ratio. Carbon isotopic values of bulk organic matter are enriched by ~5‰ to 7‰, however, relative to individual leaf wax *n*-alkanes. This is expected because lipids, including *n*-alkanes, are commonly depleted in ^{13}C relative by ~6‰ –to 8‰ relative to other biosynthetic products (Hayes, 2001). Thus, much of the terrestrial organic matter in the lake deposits owes its origin to non-lipid sources.

An important concern in analyzing the isotopes of individual *n*-alkanes is preservation potential. The carbon preference index (CPI) is often used as a proxy for the preservation potential of the organic matter when there is a clear predominance of epicuticular leaf waxes of terrestrial plants (Hedges and Prahl, 1993). CPI values are generally highest in living plants and surface sediments. Lowered values indicate increasing maturity and degradation and tend to decrease to a final value of 1 (Hedges and Prahl, 1993). However, this index cannot be used as a preservation potential proxy in all cases. For example, a CPI of 1 may indicate immature organic matter with a low contribution from higher plants rather than mature organic matter. In order to determine whether the CPI can be used as a proxy for preservation potential, the examination of the predominant *n*-alkane chain length can provide some insight into the provenance of organic matter. The predominant *n*-alkane chain length is shown in Figure 18a, which is interpreted as an indicator of the origin of the organic debris input (algae, aquatic

macrophytes or land plants) (Cranwell *et al*., 1987; Ficken *et al*., 2000). The predominance of *n*-alkanes of high-molecular-weight indicates that terrestrial plants are the predominant organic matter source and suggests that the CPI can be used as a proxy for preservation potential.

With respect to the CPI, most of the values are greater than 1.5 with few exceptions (Figure 18b). The CPI shows a predominance of immature, plant-derived material and, therefore, very little removal of components during transport and post-deposition (Ortiz *et al.*, 2004).

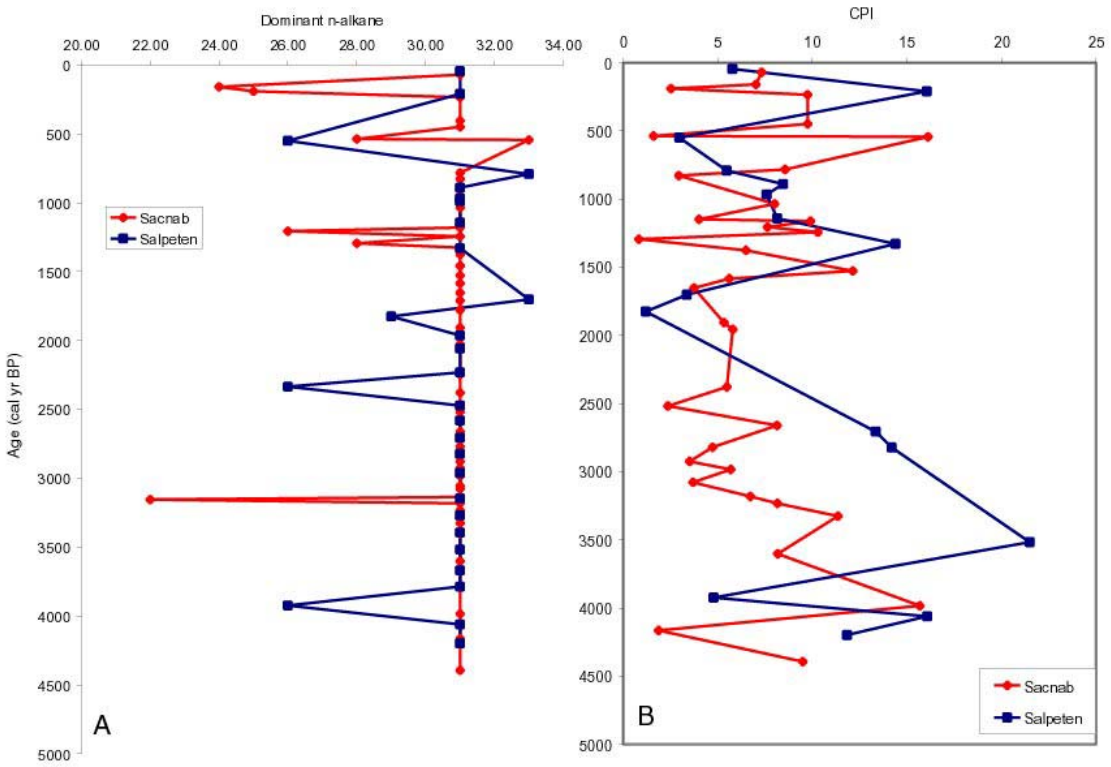

Figure 18: Predominant *n*-alkane chain length (A) and CPI (B) for Lakes Sacnab and Salpetén.

Evidence for Relative Shifts in Vegetation

Sediments from Lakes Sacnab and Salpetén show a range of values (-38‰ to -27‰,) during the last 4500 years that indicate changing relative proportions of C_3 to C_4 vegetation in the watershed (Figure 11). A comparison of the $\delta^{13}C$ records of C_{33} from Lake Sacnab and Lake Salpetén reveals similar absolute values and long-term trends over the past 4500 cal yr BP (Figure 19). At the base of the core, more depleted values suggest a higher proportion of C_3 versus C_4 vegetation. A shift towards more enriched values from 4500 cal yr BP to 3300 cal yr BP reflects an increase in the relative abundance of C_4 (grasses, etc.) to C_3 (trees) vegetation. Decreasing $\delta^{13}C$ values from 2500 cal yr BP to 2000 cal yr BP indicates some forest regrowth and a higher proportion of C_3 taxa than in the previous interval. The proportion of C_3 to C_4 vegetation is relatively unchanged from 2000 cal yr BP to 1300 cal yr BP, which is surprising given the population changes that were occurring in this period. At 1300 cal yr BP in the Sacnab watershed only, a sharp decrease in the $\delta^{13}C$ indicates a rapid transition (~100 years) to a highly C_3-dominated landscape. During the last ~1200 cal yr BP, the carbon isotopic record from both lakes suggests a gradual shift towards greater contribution of C_3 vegetation toward present.

There are several distinct differences in the δ13C records of the two cores. A peak in the $\delta^{13}C$ in Lake Salpetén at approximately 3900 cal yr BP and subsequent decrease until 3300 cal yr BP is not observed in Lake Sacnab. Rather, values are continually increasing during this time in Lake Sacnab. In addition, the $\delta^{13}C$ peaks at approximately 3100 cal yr BP in Lake Sacnab, whereas maximum δ13C values in Lake

Salpetén do not occur until 2800 cal yr BP. The rapid transition in $\delta^{13}C$ at 1300 cal yr BP in Lake Sacnab is not present in the Salpetén record. The differences in the δ13C records may be due partly to sampling resolution, which is approximately two times higher in Lake Sacnab than in Lake Salpetén. In addition, some variation may be expected in the history of vegetation changes in the two watersheds. While the general trends of land-use and human occupation are thought to be similar between watersheds, these systems are dynamic and the history of land use was probably variable throughout the region.

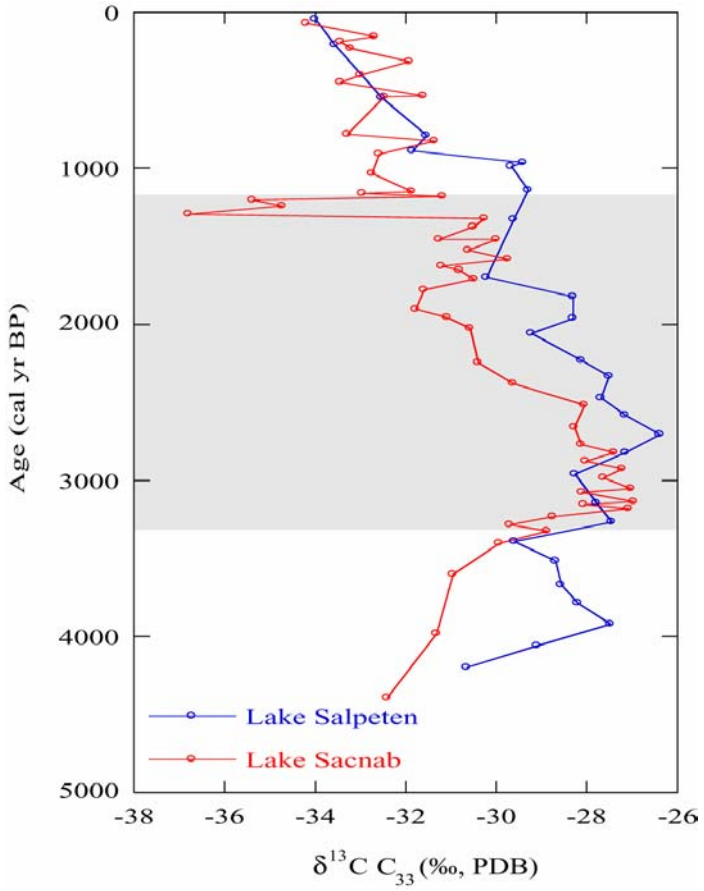

Figure 19: Comparison of $\delta^{13}C$ records for *n*-alkane chain C_{33} in Lake Sacnab and Lake Salpetén .

The rapid decline in $\delta^{13}C$ in the Lake Sacnab core at 1300 cal yr BP may reflect increased dominance of a single species with a relatively depleted carbon isotopic value after agricultural abandonment. Various chronosequence studies of abandoned agricultural fields have determined that soil nitrogen is often the limiting factor during the entire succession of vegetative regrowth (Tilman, 1984; Tilman 1987; Knops and Tilman, 2000). In many cases, legumes are the first plants to colonize abandoned fields because they are able to fix atmospheric nitrogen. If the pioneering species were legumes, then it would have a low $\delta^{15}N$ value because of nitrogen fixation ($\delta^{15}N = 0$), which involves little isotopic fractionation between plant tissues and air. In fact, the rapid transition in the $\delta^{13}C$ record in Lake Sacnab occurs at the same time (~1300 cal yr BP) as a rapid decrease in the $\delta^{15}N$ of bulk organic matter (Figure 20). These data support an increased contribution of sediment organic nitrogen from N_2 fixers because sedimentary $\delta^{15}N$ values at this time are close to zero. While the average $\delta^{13}C$ of legumes is not necessarily more negative than other plants, they are exclusively C_3 plants and thus have low $\delta^{13}C$ values relative to C_4 vegetation.

An alternative explanation for the rapid transition at 1300 cal yr BP is the result of dominance of a non-leguminous pioneer species. For example, it has been documented that in certain systems, bracken fern often dominates the vegetation in a field immediately following abandonment (Pakemen *et al.*, 1994). Eventually, other high forest taxa out-compete this weed and would thus change the isotopic composition of sediments gradually over time. While the $\delta^{13}C$ value of bracken fern is not reported in the literature and is not necessarily the source for the depleted values in this study, previous work shows that one species may dominate following agricultural abandonment.

It may be possible to determine whether a pioneer species accounts for the dramatic isotope shift by analyzing pollen samples at close intervals above, within, and below the transition.

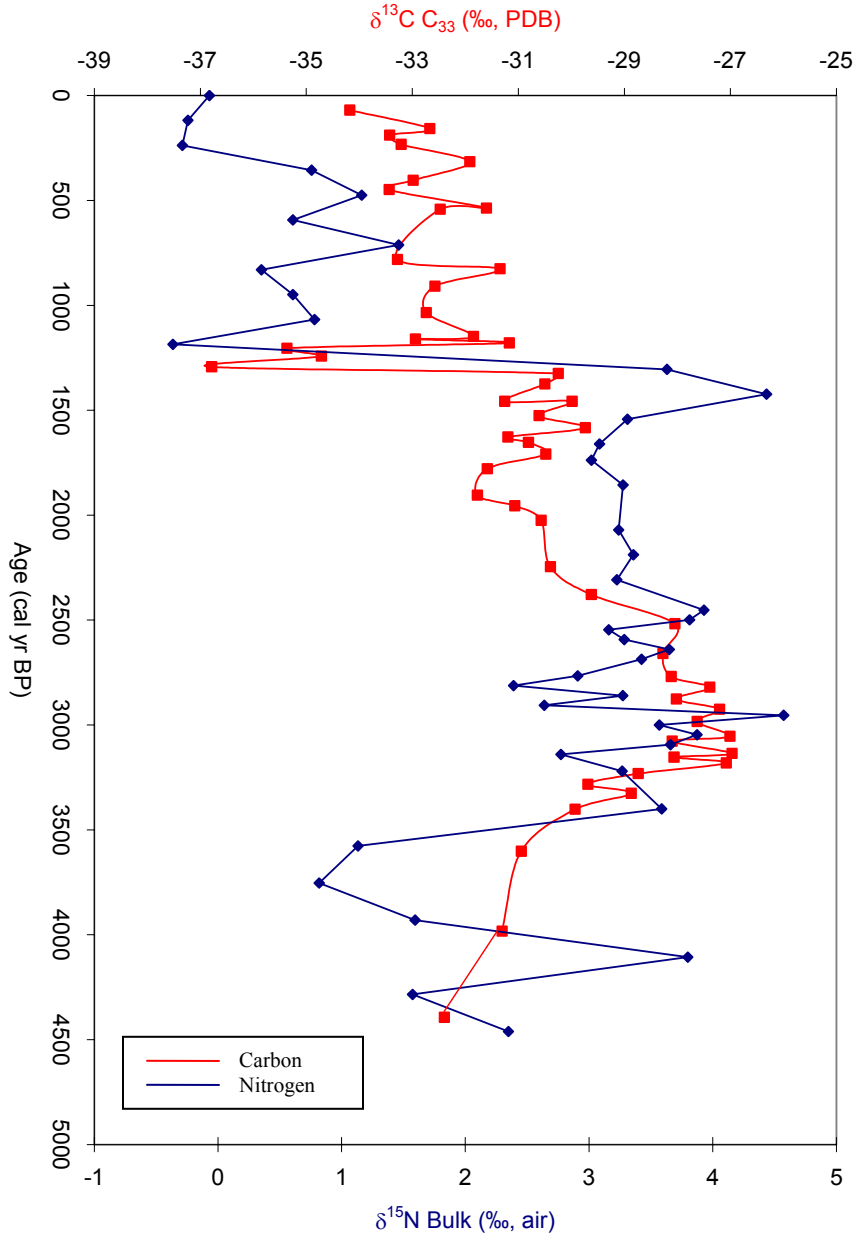

Figure 20: Diagram comparing the $\delta^{13}C$ of C_{33} to the $\delta^{15}N$ of bulk organic matter in Lake Sacnab.

Reported $\delta^{13}C$ values of *n*-alkanes in C_3 plants range from -31‰ to -38‰, whereas *n*-alkanes in leaf waxes of C_4 plants typically range from -19‰ to -25‰ (Freeman, 2001). The $\delta^{13}C$ values for *n*-alkanes in this study, however, range from -27‰ to -38‰ which might suggest that C_3 vegetation dominated throughout much of the study period. Previous studies of aerosols and sediments have translated $\delta^{13}C$ values into percentages of C_3 versus C_4 plants using a two-component mixing equation (Huang et al., 2000; Schefub et al., 2003). It has been found, however, that the isotopic values of C_3 plants usually become more depleted with increasing carbon number while C_4 plants have isotopic values that are consistent over all chain lengths (Collister et al., 1994). The variation is suggested to result from the production of different leaf wax lipids in different proportions during a leaf's growth cycle and averages approximately 2.4‰. This variation translates into a potential 16% error in the calculation of C_3 to C_4 abundance. This characteristic makes it difficult to quantify the contribution of C_3 versus C_4 plants. In order to account for this effect, the values for the lowest-number terrestrial *n*-alkane chain, C_{29}, are most often used to translate $\delta^{13}C$ values into % contributions. Because aquatic macrophytes can contribute significant amounts of C_{29}, it is preferable to calculate $\%C_4$ using an n-alkane of greater chain length. For this study, values were calculated using a two-component mixing equation assuming end-member $\delta^{13}C$ values of *n*-alkane C_{33} of -36.4‰ for C_3 plants and -19‰ for C_4 plants, respectively. These values were adapted from those of Collister *et al*. (1994), who reported -34‰ for the C_3-endmember and -19‰ for the C_{29} C_4-endmember.

For Lake Salpetén, the contribution of C_4 vegetation to the C_{33} *n*-alkane pool ranges between 14% and 57.5% (Figure 21). The % contribution of C_4 taxa increases

between 4500 and ~2700 cal yr BP when the greatest proportion of C4 occurred. The contribution of C_4 biomass declines from nearly 58% at 2700 cal yr BP to just 14% at present.

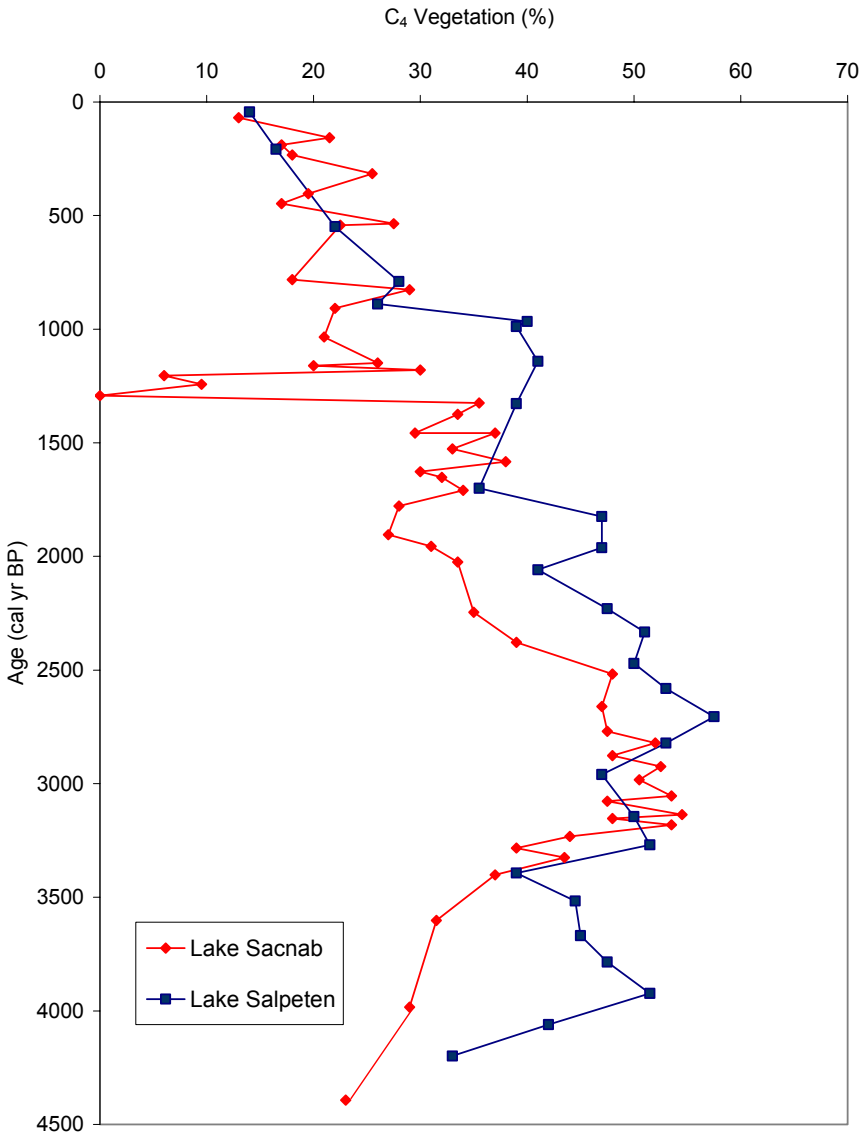

Figure 21: Relative shifts in contribution of C_4 vegetation (in %) in Lakes Sacnab and Salpetén over the last ~4500 cal yr BP. Values were calculated using a two-component mixing equation with C_3 and C_4 inputs represented by $\delta^{13}C$ values of *n*-alkane C_{33} of -36.4‰ and -19‰, respectively (Collister *et al*., 1994).

Lake Sacnab shows similar shifts to Lake Salpetén with respect to % contribution of C_4 biomass. From 4500 cal yr BP until ~3300 cal yr BP, the % contribution increases, reaching peak values of ~55‰ between 3300 and 2700 cal yr BP. From 2700 cal yr BP to 1300 cal yr BP, the contribution of C_4 vegetation generally decreases. At 1300 cal yr BP, the contribution of C_4 vegetation is 0%, but rapidly increases to a greater contribution (30%) by 1200 cal yr BP. The contribution of C_4 vegetation gradually decreases from 1200 cal yr BP to the present.

Changes in water-use efficiency (WUE), i.e. the ratio of carbon gained to water lost during gas exchange, may also affect the δ13C of vegetation. A negative correlation exists between precipitation and $\delta^{13}C$ of vegetation among tropical sites (Leffler and Enquist, 2002). Consequently, the $\delta^{13}C$ of C_3 vegetation would increase during periods when the precipitation decreased significantly. Consequently the calculated % C_4 contribution may be greater than the true value. It is thus necessary to consider the potential influence of climate on the $\delta^{13}C$ record.

The $\delta^{13}C$ values of *n*-alkanes in Lakes Sacnab and Salpetén are similar to values obtained by Huang et al. (2001) in Lake Quexil (Figure 22). The $\delta^{13}C$ values during the Maya clay interval in Quexil averaged -31‰ and are similar to values measured in the Maya clay from Lake Sacnab (average = -30‰). Values from Lake Quexil in the pre-Maya gyttja average -34‰ and increased by ~5‰ between 3300 and 1100 cal yr BP, with a peak in $\delta^{13}C$ during the time of the Maya Terminal Classic period. They attribute this increase to both anthropogenic forest clearance and regional drying. The $\delta^{13}C$ from Lake Sacnab, however, reaches peak values much earlier at ~3000 cal yr BP than in Lake

Quexil. The Quexil carbon isotope record is much lower resolution than either Lakes Sacnab or Salpetén, and may not capture the structure observed in the higher-resolution $\delta^{13}C$ records.

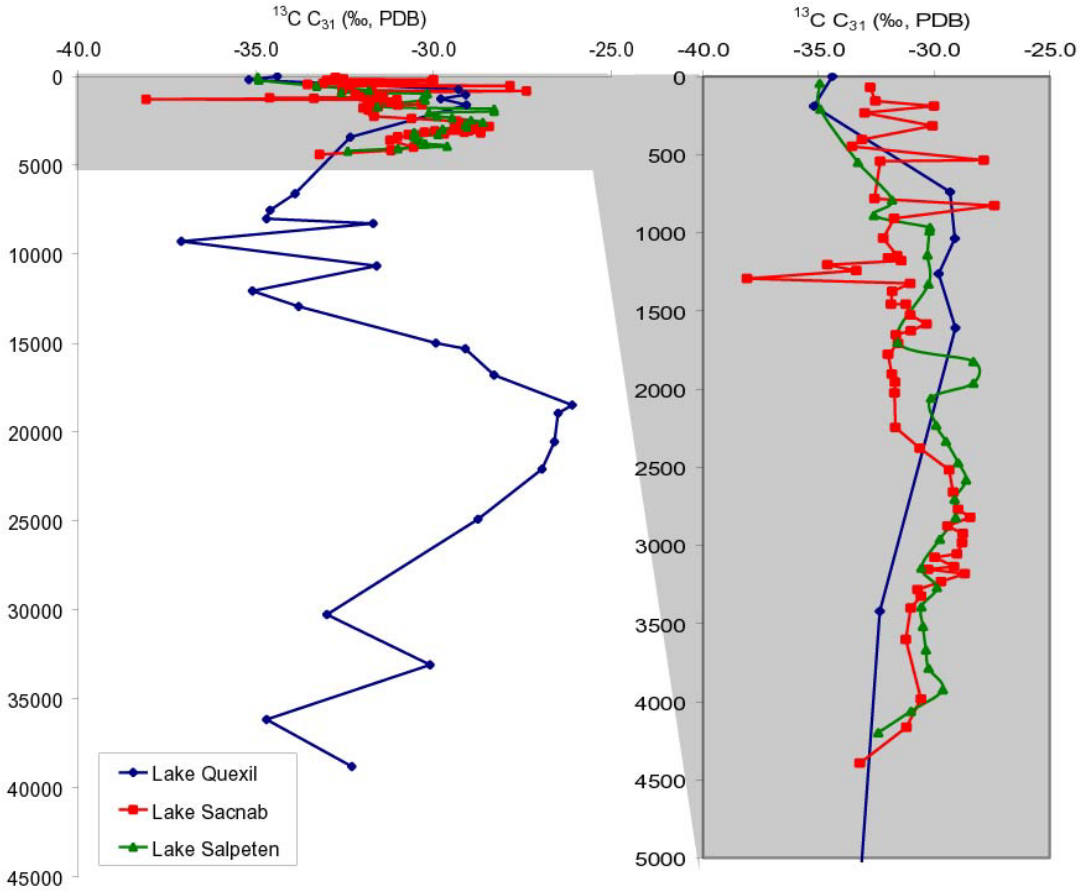

Figure 22: Diagram showing the comparison between $\delta^{13}C$ values of C_{31} from Lake Sacnab, Lake Salpeten and Lake Quexil (Huang et al., 2001).

In the records from Lake Salpetén and Sacnab, the $\delta^{13}C$ values of *n*-alkanes from 3300 cal yr BP to 2700 cal yr BP are comparable to values during the LGM in Lake Quexil, further supporting the interpretation of enhanced C_4 input. The data imply that vegetation during the period between 3300 cand 2700 cal yr BP may have been quite similar to the vegetation during the Last Glacial Maximum, when climate was significantly cooler. It is remarkable that vegetation may have changed as drastically during the period of human occupation as it did during a glacial-interglacial cycle.

Comparison with Pollen Records

Compound-specific carbon isotope records can be compared with pollen records from the same or nearby lakes to test if vegetation changes inferred from the $\delta^{13}C$ of long-chain *n*-alkanes are the same as those inferred from pollen profiles. A comparison of the % disturbance taxa from Lake Salpetén (Leyden, 1987) and the long-chain *n*-alkane $\delta^{13}C$ record from Lake Sacnab reveals significant differences in the two proxies (Figure 23). Disturbance taxa include grasses, sedges, and herbs from the following families: *Amaranthaceae* (C_3 and C_4), *Ambrosia* (C_3), *Compositae* (C_3 and C_4), *Cyperaceae* (C_3 and C_4) and *Gramineae* (C_3 and C_4). While these pollen data may provide an accurate representation of changes in the relative abundance of the selected taxa, they are not ideal for distinguishing changes in the relative contributions of C_3 versus C_4 plants because both plant types are represented by the disturbance taxa. Perhaps a better way to compare the compound-specific and disturbance taxa is to compare $\delta^{13}C$ to grasses only, which would be most representative of C_4 contribution.

A comparison of compound-specific carbon isotopes to % grasses reveals that while both records increase from the base of the record to 3300 cal yr BP, only the $\delta^{13}C$ of C_{33} peaks between 3300 and 2500 cal yr BP (Figure 24). The % grasses in the pollen record, however, is relatively low during this period (9%) and does not peak until ~2300 cal yr BP. Both the % grass and isotope records generally decline from 2300 cal yr BP to present. The pollen (% grasses) record is lower resolution than the isotope record; which may explain some of the discrepancy between the two vegetation proxies.

Perhaps the largest potential reason for the discrepancy may lie in the fact that maize pollen is not included in the total pollen count because of its large size, thus causing an over-representation of other taxa. Maize pollen has often been used in Mesoamerican studies as a proxy for agriculture and associated deforestation and it is well-documented that maize pollen is abundant during the period of Maya occupation (Leyden, 1987; Islebe et al., 1996). The $\delta^{13}C$ of *n*-alkanes, however, should be very sensitive to large stands of maize in the watershed.

There are additional potential shortcomings in using the $\delta^{13}C$ of *n*-alkanes as a proxy for vegetation change. For example, maize was probably an important (C_4) plant in the vegetation of the Petén Lake District, especially during times of high population density. Shoreline cultivation of maize would strongly influence the compound-specific $\delta^{13}C$ while not altering the pollen profile. The higher contribution of C_4 vegetation during the Preclassic (~3300 cal yr BP to 2500 cal yr BP) may represent early shoreline maize cultivation in the watershed. As populations increased into the Classic period, the more desirable shorelines may have become residential areas as opposed to agricultural areas, which would have then been moved further from the lake. Abandonment of near-shore

fields would alter the compound-specific $\delta^{13}C$ but would not be apparent in the pollen profile. Alternatively, maize cultivation on shorelines may have ceased in the Late Preclassic due to soil depletion. As the soils immediately surrounding the lake were exhausted, the ancient Maya may have moved agricultural fields further into the surrounding watershed.

While there are potential explanations for the discrepancy between pollen and compound-specific $\delta^{13}C$ values, it is necessary to fully understand that both records are recording different aspects of watershed vegetation. Vegetation inferences from pollen percentages represent the relative abundance of pollen grains in a sediment profile and do not necessarily reflect species abundance or biomass on the landscape (Bradley, 1999) whereas compound-specific carbon isotopes do not reveal any information about forest composition.

Pollen and leaf waxes are derived from different vegetative sources and thus record different aspects of watershed vegetation (Huang *et al.*, 1999). Whereas pollen is a measure of only reproduction, leaf waxes provide a more representative measure of vegetative biomass within a watershed. The exclusion of maize pollen provides yet another complication for interpreting pollen profiles. Compound-specific carbon isotopes, on the other hand, do not reveal any detailed information about forest composition. They simply allow estimation of the relative contribution of C_3 versus C_4 n-alkanes to the sedimented organic matter. When examined in conjunction with pollen accumulation rates, however, leaf waxes and pollen may provide a better estimate of vegetative biomass. The carbon isotopic composition of leaf waxes is a good

geochemical proxy for testing palynological inferences for vegetation changes within a watershed.

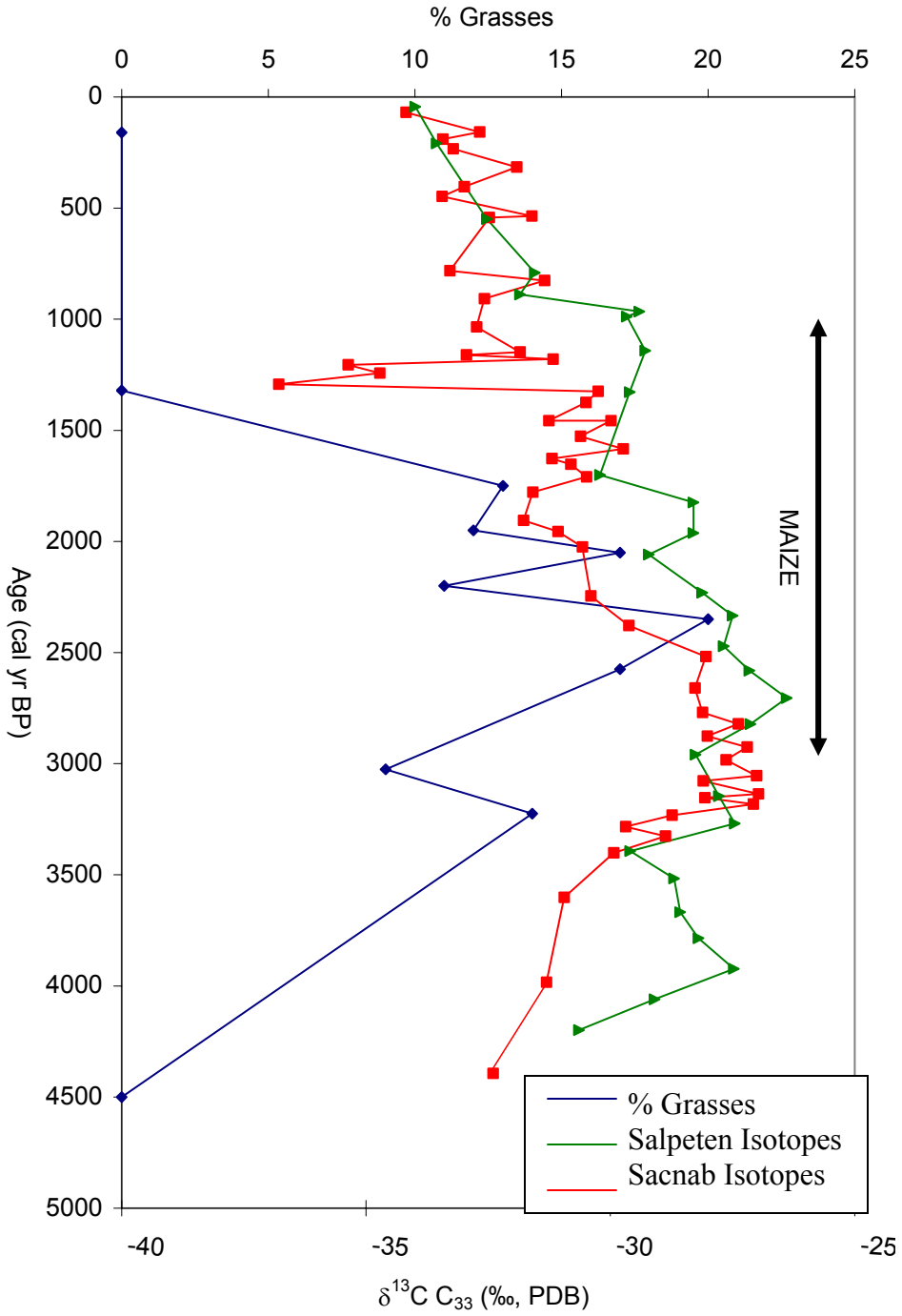

Figure 23: Diagram showing % grass pollen versus $\delta^{13}C$ of *n*-alkane C_{33} in Lakes Salpetén and Sacnab and the presence of maize pollen in Salpetén (pollen data from Leyden, 1987).

Comparison with Population Estimates

The correlation between Maya population densities and $\delta^{13}C$ values of long-chain *n*-alkanes in lake sediments suggests that while vegetation change over the past 4500 cal yr BP may have been tied to changes in population density, additional factors may have affected vegetation in the watershed in the early part of the record. Pollen records (Leyden, 1987; Islebe *et al*., 1996) reveal that disturbance taxa and maize increased as populations increased. Pollen changes were most likely tied to agricultural land clearance. Because grasses and maize are C_4 plants, one would predict an increase in the $\delta^{13}C$ of *n*-alkanes as populations grew. The largest shifts in vegetation, however, in both Lakes Sacnab and Salpetén, occurred well before the peak in late Classic Maya populations (Figure 24). The highest $\delta^{13}C$ values, indicating the largest contribution from C_4 vegetation, occurs in Lake Sacnab between 3300 cal yr BP and 2700 cal yr BP and in Lake Salpetén at 2700 cal yr BP, during the Preclassic Period. In both lakes there appears to be a decrease in C_4 biomass between 2700 cal yr BP and 1300 cal yr BP, the time period during which population density was greatest.

This decoupling of population density and the $\delta^{13}C$ of long-chain n-alkanes between 4500 cal yr BP and 1300 cal yr BP may be a result of several factors. For example, if agricultural practices changed through time from more extensive to intensive methods, a return to a C_3-dominated landscape may coincide with both population growth and agricultural developments. The question regarding whether the Maya maintained economic trees and house gardens within cities remains unanswered, but researchers have made speculations in some instances. For example, Leyden (1987) notes that the presence of *ramon* (*Bromsimum*) pollen suggests that the Maya were “arboriculturists”,

possibly growing tree gardens in typically residential and common areas. Selective clearing and/or tree planting, however, is not indicated by the rest of the pollen record. Instead, greater proportions of corn pollen during the Late Classic through Postclassic indicate intensified agricultural activities. The interpretations made from the pollen record (that ramon does not necessarily indicate arboriculture) are supported by the work of Lambert and Arnason (1982), who showed that ramon is attracted to constructions of limestone and is positively correlated with Maya sites; this would indicate not arboriculture, but instead settlement expansion.

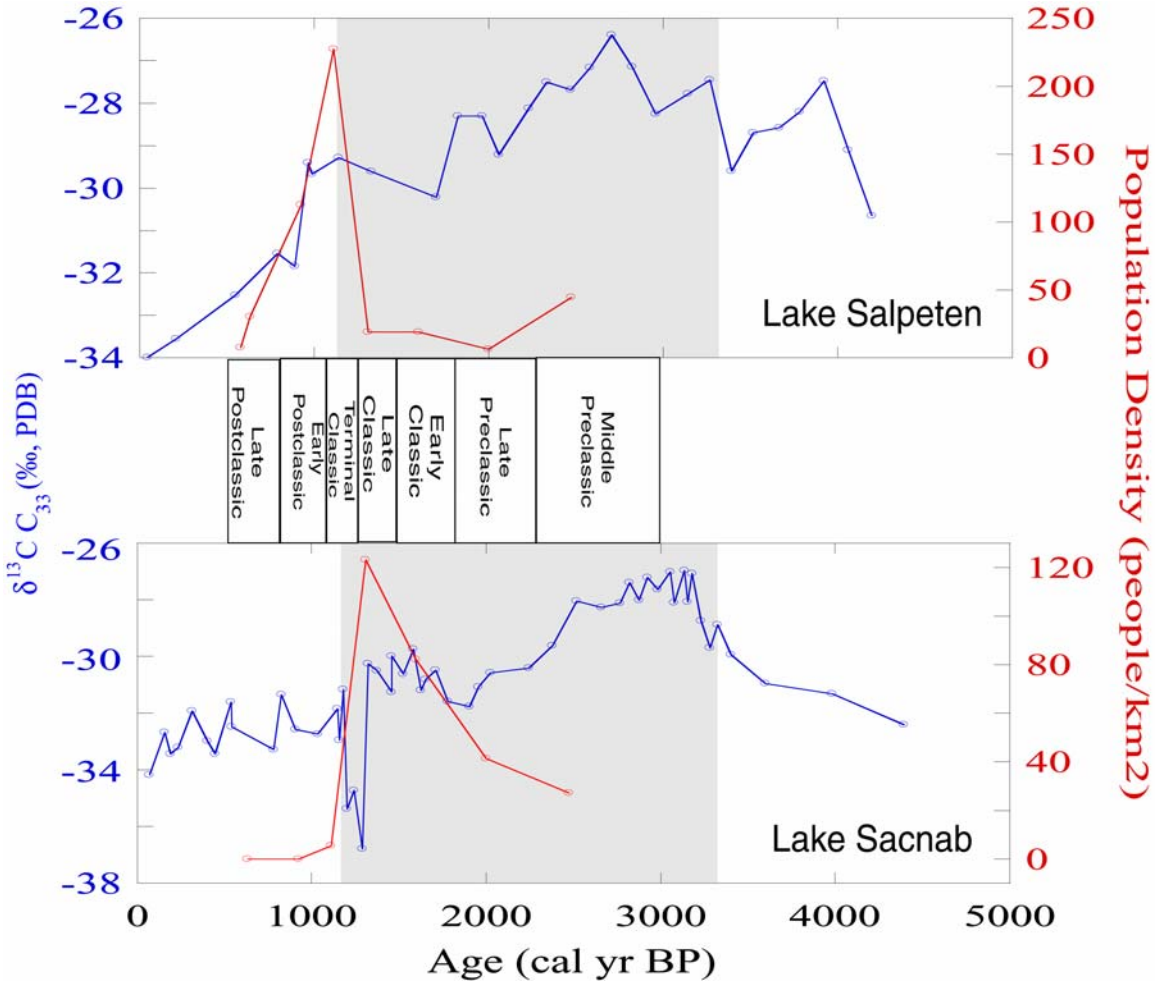

Figure 24: Comparison of the compound-specific carbon isotope records (C_{33}) and population density estimates versus time in Lakes Salpetén (top) and Sacnab (bottom).

It is also possible that, as discussed in the previous section, the higher contribution of C_4 vegetation during the Preclassic (~3300 cal yr BP to 2500 cal yr BP) may represent early shoreline maize cultivation in the watershed. As populations increased into the Classic period, the more desirable shorelines may have shifted to residential areas as opposed to agricultural areas, which would have then been relocated further from the lake. Abandonment of near-shore fields would be represented by a decoupling of the compound-specific $\delta^{13}C$ and population because the agricultural fields may have expanded away from the lake shore as populations expanded in the Classic Period.

Another possibility for the lack of coherence between population estimates and the compound-specific vegetation record may lie within the population estimates themselves. The population estimates in the Petén are based on a limited number of survey transects and house-mound excavations. There is a possibility that existing sites may not have been revealed during survey transects. In addition, older Preclassic population may have been underestimated if house mounds of the period were poorly preserved in the archaeological record. In addition, the chronology for population estimates was based on ceramic phases and inherently has a significant amount of error associated with it. While estimates of population densities in the watersheds may not be entirely accurate and may potentially be off by orders of magnitude the relative changes in population density are correct, and populations were certainly greater in the Classic than Preclassic Periods.

Despite the divergent trends in population density and proxy vegetation in the early part of the record, the records display similar trends between 1200 cal yr BP and the present. A decrease in the compound-specific carbon isotopic ratios begins at 1200 cal

yr BP and correlates with a significant decline in population associated with the decline of the Maya civilization. As human pressures on the landscape were curtailed and fields were abandoned, watershed vegetation shifted from a C_4 to a C_3-dominated landscape. This indicates that the decline in population density was likely the main cause of late Holocene vegetation change.

Relationship between Climate and Environmental Changes

Finally, the relative importance of humans versus climate for vegetation change in the Central Petén can be determined by comparing the $\delta^{13}C$ of *n*-alkanes with climate proxies that are not confounded by human impact. These comparisons may reveal whether climate played any role in environmental change. If vegetation changes in a watershed were climate-induced, long-chain *n*-alkanes should correlate with independent evidence for regional climate change. Proxy records of climate change are available for both the Yucatan and the Caribbean Sea and can be compared with compound-specific analyses and evaluated in regards to changes in Maya population densities.

A comparison with the %Ti record from the Cariaco basin (Haug *et al.*, 2001) (Figure 25) reveals a relationship between %Ti and the compound-specific records from each lake during the early part of the record. In the Cariaco Basin, %Ti in the sediments is used as a proxy for terrigenous sediment input, which is influenced by regional dry/wet cycles. Higher %Ti reflects higher terrigenous input and greater precipitation.

The %Ti record from 10,000 cal yr BP to 4000 cal yr BP is high and relatively unchanging, indicating relatively mesic conditions. At approximately 4000 cal yr BP, however, %Ti values decrease and show greater variability indicating generally reduced

precipitation, perhaps related to the southward migration of the Intertropical Convergence Zone (ITCZ). Increased variability in %Ti is especially pronounced from 4000 cal yr BP to 2000 cal yr BP. The apparent relationship of $\delta^{13}C$ of *n*-alkanes to climate suggests that vegetation may have been partly controlled by changes in regional climate rather than local cultural changes over some time period.

Increased climate variability during the period between 4000 cal yr BP and 2000 cal yr BP may have altered precipitation patterns and the vegetation in Peten. An extended dry period with sporadic periods of greater precipitation is an effective way to stress vegetation and to erode the landscape. Prior to 2000 cal yr BP, changes in regional climate may have influenced vegetation in addition to human disturbance.

Further evidence for climate-influenced vegetation change can be found in sediment records from numerous lakes in northern Yucatan. A sediment core from Lake Chichancanab provides evidence for regional drying that occurred beginning at approximately 3000 cal yr BP with a distinct interval of droughts between 1300 cal yr BP and 1100 cal yr BP, which coincided with the Terminal Classic collapse (Hodell *et al.*, 1995; Hodell *et al.,* in press). Compound-specific carbon isotopes (Figure 15) during the period between 3300 and 2700 cal yr BP in both Lakes Sacnab and Salpetén represent the highest proportion of C_4 versus C_3 vegetation, as would be expected during a period of increased climate variability. One would expect to see continued increased contribution of C_4 vegetation throughout the period of increased climate variability but this is not the case. This discrepancy may suggest that while climate influenced vegetation change beginning at 3000 cal yr BP, human land-use change exacerbated the deforestation process from 3000 cal yr BP until Maya populations decreased at 1100 cal yr BP.

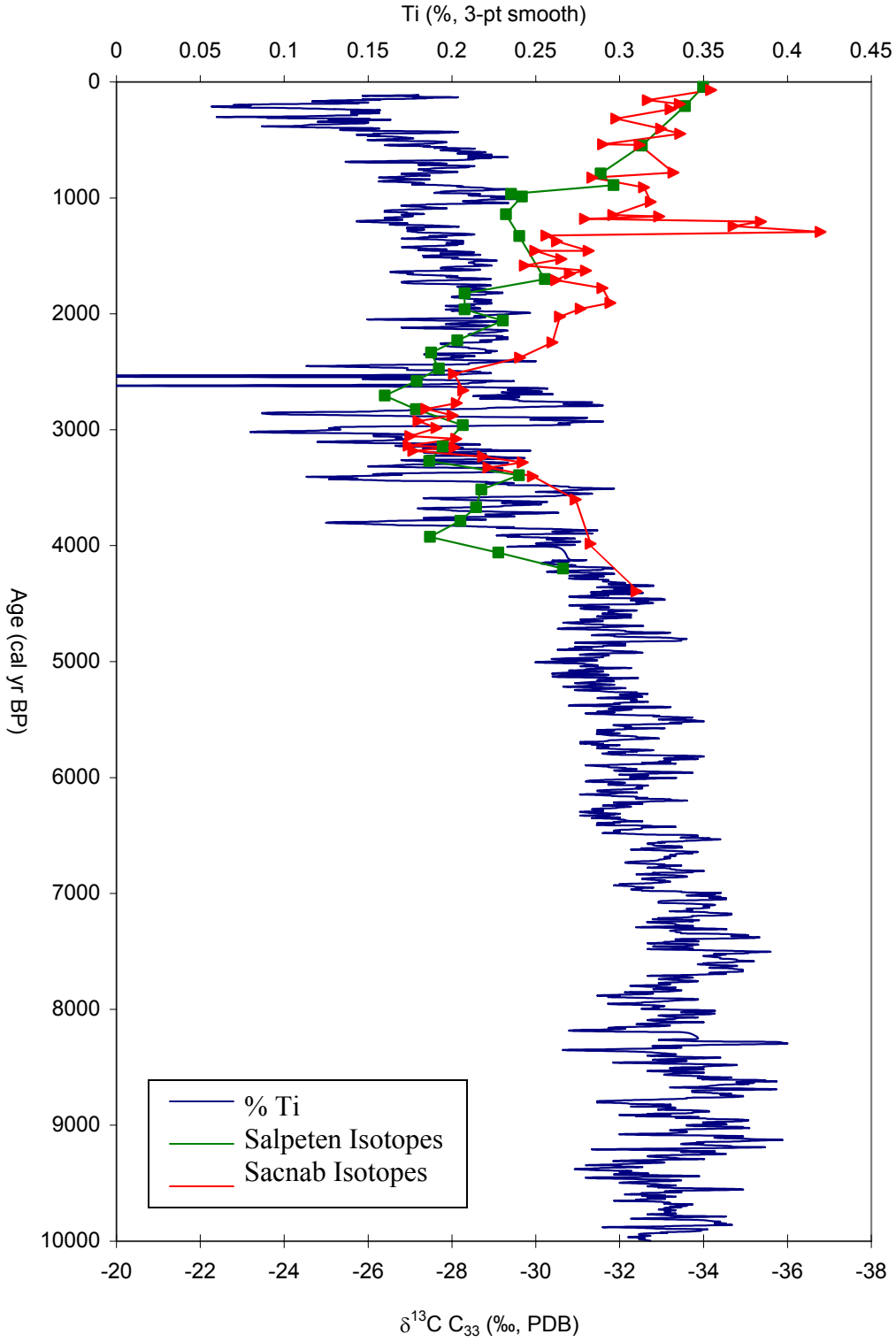

Figure 25: Comparison of the compound-specific carbon isotope records (C_{33}) and percent Ti versus time in Lakes Salpetén and Sacnab. Percent Ti data from Haug *et al.* (2001).

The $\delta^{18}O$ of ostracod carbonate in Lake Miragoane, Haiti (Hodell *et al.*, 1991) records a similar climate history to that for the Cariaco basin (Haug *et al.*, 2001). The isotope record, indicating changes in evaporation/precipitation and lake level, indicates a switch from dry forest vegetation to more mesic conditions at approximately 8200 cal yr BP. Beginning approximately 3800 cal yr BP, however, the isotopic value of shell carbonate begins to increase coincident with a loss of mesic forest trees and a regional drying event is suggested. These data correspond to local vegetation changes in the Sacnab and Salpetén basins; as climate became drier, vegetation shifted from a C_3 to a C_4-dominated landscape. This further supports the interpretation that (~4000 cal yr BP to 3000 cal yr BP), climate may have played some role in vegetation change.

Conclusions

The questions addressed in this study explore the dynamics of environmental change with respect to ancient Maya population shifts and late Holocene climate changes. While the analysis of compound-specific $\delta^{13}C$ values to study vegetation shifts is still in its infancy, this is the first late Holocene record for the Petén and the first to compare the $\delta^{13}C$ of *n*-alkanes with a local pollen record.

The data indicate that in the watersheds of Lakes Salpetén and Sacnab, shifts in the proportion of C_3 to C_4 are most likely controlled by a combination of climate change and human deforestation. The correspondence of $\delta^{13}C$ records to independent proxies for climate change from ~4500 cal yr BP until ~3000 cal yr BP suggest that regional drying and increased climate variability caused an increase in the contribution of C_4 vegetation

during that time. Following this period and beginning with the first Maya occupation in the watersheds, vegetation change was likely a result of human-driven deforestation or perhaps a combination of both climate and human impact.

The lack of concordance between the compound-specific carbon isotopic record and the pollen profiles between 3000 cal yr BP and 1100 cal yr BP may be due to the underlying ambiguities in comparing percent pollen data with compound-specific carbon isotopic measurements. The only true assessment of the C_4 pollen signal is to examine shifts in the absolute values of grass and maize pollen influx. The higher contribution of C_4 vegetation during the Preclassic inferred from compound-specific $\delta^{13}C$ (~3300 cal yr BP to 2500 cal yr BP) may represent early shoreline maize cultivation in the watershed. As populations increased into the Classic period and shorelines shifted to residential as opposed to agricultural areas, cultivated fields would have then been moved further into the surrounding watershed. This abandonment of fields and subsequent cessation of maize cultivation on the shoreline may strongly alter the compound-specific $\delta^{13}C$ but would not be apparent in the pollen profile.

Discrepancies between vegetation inferred from pollen profiles versus $\delta^{13}C$ of *n*-alkanes may also lie within the interpretation of the compound-specific $\delta^{13}C$ record itself. While $\delta^{13}C$ of *n*-alkanes is an excellent proxy for estimating the relative changes in biomass contribution of C_3 and C_4 vegetation, it cannot be used to interpret forest composition or the dynamics of tropical reforestation. In addition, there is no clear understanding of how issues such as differential leaf production and the amount of leaf wax a plant produces may affect the $\delta^{13}C$ of *n*-alkanes. Another potential problem in interpreting $\delta^{13}C$ values is that variation in canopy density that alters both light regimes

and the $\delta^{13}C$ of source CO_2 air for plants, which in turn affects the $\delta^{13}C$ of plant material. While an important factor, it is difficult to quantitatively assess the canopy effect on $\delta^{13}C$ values of *n*-alkanes. Lastly, the relationship between $\delta^{13}C$ and water-use efficiency (WUE) in C_3 plants may cause $\delta^{13}C$ values to appear more depleted and thus suggest a higher apparent contribution of C_3 vegetation. With these limitations in mind, it is necessary to interpret compound-specific carbon isotope records with caution.

While the decoupling of population density and the $\delta^{13}C$ of long-chain n-alkanes may suggest that agricultural practices changed through time from more extensive to intensive methods, it is impossible to determine this from the $\delta^{13}C$ from long-chain *n*-alkanes alone. The $\delta^{13}C$ from long-chain *n*-alkanes need not necessarily track population change if a shift in the proximity of agricultural lands (and proximity of maize pollen, which is large and does not travel far) to the lake was influencing the $\delta^{13}C$. The movement of fields and subsequent cessation of maize cultivation on the shoreline would strongly alter the compound-specific $\delta^{13}C$ but would not necessarily be reflected by changes in population densities.

The interpretation of compound-specific carbon isotopes of long-chain *n*-alkanes is dependent upon the area surrounding the lake over which the compounds integrate. There is unfortunately very little information regarding transport and deposition of *n*-alkanes in lacustrine studies. If compound-specific carbon isotopes of long-chain *n*-alkanes are more strongly influenced by vegetation on water-edge lands, than they may not provide an accurate picture of overall watershed vegetation and land-use. Studies that attempt to calibrate the compound-specific carbon isotopic value of modern sediments

with the surrounding forest structure may greatly aid in interpreting sediment records of paleoenvironmental change.

Compound-specific carbon isotopes and pollen profiles record represents different aspects of watershed vegetation , and are best used in tandem to infer past changes in watershed vegetation. While this study complements past studies that analyzed only bulk sediment or pollen and further supports the record of changes in terrestrial vegetation in the Petén region of the Maya Lowlands, further research is needed to understand the dynamic changes in forest structure associated with deforestation and reforestation. In addition, calculating grass and maize pollen accumulation rates from the same core as the $\delta^{13}C$ may provide a more robust assessment of the C_4 pollen signal. And lastly, it is important to utilize new archaeological information from surrounding watersheds to better understand how changes in land-use correlate to environmental change.

APPENDIX A
LIPID EXTRACTION PROCEDURE

Supplies:

- 33 mL stainless steel cell

- Glass filters
- Quartz sand
- 2:1 methylene chloride (DCM)/methanol
- Scintillation vials

Notes:

-All quartz sand should be ashed at 450˚C for at least two hours in a muffle furnace. ASE cells should be cleaned after each use by washing with DI water and solvent rinsing with methanol 3 times. Store ASE cells in oven, or with top and bottom screwed in place.

1) Screw base onto 33 ml Accelerated Solvent Extractor cell. Place two filters at the base and add ~5-10 mL of sand.
2) Weigh out and add approximately 10-20 μg of an internal standard (C_{34}) to each sample so as to allow calculation of yields and quantification of lipid compounds later in the process.
3) Weight out approximately 3-5 g of sample that has been frozen, freeze dried and crushed.
4) Record the weight and then add the sample to the cell.
5) Fill remaining space in the cell with sand and screw on the top.
6) Place cells in the Accelerated Solvent Extractor and use the following method to extract the phospholipids:

Solvent: 2:1 DCM/Methanol
Pressure: 1500 PSI
Temperature: 100 °C
Heat: 5 mins
Static: 5 mins
Flush: 60%
Purge: 200 sec
Cycles: 3

7) Solvent exchange to hexane using a hot water bath under a stream of nitrogen gas. This is performed by evaporating samples to dryness and then adding ~10 mL of hexane. To ensure full solvent exchange, repeat this process three times.
8) Transfer residue to a labeled 20 mL glass scintillation vial using ~15ml of hexane. For maximum compound retention, do this in multiple wash/transfer steps.
9) Evaporate sample in a hot water bath under a stream of nitrogen gas.
10) Samples (in scintillation vials) are now ready for silica gel chromatography.

APPENDIX B
SILICA GEL CHROMOTAGRAPHY

Supplies:

- Glass column
- Teflon stopcock
- Glass rod
- Glass funnels
- Glass wool
- GC Resolv or Optima grade Hexane
- GC Resolv or Optima grade methylene chloride (DCM)
- Teflon squirt bottle
- Small stainless steel spatula
- 5% deactivated silica gel
- Pasteur pipette with long pipette tips
- 20 mL beaker
- 2 graduates cylinders

Notes:

-All glassware, glass wool, and silica gel should be solvent rinsed and ashed at 450˚C for at least two hours in a muffle furnace.

1) To make 5% deactivated silica gel, use the following relation:
    a. (%deactivation/ (100-%deactivation)) = (mL water/weight of silica (g))
    b. (%deactivation/(100-%deactivation)) (weight of silica (g)) = mL of water
        - Add 1 mL of DI water to 20g of 100% activated silica gel
    c. Shake bottle for 10 minutes.
    d. Store in dessicator (good for only three days).
2) Assemble stopcock to the base of the column to regulate flow.
3) Set up column by placing glass wool at the base of a glass column and pushing it down with a glass rod until the column is clogged.
4) Set up column vertically in the hood with a clamp.
5) Add approximately one column full of hexane and allow the hexane to drain to clean the glass plug.
6) Weight out 2.5 grams of 5% deactivated silica gel in a 20-ml beaker. Cover with hexane quickly to keep if from absorbing any moisture from the air.

7) Place a glass funnel in the top of the column. Mix silica gel/hexane thoroughly with the spatula creating a suspension. Add the mixture to the column using the funnel and allow the silica to settle while tapping gently to avoid gas bubbles. Be sure to scrape all silica gel from the sides of the beaker into the funnel. Squirt the gel with hexane to force it through the funnel.
8) Remove the funnel and fill with hexane.
9) Drain excess hexane while tapping the column to guarantee full settling. Close the stopcock when the hexane level reaches just above the silica gel. Free any remaining silica gel adhering to the sides by tapping the column gently.
10) Rinse the column with ~10ml of hexane to wash remaining silica gel, again stopping when the solvent level reaches just above the silica-gel. Rinse the stopcock tip with hexane.
11) Place a collection vial labeled for n-alkanes under the column.
12) Fill a graduated cylinder with 16-17 mL of hexane. Use a pipette to bring the level to 15 mL, thus rinsing the pipette.
13) Add 1 mL of hexane from the graduated cylinder to the scintillation vial containing the sample. Rotate the sample vial between fingers while holding the vial at a 45˚ angle to dissolve the residue.
14) Transfer the sample in hexane to the column, gently dispensing sample ~1cm above silica gel.
15) Drain and collect the sample and solvent.
16) Repeat steps 13-15 twice more before adding the remaining hexane (~12 mL) in the graduated cylinder to the column.
17) Drain the sample and solvent to just above the level of the silica gel.
18) Remove the collection vial and a place second vial labeled for the "non-n-alkane organic fraction" under the column.
19) Using a graduated cylinder, measure 15 mL of DCM and add it to the column.
20) Drain the DCM into the collection vial, thus eluting all other lipid compounds.
21) Archive for potential later use.
22) Concentrate *n*-alkane fractions in collection vials by evaporating to dryness under a stream of N_2.
23) Re-dissolve *n*-alkanes in 200 µL of hexane.
24) Run samples on a Perkin Elmer 8500 Gas Chromatograph (PE 8500 GC) injecting 4 µL of sample in order to determine purity and approximate concentrations using the following oven program:

T ramp Rate ˚C/min	Hold Temp. ˚C	Hold Time (min)
	50	1
6	300	20

APPENDIX C
UREA ADDUCTION AND GC ANALYSIS

Supplies:

- GC Resolv or Optima grade hexane
- GC Resolv or Optima grade acetone
- GC Resolv or Optima grade pentane
- GC Resolv or Optima grade urea-saturated methanol
- DCM-extracted DI water
- GC Resolv or Optima grade methanol
- Pasteur pipette with long pipette tips
- 20 mL beaker
- 2 graduates cylinders
- gas-tight Teflon coated syringes

Notes:

-All glassware should be solvent rinsed and ashed at 450˚C for at least two hours in a muffle furnace. All of the following solvent transfers are performed using glass pipettes or Teflon-coated gas-tight syringes.

1) After running each alkane sample on the PE 8500 GC, transfer samples to a 4 mL glass screw top vial and evaporate to dryness under a stream of nitrogen.
2) Add 1 mL each of acetone, pentane, and urea-saturated methanol to each sample. Replace caps.
3) Place in a -4˚C freezer for ~30 minutes.
4) After 30 minutes, remove samples from freezer. Evaporate excess solvent under a stream of nitrogen. The urea crystals that remain contain the straight-chain n-alkanes only, while the non-adducts, branched and cyclic compounds, remain outside of the crystals.
5) Wash urea crystals with hexane three times, with the wash hexane being pipetted into a separate 4 mL vial labeled as “non-adducts” to be archived for potential later use.
6) Dissolve the remaining urea crystals in 1 mL of methanol and 1 mL of DCM-extracted DI water. This fraction contains the straight-chain n-alkanes.
7) Add approximately 2 mL of hexane to this fraction. Shake vigorously using a Vortex vibrator to extract hydrocarbons.
8) Centrifuge vials at 500 rpm for 5 minutes or until hexane and urea/methanol/water separate.

9) Remove the hexane from the top with a gas-tight syringe and place into a separate 4 mL vial labeled as "adducts". Repeat the hydrocarbon extraction (Steps 7-8) twice more to guarantee full recovery of *n*-alkanes.
10) Evaporate excess solvent from the adduct fraction under a stream of nitrogen.
11) Repeat steps 2-10 twice more on the adduct fraction.
12) After triple adduction, evaporate the adduct fraction to dryness under a stream of nitrogen and re-dissolve in 200 µL of hexane.
13) Run samples on a Perkin Elmer 8500 GC using the following oven program and injecting 4 µL of sample:

Rate ˚C/min	Temperature ˚C	Time (min)
	50	1
6	300	20

14) Evaporate the sample to dryness again under a stream of nitrogen and transfer to a 1 mL glass crimp-top autosampler vial using multiple washes to ensure full transfer of *n*-alkanes.
15) Evaporate the sample to dryness under a stream of nitrogen. Dissolve in a known amount of hexane according to obtain the approximate concentration necessary for GC-IRMS analysis (ex.: samples that had a voltage of ~20-30 mV on the PE 8500 GC should be dissolved in 100 µL of hexane whereas samples with a voltage of ~10 should be dissolved in 25 µL of hexane).
16) The adduct fraction containing straight-chain n-alkanes is now ready for GC-Isotope Ratio Mass Spectrometry (IRMS) analysis.

APPENDIX D
DATA TABLES

Table 6: Values for %N, %C, C:N, %TIC, %$CaCO_3$, %TOC, %Organic matter and %Other from Sacnab.Lake

Sample ID	Nominal Depth (cm)	Composite Depth (cm)	Age (cal yr BP)	%N	%C	C:N	%TIC, Corrected	%CaCO3	% TOC	% Organic Matter	% OTHER
sn mwi 1.5	1.5	1.5	17.7945	2.46	22.50	9.14	0.20	1.62	22.31	55.77	42.60
sn MWI 6.5	6.5	6.5	77.1095	2.49	22.22	8.94	0.18	1.46	22.04	55.10	43.44
sn MWI 11.5	11.5	11.5	136.4245	2.43	22.21	9.13	0.12	0.96	22.09	55.23	43.81
sn MWI 16.5	16.5	16.5	195.7395	2.09	19.97	9.57	0.15	1.21	19.83	49.57	49.22
sn MWI 21.5	21.5	21.5	255.0545	1.93	20.12	10.45	0.28	2.29	19.85	49.61	48.10
sn MWI 26.5	26.5	26.5	314.3695	1.58	17.68	11.18	0.10	0.81	17.58	43.96	55.23
sn MWI 31.5	31.5	31.5	373.6845	1.15	13.88	12.09	0.30	2.46	13.58	33.96	63.59
sn MWI 36.5	36.5	36.5	432.9995	1.19	14.66	12.33	0.47	3.87	14.19	35.48	60.64
sn MWI 41.5	41.5	41.5	492.3145	1.28	15.36	11.98	0.30	2.46	15.07	37.66	59.88
sn MWI 46.5	46.5	46.5	551.6295	1.18	13.97	11.86	0.09	0.79	13.87	34.68	64.53
sn MWI 51.5	51.5	51.5	610.9445	1.09	13.91	12.73	0.16	1.29	13.75	34.38	64.32
sn MWI 56.5	56.5	56.5	670.2595	0.91	11.70	12.84	0.45	3.71	11.25	28.13	68.16
sn MWI 61.5	61.5	61.5	729.5745	0.84	10.15	12.07	0.47	3.87	9.68	24.21	71.92
sn MWI 66.5	66.5	66.5	788.8895	0.76	10.03	13.12	0.86	7.12	9.18	22.94	69.93
sn MWI 71.5	71.5	71.5	848.2045	0.98	12.03	12.33	0.42	3.46	11.61	29.03	67.51
sn MWI 76.5	76.5	76.5	907.5195	0.96	12.50	13.02	0.56	4.62	11.95	29.87	65.50
sn MWI 81.5	81.5	81.5	966.8345	0.92	12.52	13.60	0.76	6.29	11.76	29.40	64.31
sn MWI 86.5	86.5	86.5	1026.1495	0.85	11.23	13.25	0.70	5.79	10.54	26.34	67.87
sn MWI 91.5	91.5	91.5	1085.4645	0.66	8.41	12.80	0.47	3.87	7.94	19.85	76.27
sn MWI 96.5	96.5	96.5	1144.7795	0.55	7.01	12.64	0.63	5.21	6.38	15.95	78.84
sn MWI 104.5	104.5	104.5	1239.6835	0.14	2.39	17.48	1.48	12.29	0.91	2.28	85.43
sn MWI 109.5	109.5	109.5	1298.9985	0.13	2.74	21.39	1.87	15.54	0.87	2.18	82.27
sn MWI 114.5	114.5	114.5	1358.3135	0.17	2.85	17.18	2.11	17.54	0.74	1.86	80.60
sn MWI 119.5	119.5	119.5	1417.6285	0.12	3.36	27.85	2.64	22.00	0.72	1.80	76.20
sn lex1 149.5	149.5	124	1471.012	0.14	3.90	27.87	2.62	21.83	1.28	3.21	74.95
sn lex1 154.5	154.5	129	1530.327	0.17	3.34	20.13	2.42	20.17	0.92	2.30	77.53
sn lex1 159.5	159.5	134	1589.642	0.15	4.64	31.85	3.97	33.08	0.67	1.67	65.24

Table 6: Continued.

Sample ID	Nominal Depth (cm)	Composite Depth (cm)	Age (cal yr BP)	%N	%C	C:N	%TIC, Corrected	%CaCO3	% TOC	% Organic Matter	% OTHER
sn lex1 164.5	164.5	139	1648.957	0.12	4.69	38.71	3.95	32.92	0.74	1.86	65.23
sn lex1 169.5	169.5	144	1708.272	0.13	4.35	33.89	3.80	31.67	0.55	1.39	66.95
sn lex1 174.5	174.5	149	1767.587	0.13	4.50	34.63	4.10	34.17	0.40	1.00	64.83
sn lex1 179.5	179.5	154	1826.902	0.10	4.75	45.46	4.40	36.67	0.35	0.87	62.46
sn lex1 184.5	184.5	159	1886.217	0.11	5.04	47.13	4.66	38.83	0.38	0.95	60.22
sn lex1 199.5	199.5	174	2064.162	0.12	5.17	42.81	4.49	37.42	0.68	1.70	60.88
sn lex2 204.5	204.5	179	2123.477	0.15	4.20	27.89	3.59	29.92	0.61	1.53	68.56
sn lex2 209.5	209.5	184	2182.792	0.14	4.79	34.92	3.97	33.08	0.82	2.05	64.86
sn lex2 214.5	214.5	189	2242.107	0.14	5.04	35.08	4.51	37.58	0.53	1.33	61.09
sn lex2 219.5	219.5	194	2301.422	0.14	6.21	45.18	5.28	44.00	0.93	2.32	53.68
sn lex2 224.5	224.5	199	2426.7379	0.17	4.75	27.93	3.66	30.52	1.09	2.71	66.76
sn lex2 229.5	229.5	204	2450.1484	0.13	4.78	37.36	4.02	33.52	0.76	1.89	64.58
sn lex2 234.5	234.5	209	2473.5589	0.15	4.52	31.02	3.86	32.19	0.66	1.64	66.17
sn lex2 239.5	239.5	214	2496.9694	0.16	5.48	34.18	4.68	39.02	0.80	1.99	58.98
sn lex2 244.5	244.5	219	2520.3799	0.15	5.24	34.19	4.16	34.69	1.07	2.68	62.63
sn lex2 249.5	249.5	224	2543.7904	0.16	4.46	27.82	3.46	28.86	1.00	2.50	68.64
sn lex2 254.5	254.5	229	2567.2009	0.10	1.94	19.40	2.99	24.94	0.00	0.00	75.06
sn lex2 259.5	259.5	234	2590.6114	0.19	3.04	15.77	2.15	17.94	0.88	2.21	79.85
sn lex2 264.5	264.5	239	2614.0219	0.13	1.98	14.67	1.75	14.61	0.23	0.56	84.83
sn lex2 269.5	269.5	244	2637.4324	0.12	2.42	20.84	2.04	17.02	0.38	0.95	82.02
sn lex2 274.5	274.5	249	2660.8429	0.15	4.64	30.29	3.79	31.61	0.85	2.12	66.27
sn lex2 279.5	279.5	254	2684.2534	0.14	2.50	17.44	2.23	18.57	0.27	0.67	80.76
sn lex2 284.5	284.5	259	2707.6639	0.13	2.20	17.37	2.32	19.32	0.00	0.00	80.68
sn lex3 294.5	294.5	269	2754.4849	0.11	2.21	20.39	1.86	15.48	0.35	0.88	83.64
sn lex3 304.5	304.5	279	2801.3059	0.18	2.56	13.97	1.90	15.82	0.66	1.65	82.54
sn lex3 309.5	309.5	284	2824.7164	0.24	2.16	8.93	1.45	12.07	0.71	1.77	86.16
sn lex3 314.5	314.5	289	2848.1269	0.19	2.41	12.53	1.60	13.32	0.82	2.04	84.64
sn lex3 319.5	319.5	294	2871.5374	0.21	2.26	10.98	1.38	11.48	0.88	2.21	86.31

Table 6: Continued.

Sample ID	Nominal Depth (cm)	Composite Depth (cm)	Age (cal yr BP)	%N	%C	C:N	%TIC, Corrected	%CaCO3	% TOC	% Organic Matter	% OTHER
sn lex3 324.5	324.5	299	2894.9479	0.17	1.34	8.01	0.69	5.73	0.65	1.63	92.63
sn lex3 329.5	329.5	304	2918.3584	0.19	1.43	7.69	0.48	3.98	0.95	2.38	93.64
sn lex3 334.5	334.5	309	2941.7689	0.18	2.54	14.30	2.01	16.73	0.53	1.32	81.95
sn lex3 339.5	339.5	314	2965.1794	0.18	2.17	12.28	1.41	11.73	0.76	1.89	86.37
sn lex3 344.5	344.5	319	2988.5899	0.15	1.85	12.12	0.17	1.39	1.69	4.22	94.39
sn lex3 349.5	349.5	324	3012.0004	0.12	1.61	13.87	1.36	11.32	0.25	0.62	88.06
sn lex3 354.5	354.5	329	3035.4109	0.21	2.66	12.96	1.33	11.07	1.33	3.33	85.60
sn lex3 359.5	359.5	334	3058.8214	0.15	3.22	21.21	2.49	20.73	0.73	1.83	77.43
sn lex3 364.5	364.5	339	3082.2319	0.20	2.32	11.79	0.81	6.73	1.51	3.78	89.48
sn lex3 370.5	370.5	345	3110.3245	0.24	2.27	9.36	0.58	4.82	1.69	4.22	90.97
sn lex3 374.5	374.5	349	3129.0529	0.33	3.44	10.28	1.04	8.65	2.40	6.00	85.35
sn lex3 379.5	379.5	354	3152.4634	0.31	3.24	10.44	0.73	6.07	2.51	6.29	87.65
sn lex4 391.5	391.5	366	3208.6486	0.26	2.47	9.62	0.09	0.73	2.38	5.96	93.31
sn lex4 396.5	396.5	371	3267.193	0.25	2.38	9.47	0.23	1.90	2.15	5.37	92.73
sn lex4 401.5	401.5	376	3355.608	0.25	2.08	8.20	0.12	0.98	1.96	4.90	94.12
sn lex4 406.5	406.5	381	3444.023	0.54	7.58	14.07	0.64	5.36	6.94	17.34	77.30
sn lex4 411.5	411.5	386	3532.438	0.70	9.65	13.75	0.89	7.44	8.76	21.90	70.66
sn lex4 416.5	416.5	391	3620.853	0.54	8.01	14.70	1.05	8.77	6.96	17.39	73.84
sn lex4 421.5	421.5	396	3709.268	0.73	10.64	14.50	0.59	4.94	10.05	25.13	69.93
sn lex4 426.5	426.5	401	3797.683	0.65	9.24	14.21	0.65	5.44	8.59	21.47	73.09
sn lex4 431.5	431.5	406	3886.098	0.98	14.19	14.51	0.29	2.44	13.90	34.75	62.81
sn lex4 436.5	436.5	411	3974.513	0.57	8.64	15.07	0.77	6.44	7.87	19.67	73.89
sn lex4 441.5	441.5	416	4062.928	0.57	9.99	17.43	1.58	13.19	8.41	21.03	65.78
sn lex4 447.5	447.5	422	4169.026	0.41	9.69	23.91	4.08	34.02	5.60	14.01	51.97
sn lex4 451.5	451.5	426	4239.758	0.46	9.39	20.35	2.88	24.02	6.50	16.26	59.72
sn lex4 456.5	456.5	431	4328.173	1.24	17.23	13.88	0.35	2.94	16.88	42.20	54.86
sn lex4 466.5	466.5	441	4505.003	0.69	16.42	23.66	5.54	46.19	10.88	27.19	26.62

Table 7: Values for bulk organic matter isotopes from Lake Sacnab.

Core section	Nominal Depth (cm)	Composite Depth (cm)	Age (cal yr BP)	$\delta^{15}N$ corrected	$\delta^{13}C$
SN-19-VII-97-MWI	0	0	0	-0.07	-25.14
SN-19-VII-97-MWI	10	10	119	-0.24	-24.97
SN-19-VII-97-MWI	20	20	237	-0.29	-24.74
SN-19-VII-97-MWI	30	30	356	0.76	-25.48
SN-19-VII-97-MWI	40	40	475	1.16	-25.75
SN-19-VII-97-MWI	50	50	593	0.61	-24.99
SN-19-VII-97-MWI	60	60	712	1.46	-25.60
SN-19-VII-97-MWI	70	70	830	0.35	-25.67
SN-19-VII-97-MWI	80	80	949	0.61	-26.76
SN-19-VII-97-MWI	90	90	1068	0.78	-26.18
SN-19-VII-97-MWI	100	100	1186	-0.36	-27.07
SN-19-VII-97-MWI	110	110	1305	3.63	-24.45
SN-19-VII-97-MWI	120	120	1424	4.44	-24.54
SN-19-VII-97-MWI	130	130	1542	3.31	-24.43
SN-19-VII-97-MWI	140	140	1661	3.09	-23.69
SN-19-VII-97-LEX-1	172	146.5	1738	3.02	-23.85
SN-19-VII-97-LEX-1	182	156.5	1857	3.27	-23.67
SN-19-VII-97-LEX-2	200	174.5	2070	3.24	-24.16
SN-19-VII-97-LEX-2	210	184.5	2189	3.36	-24.04
SN-19-VII-97-LEX-2	220	194.5	2307	3.22	-23.87
SN-19-VII-97-LEX-2	230	204.5	2452	3.93	-22.89
SN-19-VII-97-LEX-2	240	214.5	2499	3.81	-23.16
SN-19-VII-97-LEX-2	250	224.5	2546	3.16	-22.12
SN-19-VII-97-LEX-2	260	234.5	2593	3.28	-22.32
SN-19-VII-97-LEX-2	270	244.5	2640	3.65	-22.91
SN-19-VII-97-LEX-2	280	254.5	2687	3.42	-21.68
SN-19-VII-97-LEX-3	297	271.5	2766	2.91	-22.12
SN-19-VII-97-LEX-3	307	281.5	2813	2.39	-20.52
SN-19-VII-97-LEX-3	317	291.5	2860	3.27	-21.61
SN-19-VII-97-LEX-3	327	301.5	2907	2.64	-21.45
SN-19-VII-97-LEX-3	337	311.5	2953	4.57	-21.74
SN-19-VII-97-LEX-3	347	321.5	3000	3.57	-21.75
SN-19-VII-97-LEX-3	357	331.5	3047	3.87	-22.05
SN-19-VII-97-LEX-3	367	341.5	3094	3.66	-21.96
SN-19-VII-97-LEX-3	377	351.5	3141	2.77	-23.72
SN-19-VII-97-LEX-4	394	368.5	3220	3.27	-22.03
SN-19-VII-97-LEX-4	404	378.5	3400	3.59	-22.04
SN-19-VII-97-LEX-4	414	388.5	3577	1.13	-23.04
SN-19-VII-97-LEX-4	424	398.5	3753	0.82	-23.36
SN-19-VII-97-LEX-4	434	408.5	3930	1.59	-21.98
SN-19-VII-97-LEX-4	444	418.5	4107	3.80	-26.95
SN-19-VII-97-LEX-4	454	428.5	4284	1.57	-22.38
SN-19-VII-97-LEX-4	464	438.5	4461	2.35	-26.72

.Table 8: Values for compound-specific carbon isotopes from Lake Sacnab.

Sample ID	Core	Nominal Depth (cm)	Composite Depth (cm)	Age (cal yr BP)	δ^{13}C C21	δ^{13}C C23	δ^{13}C C25	δ^{13}C C27	δ^{13}C C29	δ^{13}C C31	δ^{13}C C33	δ^{13}C C34
1139	SN-19-VII-97 MWI	5.5	5.5	69.388	-25.66	-21.51	-21.07	-24.44	-30.42	-32.76	-34.18	-30.59
1140	SN-19-VII-97 MWI	12.5	12.5	157.7	-27.36	-22.61	-22.49	-25.71	-30.64	-32.53	-32.67	-30.13
1012	SN-19-VII-97 MWI	15	15	189.24					-25.66	-30.00	-33.43	
1141	SN-19-VII-97 MWI	18.5	18.5	233.396	-27.48	-22.22	-22.11	-25.46	-30.84	-33.01	-33.22	-30.29
	SN-19-VII-97 MWI	25	25	315.4					-26.53	-30.06	-31.92	-30.93
1121	SN-19-VII-97 MWI	32	32	403.712			-25.26	-27.19	-31.07	-33.11	-32.99	-29.60
1142	SN-19-VII-97 MWI	35.5	35.5	447.868	-29.17	-24.88	-25.07	-27.21	-31.49	-33.55	-33.44	-30.10
1018	SN-19-VII-97 MWI	42.5	42.5	536.18					-24.98	-27.85	-31.61	-30.46
1122	SN-19-VII-97 MWI	43	43	542.488		-22.97	-23.98	-26.07	-30.15	-32.33	-32.48	-29.71
1123	SN-19-VII-97 MWI	62	62	782.192	-28.66	-25.49	-24.83	-26.99	-30.37	-32.58	-33.29	-30.33
1019	SN-19-VII-97 MWI	65.5	65.5	826.348					-22.68	-27.39	-31.35	-30.11
1124	SN-19-VII-97 MWI	72	72	908.352	-29.51	-25.69	-25.35	-27.11	-29.53	-31.73	-32.58	-29.91
1125	SN-19-VII-97 MWI	82	82	1034.512	-29.94	-26.05	-25.50	-27.21	-30.32	-32.20	-32.74	-29.70
1091	SN-19-VII-97 LEX 1	116.5	91	1148.056					-31.03	-31.60	-31.85	-30.43
1126	SN-19-VII-97 MWI	92	92	1160.672		-24.18	-23.61	-26.27	-29.50	-31.98	-32.95	-30.04
1116	SN-19-VII-97 LEX 1	119	93.5	1179.596					-31.34	-31.41	-31.17	-29.88
1080	SN-19-VII-97 MWI	95.5	95.5	1204.828					-33.64	-34.62	-35.37	-30.00
1115	SN-19-VII-97 MWI	98.5	98.5	1242.676		-26.54	-26.71	-29.06	-31.58	-33.36	-34.72	-29.88
1013	SN-19-VII-97 MWI	102.5	102.5	1293.14					-33.83	-38.09	-36.79	
1117	SN-19-VII-97 LEX 1	130.5	105	1324.68					-30.69	-31.03	-30.25	-29.75
1085	SN-19-VII-97 LEX 1	134.5	109	1375.144					-31.57	-31.81	-30.50	-29.68
1081	SN-19-VII-97 MWI	115.5	115.5	1457.148					-31.44	-31.86	-31.26	-30.10
1118	SN-19-VII-97 LEX 1	141	115.5	1457.148					-30.79	-31.22	-29.99	-31.04
1094	SN-19-VII-97 LEX 1	146.5	121	1526.536					-30.94	-31.03	-30.61	-30.26
1119	SN-19-VII-97 LEX 1	151	125.5	1583.308			-27.15	-27.59	-30.70	-30.32	-29.74	-29.70
1021	SN-19-VII-97 LEX 1	154.5	129	1627.464					-26.24	-31.00	-31.20	-29.84
1086	SN-19-VII-97 LEX 1	156.5	131	1652.696					-30.85	-31.65	-30.81	-30.23

.Table 8: Continued.

Sample ID	Core	Nominal Depth (cm)	Composite Depth (cm)	Age (cal yr BP)	δ^{13}C C21	δ^{13}C C23	δ^{13}C C25	δ^{13}C C27	δ^{13}C C29	δ^{13}C C31	δ^{13}C C33	δ^{13}C C34
1120	SN-19-VII-97 LEX 1	161	135.5	1709.468					-31.49	-31.56	-30.49	-29.95
1095	SN-19-VII-97 LEX 1	166.5	141	1778.856					-31.47	-31.98	-31.59	-30.29
1082	SN-19-VII-97 LEX 1	176.5	151	1905.016					-29.06	-31.83	-31.78	-31.06
1096	SN-19-VII-97 LEX 1	180.5	155	1955.48					-31.53	-31.69	-31.07	-30.13
1143	SN-19-VII-97 LEX 1	186	160.5	2024.868					-32.34	-31.71	-30.57	-30.30
1087	SN-19-VII-97 LEX 2	203.5	178	2245.648					-31.16	-31.68	-30.40	-30.17
1144	SN-19-VII-97 LEX 2	214	188.5	2378.116		-27.65	-28.95	-28.63	-30.86	-30.62	-29.62	-30.04
1088	SN-19-VII-97 LEX 2	224.5	199	2517.753					-30.07	-29.35	-28.05	-30.03
1097	SN-19-VII-97 LEX 2	252.5	227	2660.181					-28.24	-29.18	-28.27	-30.33
1145	SN-19-VII-97 LEX 2	274	248.5	2769.545				-27.33	-29.35	-28.96	-28.12	-30.08
1146	SN-19-VII-97 LEX 2	284	258.5	2820.412			-26.52	-26.52	-29.23	-28.43	-27.39	-30.12
1147	SN-19-VII-97 LEX 3	295	269.5	2876.366					-29.81	-29.42	-28.02	-29.77
1089	SN-19-VII-97 LEX 3	304.5	279	2924.689				-26.92	-29.57	-28.75	-27.21	-29.97
1148	SN-19-VII-97 LEX 3	316	290.5	2983.186		-25.54	-26.90	-26.55	-29.07	-28.79	-27.63	-30.05
1149	SN-19-VII-97 LEX 3	330	304.5	3054.4			-28.34	-27.60	-29.88	-29.00	-27.01	-30.27
1090	SN-19-VII-97 LEX 3	334.5	309	3077.29					-30.06	-29.97	-28.10	-29.81
1150	SN-19-VII-97 LEX 3	346	320.5	3135.787					-30.10	-29.13	-26.97	-29.54
1098	SN-19-VII-97 LEX 3	349.5	324	3153.591					-29.50	-30.26	-28.07	-30.71
1151	SN-19-VII-97 LEX 3	355	329.5	3181.568		-25.41	-25.36	-26.26	-28.29	-28.67	-27.08	-29.85
1152	SN-19-VII-97 LEX 3	365	339.5	3232.435		0.00	-24.48	-25.85	-29.43	-29.70	-28.74	-29.90
1153	SN-19-VII-97 LEX 3	375	349.5	3283.302		-27.21	-25.66	-25.81	-29.60	-30.71	-29.69	-30.13
1154	SN-19-VII-97 LEX 4	392.5	367	3325.489		-27.47	-26.86	-27.01	-30.27	-30.56	-28.87	-30.27
1084	SN-19-VII-97 LEX 4	396.5	371	3401.757					-29.71	-31.01	-29.93	-30.26
1155	SN-19-VII-97 LEX 4	407	381.5	3601.961		-25.81	-24.42	-24.70	-29.08	-31.22	-30.95	-30.05
1156	SN-19-VII-97 LEX 4	427	401.5	3983.301		-24.27	-21.80	-23.15	-27.66	-30.56	-31.31	-29.98
1101	SN-19-VII-97 LEX 4	436.5	411	4164.437					-28.11	-31.20		-30.90
1102	SN-19-VII-97 LEX 4	448.5	423	4393.241					-31.64	-33.21	-32.40	-30.74

. Table 9: Values for compound-specific carbon isotopes from Lake Salpeten.

Sample ID	Core	Nominal Depth (cm)	Composite Depth (cm)	Age (cal yr BP)	δ^{13}C C21	δ^{13}C C23	δ^{13}C C25	δ^{13}C C27	δ^{13}C C29	δ^{13}C C31	δ^{13}C C33	δ^{13}C C34
1181	SP-12-VI-01	4	4	44					-32.59	-34.95	-33.99	-29.71
1182	SP-12-VI-02	19	19	209					-32.12	-34.92	-33.56	-29.59
1183	SP-12-VI-02	50	50	549					-30.63	-33.29	-32.52	-29.58
1184	SP-12-VI-02	72	72	790					-29.33	-31.82	-31.54	-29.57
1185	SP-12-VI-02	81	81	889				-29.33	-30.72	-32.60	-31.85	-29.63
1186	SP-12-VI-02	88	88	966				-29.22	-30.23	-30.17	-29.41	-29.97
1157	SP-12-VI-02	83	90	988			-28.30	-30.21	-30.32	-30.20	-29.66	-29.69
1160	SP-12-VI-02	97	104	1142			-31.27	-31.10	-30.86	-30.29	-29.29	-30.22
1158	SP-12-VI-02	114	121	1328			-29.02	-28.16	-30.46	-30.24	-29.60	-29.85
1159	SP-12-VI-02	153	160	1701					-32.38	-31.58	-30.21	-30.01
1161	SP-12-VI-02	171	178	1824		-28.10	-30.36	-30.21	-28.30	-28.30	-28.30	-28.30
1162	SP-12-VI-02	191	198	1962		-28.10	-30.36	-30.21	-28.30	-28.30	-28.30	-28.30
1163	SP-12-VI-02	205	212	2058					-31.42	-30.13	-29.21	-30.40
1164	SP-12-VI-02	230	237	2230					-31.34	-29.91	-28.12	-30.14
1165	SP-12-VI-02	245	252	2334					-31.07	-29.49	-27.50	-29.81
1166	SP-12-VI-02	265	272	2471				-28.44	-29.82	-28.95	-27.68	-30.00
1167	SP-12-VI-02	281	288	2581					-29.60	-28.61	-27.15	-29.71
1168	SP-12-VI-02	299	306	2705				-29.10	-30.26	-29.10	-26.39	-29.64
1169	SP-12-VI-02	316	323	2822				-27.95	-30.65	-29.06	-27.14	-29.87
1170	SP-12-VI-02	336	343	2960				-28.17	-30.78	-29.75	-28.25	-29.83
1171	SP-12-VI-02	363	370	3145					-31.83	-30.55	-27.78	-29.85
1172	SP-12-VI-02	381	388	3269				-29.42	-30.99	-29.88	-27.45	-29.90
1173	SP-12-VI-02	399	406	3393				-28.19	-31.35	-30.55	-29.59	-30.20
1174	SP-12-VI-02	417	424	3517			-28.87	-27.39	-31.06	-30.48	-28.70	-29.59
1175	SP-12-VI-02	439	446	3668			-29.73	-28.93	-31.09	-30.35	-28.57	-29.91
1176	SP-12-VI-02	456	463	3785			-28.03	-28.84	-31.20	-30.23	-28.20	-30.11
1177	SP-12-VI-02	476	483	3923				-28.30	-31.35	-29.62	-27.47	-29.63
1178	SP-12-VI-02	496	503	4061				-28.23	-31.20	-31.00	-29.10	-29.91
1179	SP-12-VI-02	516	523	4198				-34.50	-32.31	-32.42	-30.64	-30.10

. Table 10: Concentrations of *n*-alkanes in µg/g from Lake Sacnab.

Sample ID	Core	Nominal Depth (cm)	Composite Depth (cm)	Age (cal yr BP)	C21	C22	C23	C24	C25	C26	C27	C28	C29	C30	C31	C32	C33	C34	Dominant *n*-alkane Log	CPI
1139	SN-19-VII-97 MWI	5.5	5.5	69	1.13	1.00	2.40	0.51	3.50	0.61	4.97	1.01	6.62	0.80	7.48	0.76	5.23	15.73	31	7.32
1140	SN-19-VII-97 MWI	12.5	12.5	158	0.81	0.48	1.39	7.97	1.94	0.31	2.86	0.49	4.91	0.91	6.33	0.59	5.51	9.77	24	7.02
1012	SN-19-VII-97 MWI	15	15	189	9.67	5.57	11.15	9.67	16.01	6.47	11.04	6.43	11.03	2.31	14.98	1.78	9.04	8.66	25	2.52
1141	SN-19-VII-97 MWI	18.5	18.5	233	0.82	0.61	1.59	0.41	2.81	0.51	4.64	0.71	8.13	0.96	10.48	0.82	9.50	8.52	31	9.75
1121	SN-19-VII-97 MWI	32	32	404	0.00	0.00	0.00	0.00	1.32	0.00	2.12	0.00	3.60	0.00	5.19	0.00	4.78	8.43	31	N/A
1142	SN-19-VII-97 MWI	35.5	35.5	448	0.77	0.34	1.15	0.33	1.99	0.47	3.46	0.44	5.60	0.71	8.08	0.54	6.80	6.62	31	9.75
1018	SN-19-VII-97 MWI	42.5	42.5	536	2.45	1.84	0.82	2.36	1.31	4.00	1.09	8.42	8.74	2.48	6.87	1.06	3.64	6.51	28	1.61
1122	SN-19-VII-97 MWI	43	43	542	0.00	0.00	1.18	0.00	2.12	0.00	3.48	0.00	4.36	0.54	6.06	0.03	6.29	6.39	33	16.11
1123	SN-19-VII-97 MWI	62	62	782	2.89	1.30	4.75	1.32	8.03	1.48	10.56	1.55	13.05	1.50	15.36	1.11	12.53	5.24	31	8.56
1019	SN-19-VII-97 MWI	65.5	65.5	826	0.93	1.69	1.20	1.46	3.20	0.50	4.44	1.82	4.40	1.18	4.95	0.68	2.43	7.59	31	2.94
1124	SN-19-VII-97 MWI	72	72	908	0.49	0.00	0.97	0.00	1.73	0.00	2.38	0.00	3.64	0.00	4.32	0.00	12.40	3.99	31	N/A
1125	SN-19-VII-97 MWI	82	82	1035	0.89	0.00	1.70	0.00	3.37	0.58	5.16	1.12	8.36	0.97	10.71	0.76	10.35	4.87	31	8.00
1091	SN-19-VII-97 LEX 1	116.5	91	1148	0.00	0.00	0.00	0.00	0.62	0.38	0.58	0.41	1.06	0.11	0.88	0.10	0.51	2.53	31	4.01
1126	SN-19-VII-97 MWI	92	92	1161	0.00	0.00	0.46	0.00	1.06	0.00	1.97	0.32	3.53	0.39	4.29	0.25	3.99	3.58	31	9.90
1116	SN-19-VII-97 LEX 1	119	93.5	1180	0.00	0.00	0.00	0.00	0.00	0.00	0.00	0.00	0.37	0.00	0.52	0.00	0.36	3.02	31	N/A
1080	SN-19-VII-97 MWI	95.5	95.5	1205	0.30	2.31	0.75	13.42	0.82	18.12	1.57	0.31	2.45	0.34	2.87	0.38	2.48	13.76	26	7.63
1115	SN-19-VII-97 MWI	98.5	98.5	1243	0.00	0.00	0.16	0.00	0.41	0.00	0.75	0.14	1.60	0.18	2.11	0.19	1.97	1.94	31	10.29
1013	SN-19-VII-97 MWI	102.5	102.5	1293	4.38	17.13	3.44	5.87	5.51	2.76	5.67	17.39	7.33	0.35	2.21	0.59	1.31	5.89	28	0.83
1117	SN-19-VII-97 LEX 1	130.5	105	1325	0.00	0.00	0.00	0.00	0.00	0.00	0.00	0.00	0.17	0.00	0.28	0.00	0.20	4.16	31	N/A
1085	SN-19-VII-97 LEX 1	134.5	109	1375	0.00	0.00	0.00	0.00	0.03	0.04	0.08	0.03	0.21	0.04	0.31	0.05	0.21	2.47	31	6.49
1081	SN-19-VII-97 MWI	115.5	115.5	1457	0.00	0.00	0.00	0.00	0.00	0.00	0.00	0.00	0.63	0.00	0.75	0.00	0.48	7.29	31	N/A
1118	SN-19-VII-97 LEX 1	141	115.5	1457	0.00	0.00	0.00	0.00	0.00	0.00	0.00	0.00	0.19	0.00	0.32	0.00	0.20	2.81	31	N/A
1094	SN-19-VII-97 LEX 1	146.5	121	1527	0.00	0.00	0.00	0.38	0.39	0.25	0.84	0.00	1.66	0.27	1.95	0.35	1.25	2.42	31	12.13
1119	SN-19-VII-97 LEX 1	151	125.5	1583	0.00	0.00	0.00	0.00	0.09	0.00	0.15	0.07	0.43	0.08	0.63	0.08	0.40	3.77	31	5.60
1086	SN-19-VII-97 LEX 1	156.5	131	1653	0.00	0.03	0.11	0.04	0.04	0.08	0.14	0.05	0.32	0.12	0.41	0.06	0.25	2.51	31	3.74
1120	SN-19-VII-97 LEX 1	161	135.5	1709	0.00	0.00	0.00	0.00	0.00	0.00	0.00	0.00	0.26	0.00	0.35	0.00	0.24	3.18	31	N/A
1095	SN-19-VII-97 LEX 1	166.5	141	1779	0.00	0.00	0.00	0.00	0.00	0.00	0.10	0.00	0.25	0.00	0.27	0.00	0.19	3.28	31	N/A

.Table 10: Continued

Sample ID	Core	Nominal Depth (cm)	Composite Depth (cm)	Age (cal yr BP)	C21	C22	C23	C24	C25	C26	C27	C28	C29	C30	C31	C32	C33	C34	Dominant *n*-alkane Log	CPI
1082	SN-19-VII-97 LEX 1	176.5	151	1905	0.45	0.00	0.09	0.12	0.12	0.22	0.42	0.20	1.07	0.21	1.46	0.26	0.41	9.62	31	5.33
1096	SN-19-VII-97 LEX 1	180.5	155	1955	0.00	0.00	0.00	0.00	0.09	0.09	0.17	0.06	0.38	0.07	0.39	0.08	0.27	2.95	31	5.79
1143	SN-19-VII-97 LEX 1	186	160.5	2025	0.00	0.00	0.00	0.00	0.00	0.00	0.00	0.00	0.28	0.00	0.39	0.00	0.28	3.30	31	N/A
1087	SN-19-VII-97 LEX 2	203.5	178	2246	0.00	0.00	0.27	0.13	0.41	0.17	0.16	0.00	0.39	0.00	0.45	0.00	0.35	3.40	31	N/A
1144	SN-19-VII-97 LEX 2	214	188.5	2378	0.00	0.00	0.09	0.00	0.13	0.06	0.22	0.09	0.50	0.10	0.64	0.08	0.43	2.97	31	5.48
1088	SN-19-VII-97 LEX 2	224.5	199	2518	0.00	0.00	0.00	0.00	0.11	0.08	0.20	0.19	0.35	0.11	0.52	0.11	0.40	3.15	31	2.37
1097	SN-19-VII-97 LEX 2	252.5	227	2660	0.00	0.15	0.16	0.18	0.33	0.20	0.51	0.10	0.83	0.11	0.85	0.20	0.66	2.15	31	8.13
1145	SN-19-VII-97 LEX 2	274	248.5	2770	0.00	0.00	0.00	0.00	0.00	0.00	0.18	0.00	0.31	0.00	0.42	0.00	0.24	2.85	31	N/A
1146	SN-19-VII-97 LEX 2	284	258.5	2820	0.00	0.00	0.00	0.00	0.07	0.04	0.15	0.07	0.33	0.07	0.44	0.05	0.25	2.22	31	4.72
1147	SN-19-VII-97 LEX 3	295	269.5	2876	0.00	0.00	0.00	0.00	0.00	0.00	0.00	0.00	0.23	0.00	0.49	0.00	0.34	2.17	31	N/A
1089	SN-19-VII-97 LEX 3	304.5	279	2925	0.00	0.00	0.00	0.00	0.09	0.09	0.20	0.12	0.39	0.10	0.57	0.10	0.42	2.87	31	3.52
1148	SN-19-VII-97 LEX 3	316	290.5	2983	0.00	0.00	0.06	0.04	0.15	0.06	0.23	0.07	0.39	0.07	0.50	0.03	0.34	3.27	31	5.69
1149	SN-19-VII-97 LEX 3	330	304.5	3054	0.00	0.00	0.00	0.00	0.15	0.00	0.22	0.00	0.44	0.00	0.69	0.00	0.51	2.20	31	N/A
1090	SN-19-VII-97 LEX 3	334.5	309	3077	0.00	0.21	0.03	0.11	0.11	0.13	0.19	0.09	0.40	0.13	0.48	0.09	0.41	3.08	31	3.68
1150	SN-19-VII-97 LEX 3	346	320.5	3136	0.00	0.00	0.00	0.00	0.00	0.00	0.00	0.00	0.35	0.00	0.58	0.00	0.42	2.25	31	N/A
1098	SN-19-VII-97 LEX 3	349.5	324	3154	0.00	5.16	0.00	1.72	0.00	0.00	0.90	0.00	1.90	0.00	2.23	0.00	1.52	1.94	22	N/A
1151	SN-19-VII-97 LEX 3	355	329.5	3182	0.00	0.00	0.09	0.04	0.20	0.07	0.32	0.08	0.58	0.09	0.73	0.08	0.54	2.40	31	6.72
1152	SN-19-VII-97 LEX 3	365	339.5	3232	0.00	0.00	0.12	0.00	0.28	0.09	0.44	0.09	0.76	0.10	0.90	0.08	0.63	3.06	31	8.15
1153	SN-19-VII-97 LEX 3	375	349.5	3283	0.00	0.00	0.18	0.00	0.38	0.11	0.59	0.00	1.01	0.00	1.20	0.00	0.81	3.89	31	N/A
1154	SN-19-VII-97 LEX 4	392.5	367	3325	0.00	0.00	0.11	0.00	0.22	0.00	0.36	0.00	0.69	0.12	0.99	0.13	0.65	6.12	31	11.35
1084	SN-19-VII-97 LEX 4	396.5	371	3402	0.00	0.00	0.00	0.00	0.00	0.00	1.88	0.00	3.71	0.00	4.48	0.00	3.55	8.90	31	N/A
1155	SN-19-VII-97 LEX 4	407	381.5	3602	0.00	0.00	0.52	0.13	1.00	0.24	1.46	0.26	2.62	0.39	3.66	0.38	2.84	4.09	31	8.17
1156	SN-19-VII-97 LEX 4	427	401.5	3983	0.00	0.00	0.37	0.00	0.93	0.00	1.77	0.00	3.52	0.45	4.54	0.28	3.51	3.89	31	15.68
1101	SN-19-VII-97 LEX 4	436.5	411	4164	0.00	4.51	1.58	1.03	3.19	1.24	6.18	7.36	7.97	1.15	9.89	2.14	2.53	2.72	31	1.87
1102	SN-19-VII-97 LEX 4	448.5	423	4393	0.00	1.88	0.00	0.78	0.47	0.00	0.80	0.39	1.86	0.00	2.40	0.46	2.19	3.15	31	9.49

. Table 11: Concentrations of *n*-alkanes in µg/g from Lake Salpetén.

Sample ID	Core	Nominal Depth (cm)	Composite Depth (cm)	Age (cal yr BP)	C21	C22	C23	C24	C25	C26	C27	C28	C29	C30	C31	C32	C33	C34	Dominant *n*-alkane Log	CPI
1181	SP-12-VI-01	4	4	44	0.00	0.00	0.00	0.00	1.25	0.00	2.22	0.84	4.68	0.78	7.87	1.46	5.34	4.73	31.00	5.30
1182	SP-12-VI-02	19	19	209	0.00	0.00	0.00	0.00	0.61	1.16	1.48	0.00	3.44	0.43	4.27	0.56	3.68	5.10	31.00	2.56
1183	SP-12-VI-02	50	50	549	0.00	0.00	0.00	0.00	0.78	3.47	1.44	1.13	2.66	0.66	3.31	0.70	3.32	5.93	26.00	0.63
1184	SP-12-VI-02	72	72	790	0.00	0.00	0.00	0.00	0.52	0.35	0.62	0.16	1.01	0.21	1.58	0.10	1.59	3.23	33.00	2.41
1185	SP-12-VI-02	81	81	889	0.20	0.12	0.98	0.01	1.21	0.50	1.84	0.34	2.80	0.32	4.11	0.62	2.98	4.02	31.00	4.37
1186	SP-12-VI-02	88	88	966	0.00	0.00	0.18	0.00	0.26	0.17	0.34	0.09	0.69	0.09	0.98	0.04	0.61	2.74	31.00	2.60
1157	SP-12-VI-02	83	90	988	0.00	0.00	0.11	0.00	0.22	0.00	0.55	0.00	0.81	0.00	1.00	0.00	0.71	3.69	31.00	N/A
1160	SP-12-VI-02	97	104	1142	0.17	0.15	0.25	0.07	0.35	0.13	0.90	0.20	1.72	0.22	2.17	0.19	1.75	3.36	31.00	5.55
1158	SP-12-VI-02	114	121	1328	0.00	0.00	0.18	0.35	0.27	0.28	0.46	0.00	1.15	0.16	1.43	0.15	1.11	3.34	31.00	3.30
1159	SP-12-VI-02	153	160	1701	0.09	0.11	0.16	0.00	0.17	0.00	0.29	0.25	0.57	0.09	0.82	0.13	0.73	2.55	33.00	2.39
1161	SP-12-VI-02	171	178	1824	0.00	0.00	0.00	0.26	1.25	2.02	2.97	2.80	3.00	2.23	2.42	1.71	1.60	4.52	29.00	1.23
1162	SP-12-VI-02	191	198	1962	0.05	0.07	0.07	0.02	0.04	0.00	0.08	0.00	0.25	0.00	0.32	0.00	0.21	2.98	31.00	N/A
1163	SP-12-VI-02	205	212	2058	0.00	0.00	0.00	0.00	0.00	0.00	0.00	0.00	0.17	0.00	0.28	0.00	0.15	2.53	31.00	N/A
1164	SP-12-VI-02	230	237	2230	0.00	0.00	0.00	0.00	0.00	0.00	0.10	0.00	0.29	0.00	0.41	0.00	0.32	2.63	31.00	N/A
1165	SP-12-VI-02	245	252	2334	0.00	0.00	0.00	0.00	0.08	3.47	0.13	0.00	0.31	0.00	0.50	0.00	0.43	2.62	26.00	0.07
1166	SP-12-VI-02	265	272	2471	0.00	0.00	0.00	0.00	0.00	0.00	0.12	0.00	0.33	0.00	0.44	0.00	0.30	2.27	31.00	N/A
1167	SP-12-VI-02	281	288	2581	0.00	0.00	0.00	0.00	0.00	0.00	0.00	0.00	0.28	0.00	0.38	0.00	0.26	3.03	31.00	N/A
1168	SP-12-VI-02	299	306	2705	0.07	0.08	0.08	0.00	0.07	0.00	0.16	0.00	0.45	0.07	0.63	0.05	0.54	1.78	31.00	N/A
1169	SP-12-VI-02	316	323	2822	0.00	0.00	0.00	0.00	0.00	0.00	0.15	0.00	0.43	0.06	0.66	0.07	0.51	1.99	31.00	N/A
1170	SP-12-VI-02	336	343	2960	0.00	0.00	0.00	0.00	0.00	0.00	0.14	0.00	0.50	0.00	0.60	0.00	0.44	1.84	31.00	N/A
1171	SP-12-VI-02	363	370	3145	0.00	0.00	0.00	0.00	0.00	0.00	0.13	0.00	0.36	0.00	0.49	0.00	0.45	2.34	31.00	N/A
1172	SP-12-VI-02	381	388	3269	0.00	0.00	0.00	0.00	0.18	0.00	0.43	0.00	0.81	0.00	1.09	0.00	0.98	4.34	31.00	N/A
1173	SP-12-VI-02	399	406	3393	0.00	0.00	0.00	0.00	0.00	0.00	0.25	0.00	0.73	0.00	0.88	0.00	0.52	2.24	31.00	N/A
1174	SP-12-VI-02	417	424	3517	0.09	0.10	0.10	0.00	0.11	0.00	0.29	0.00	1.03	0.10	1.19	0.09	0.81	2.33	31.00	N/A
1175	SP-12-VI-02	439	446	3668	0.00	0.00	0.00	0.00	0.10	0.00	0.29	0.00	0.85	0.00	0.94	0.00	0.67	1.65	31.00	N/A
1176	SP-12-VI-02	456	463	3785	0.00	0.00	0.00	0.00	0.06	0.00	0.17	0.00	0.47	0.00	0.57	0.00	0.39	2.26	31.00	N/A
1177	SP-12-VI-02	476	483	3923	0.00	0.00	0.00	0.00	0.14	2.96	0.37	0.16	0.53	0.07	0.73	0.08	0.52	2.25	26.00	0.24
1178	SP-12-VI-02	496	503	4061	0.00	0.00	0.00	0.00	0.09	0.00	0.36	0.00	0.76	0.09	0.93	0.00	0.55	2.60	31.00	N/A
1179	SP-12-VI-02	516	523	4198	0.08	0.06	0.10	0.00	0.23	0.08	1.45	0.11	1.51	0.15	1.90	0.08	1.28	2.40	31.00	15.21

LIST OF REFERENCES

Anselmetti, F., Ariztegui, D., Hodell, D.A., Brenner, M., Curtis, J.H., Guilderson, T.P., and Rosenmeier, M., *in preparation*. Enhanced soil erosion rates in the southern Maya Lowlands: The Lago Salpeten record, Guatemala.

Binford, M.W., Brenner, M., Whitmore, T.J., Higuera-Gundy, A., Deevey, E.S., and Leyden, B.W., 1987. Ecosystems, paleoecology and human disturbance in subtropical and tropical America. Quaternary Science Reviews 6: 115-128.

Bradley, R.S. 1999. *Paleoclimatology*. Academic Press, San Diego, CA.

Brenner, M., 1983. Paleolimnology of the Petén Lake District, Guatemala, 2: Mayan population density and sediment and nutrient loading of Lake Quexil. Hydrobiologia 103: 205-210.

Bronk Ramsey, C., 1995. Radiocarbon calibration and analysis of stratigraphy: The OxCal Program. Radiocarbon 37(2): 425-430.

Bronk Ramsey C., 2001. Development of the Radiocarbon Program OxCal. Radiocarbon 43 (2A): 355-363.

Brezonik, P.L. and Fox, J.L., 1974. The limnology of selected Guatemalan lakes. Hydrobologia 45: 467-487.

Butzer, K.W., 1992. The Americas before and after 1492: An introduction to current geographical research. Annals of the Association of American Geographers 82(3): 345-368.

Coe, M.D., 1999. *The Maya*: Sixth Edition. Thames and Hudson, New York, New York.

Collister, J.W., Rieley, G., Stern, B., Eglinton, G., and Fry, B., 1994. Compound-specific $\delta^{13}C$ analyses of leaf lipids from plants with differing carbon dioxide metabolism. Organic Geochemistry 21: 619-627.

Conte, M.H and Weber, J.C, 2002. Plant biomarkers in aerosols record isotopic discrimination of terrestrial photosynthesis. Nature 417: 639-641.

Cowgill, U.M. and Hutchinson, G.E., 1966. A general account of the basin and the chemistry and mineralogy of the sediment cores. In: U.M Cowgill, C.E. Goulden, G.E. Hutchinson, R. Patrick. A.A. Racek and M. Tsukada (eds): *The history of*

Laguna de Petenxil. Memoirs of the Connecticut Academy of Arts and Sciences, New Haven, 17: 2-62.

Cranwell, P.A., 1981. Diagenesis of free and bound lipids in terrestrial detritus deposited in a lacustrine sediment. Organic Geochemistry 3:79-89.

Cranwell, P.A., Eglinton, G. and Robinson, N., 1987. Lipids of aquatic organisms as potential contributors to lacustrine sediments-II, Organic Geochemistry 11: 513–527

Curtis, J.H., Brenner, M., Hodell, D.A., Balser, R.A., Islebe, G.A., Hooghiemstra, H., 1998. A multi-proxy study of Holocene environmental change in the Maya Lowlands of Petén, Guatemala. Journal of Paleolimnology 19: 139-159.

Deevey, E.S., 1969. Coaxing history to conduct experiments. Bioscience 19 (1):40-43.

Deevey, E.S., 1978. Holocene forests and Maya disturbance near Quexil Lake, Petén, Guatemala. Polish Archives of Hydrobiology 25 (1/2): 117-129.

Deevey, E.S., Brenner, M., and Binford, M.W., 1983. Paleolimnology of the Petén Lake District, Guatemala. III. Late Pleistocene and Gamblian environments of the Maya area. Hydrobiologia 103: 211-216.

Deevey, E.S., Brenner, M., Flannery, M.S., and Yezdani, G.H., 1980. Lakes Yaxha and Sacnab, Petén, Guatemala: Limnology and hydrology. Arch. Hydrobiol. 57: 418-460.

Deevey, E.S., Rice, D.S., Rice, R.M., Vaughan, H.H., Brenner, M., and Flannery, M.S., 1979. Mayan urbanism: Impact on a tropical karst environment. Science 206: 298-306.

Demarest, A.A., 1997. The Vanderbuilt Petexbatun Regional Archaeological Project 1989-1994: Overview, history, and major results of a multidisciplinary study of the Classic Maya collapse. Ancient Mesoamerica 8: 209-227.

Dunning, N., Beach, T., and Rue, D., 1997. The paleoecology and ancient settlement of the Petexbatun region, Guatemala. Ancient Mesoamerica 8: 255-266.

Dunning, N., Rue, D.J., Beach, T., Covich, A., and Traverse, A., 1998. Human-environment interactions in a tropical watershed: The paleoecology of Laguna Tamarindito, El Petén, Guatemala. Journal of Field Archaeology 25:139-151.

Emery, K.F. (in press). *Dietary, environmental, and societal implications of ancient Maya animal use in the Petexbatun: A zooarchaeological perspective on the collapse*. Vanderbilt University Press, Nashville.

Eglinton, G. and Hamilton, R.J., 1967. Leaf epicuticular waxes. Science 156: 1322-1335.

Ertel. J.R. and Hedges, J.I., 1985. Sources of sedimentary humic substances: vascular plant debris. Geochimica et Cosmochimica Acta 49: 2097–2107.

Ficken, K.J., Li, B., Swain, D.L., and Eglinton, G., 2000. An *n*-alkane proxy for the sedimentary input of submerged/floating freshwater aquatic macrophytes. Organic Geochemistry 31: 745-749.

Filley T. R., Freeman K. H., Bianchi T., Colarusso L. A. and P. Hatcher (2001) An isotopic biogeochemical assessment of shifts in organic matter input to Holocene sediments from Mud Lake, Florida. Organic Geochemistry 32: 1153-1167.

Hayes, J.M., 1993. Factors controlling ^{13}C contents of sedimentary organic compounds: principles and evidence. Marine Geology 113: 111-125.

Hayes, J.M., 2001. Fractionation of the isotopes carbon and hydrogen in biosynthetic processes; prepared for short course of Mineralogical Society of America, GSA 2001.

Haug, G.H., Hughen, K.A., Sigman, D.M., Peterson, L.C., and Rohl, U., 2001. Southward migration of the Intertropical Convergence Zone through the Holocene. Science 293: 1304-1308.

Hedges, J.I. and Prahl, F.G., 1993. Early diagenesis: consequences for applications of molecular biomarkers In: M.H. Engel and S.A. Macko, Editors, *Organic Geochemistry. Principles and Applications*, Plenum Press, New York, pp. 237–253.

Hodell, D.A, Brenner, M., Curtis, J.H., and Guilderson, T., 2001. Solar forcing of drought in the Maya Lowlands. Science 292: 1367-1370.

Hodell, D.A, Curtis, J.H., and Brenner, M., 1995. Possible role of climate in the collapse of the Classic Maya civilization. Nature 375: 391-394.

Huang, Y., Street-Perrott, F.A., Metcalfe, S.E., Brenner, M., Moreland, M., and Freeman, K.H., 2001. Climate change as the dominant control on Glacial-Interglacial variations in C_3 and C_4 plant abundance. Science: 293 (5535).

Huang, Y., Street-Perrott, F.A., Perrott, A., Metzger, P., and Eglinton, G., 1999. Glacial-interglacial environmental changes inferred from molecular and compound-specific $d^{13}C$ analysis of sediments from Sacred Lake, Mt. Kenya. Geochimica et Cosmochimica Acta 63: 1383-1404.

Hughen, K. A., Eglinton, T.I., Xu, L., and Makou, M., 2004. Abrupt tropical vegetation response to rapid climate change. Science 304: 1955-1959.

Islebe, G.A., Hooghiemstra, H., Brenner, M., Curtis, J.H., and Hodell, D.A, 1996. A Holocene vegetation history from lowland Guatemala. The Holocene 6: 265-271.

Kaushal, S. and Bindford, M.W., 1999. Relationship between C:N ratios of lake sediments, organic matter sources, and historical deforestation of Lake Pleasant, Massachusetts, USA. Journal of Paleolimnology 22: 439–442.

Knops, J.M.H. and Tilman, D., 2000. Dynamics of soil nitrogen and carbon accumulation for 61 years after agricultural abandonment. Ecology 81: 88-98.

Lajtha, K. and Marshall, J.D., 1994. Sources of variation in the stable isotopic composition of plants. In K. Lajtha and R.H. Michener, eds., *Stable Isotopes in Ecology and Environmental Science*. Oxford, Great Britain: Blackwell Scientific Publications, Oxford, pp 1-21.

Lambert, J.D.H.; Arnason, J. T. 1982. Ramon and Maya ruins: An ecological, not an economic, relation. Science 216: 298–299.

Leffler, A.J. and Enquist, B.J., 2002. Carbon isotope composition of tree leaves from Guanacaste, Costa Rica: Comparison across tropical forests and tree life history. Journal of Tropical Ecology 18: 151-159.

Leyden, B.W., 1987. Man and climate in the Maya Lowlands. Quaternary Research 28:407-414.

Leyden, B.W., 2002. Pollen evidence for climatic variability and cultural disturbance in the Maya Lowlands. Ancient Mesoamerica 13: 85-101.

Leyden, B.W., Brenner, M., and Dahlin, B.H., 1998. Cultural and climatic history of Coban a lowland Maya city in Quintana Too, Mexico. Quaternary Research 49: 111-122.

Leyden, B. W., Brenner, M., Hodell, D.A., and Curtis, J.H., 1993. Late Pleistocene climate in the Central American lowlands. In *Climate change in continental isotopic records*. Geophysical Monograph 78, Washington, DC: pp.165-178.

Lundell, C.L., 1937. The vegetation of Petén. Carnegie Institute, Washington, DC.

Meyers, P.A., 1994. Preservation of elemental and isotopic source identification of sedimentary organic matter. Chemical Geology 144: 289–302.

Meyers, P. A., 1997. Organic geochemical proxies of paleoceanographic, paleolimnologic, and paleoclimatic processes. Organic Geochemistry 27: 213-250.

Meyers, P.A. and Eadie, B.J., 1993. Sources, degradation and recycling of organic matter associated with sinking particles in Lake Michigan. Organic Geochemistry 20: 47–56.

Meyers, P.A., and R. Ishiwatari. 1993. Lacustrine organic geochemistry - An overview of indicators of organic matter sources and diagenesis in lake sediments. Organic Geochemistry 20: 867-900.

Meyers, P.A., Kawka, O.E., and Whitehead, D.R., 1984. Geolipid, pollen and diatom stratigraphy in postglacial lacustrine sediments. Organic Geochemistry 6: 727–732.

Müller, A. and Mathesius, U., 1999. The palaeoenvironments of coastal lagoons in the southern Baltic Sea. The application of sedimentary C_{org}/N ratios as source indicators of organic matter. Palaeogeography, Palaeoclimatology, Palaeoecology 145: 1–16.

Paillard D., L. Labeyrie, and P. Yiou, 1996. Macintosh program performs time-series analysis. Eos, Transactions, American Geophysical Union 77: 379.

Pakeman, R.J., Marrs, R.H., and Jacob, P.J., 1994. A model of bracken (*Pteridium aquilinum*) growth and the effects of control strategies and changing climate. Journal of Applied Ecology 31: 145-154.

Prahl, F.G., Bennett, J.T. and Carpenter, R., 1980. The early diagenesis of aliphatic hydrocarbons and organic matter in sedimentary particulates from Dabob Bay, Washington. Geochimica et Cosmochimica Acta 44: 1967–1976.

Rice, D.S., 1993. Eighth-Century Physical Geography, Environment, and Natural Resources in the Maya Lowlands. In Sabloff, J.A. and Henderson, J.S. (ed.): Lowland Maya Civilization in the Eighth Century A.D.: 11-64. Dumbarton Oaks Research Library and Collection, Washington D.C.

Rice, D.S., and P.M. Rice, 1990. Population Size and Population Change in the Central Petén Lakes Region, Guatemala. In: Precolumbian Population History in the Maya Lowlands, edited by T. Patrick Culbert and Don S. Rice, pp. 123-148. University of New Mexico Press, Albuquerque, New Mexico.

Rice, P.M. and Rice, D.S., 2004. Late Classic to Postclassic Transformations in the Petén Lakes Region, Guatemala. In: A.A. Demarest, P.M. Rice, and D.S. Rice (eds.): The terminal Classis in the Maya lowlands: Collapse, transition, and transformation. University Press of Colorado, Colorado.

Rice, D.S., Rice, P.M., and Deevey, E.S., 1985. Paradise Lost: Classic Maya Impact on a Lacustrine environment. In M. Pohl, ed., *Prehistoric Lowland Maya Environment and Subsistence Economy,* pp. 91-105, Peabody Museum Papers 77. Harvard University Press, Cambridge, MA.

Robinson, N., Cranwell, P.A., Finlay, B.J., and Englinton, G., 1984. Lipids of aquatic organisms as potential contributors to lacustrine sediments. Organic Geochemistry 6: 143-152.

Rosenmeier, M.F., Hodell, D.A., Brenner, M., Curtis, J.H., Martin, J.B., Anselmetti, F.A., Ariztegui, D., and Guilderson, T.P., 2002. Influence of vegetation change on watershed hydrology: Implications for paleoclimatic interpretation of lacustrine $\delta^{18}O$ records. Journal of Paleolimnology 27: 117-131.

Schefub, E., Ratmeyer, V., Stuut, J.-B. W., Jansen, J.H.F., and Sinninghe Damsté, J.S., 2003. Carbon isotope analyses of *n*-alkanes in dust from the lower atmosphere over the central eastern Atlantic. Geochimica et Cosmochimica Acta 67: 1757-1767.

Schmitt, J., Glaser, B., Zech, W., 2003. Amount-dependent isotopic fractionation during compound-specific isotope analysis. Rapid Communications in Mass Spectrometry, 17: 970-977.

Sharer, R.J., 1994. The ancient Maya: Fifth Edition. Stanford University Press, Stanford, California.

Simoneit, B.R.T., 1977. Organic matter in eolian dusts over the Atlantic Ocean. Marine Chemistry 5: 443-464.

Tilman, D., 1984. Plant dominance along an experimental nutrient gradient. Ecology 65: 1445-1453.

Tilman, D., 1987. Secondary succession and the pattern of plant dominance along experimental nitrogen gradients. Ecological Monographs 57: 189-214.

Turner, B.L., Klepeis, P., and Schneider, L.C., 2003. Three Millennia in the Southern Yucatan Peninsula: Implications for Occupancy, Use, and Carrying Capacity. In A. Gomez-Pompa, M.F. Allen, S.L. Fedick, and J.J. Jiminez-Osornio: The lowlands Maya area: Three millennia at the human-wildland interface: Food Products Press, New York, pp. 361-387.

Vaughan, H.H., Deevey, E.S. and Garrett-Jones, S.E., 1985. Pollen stratigraphy of two cores from the Petén Lake District. In M. Pohl, ed., *Prehistoric lowland Maya*

environment and subsistence economy. Peabody Museum Papers 77. Harvard University Press, Cambridge, MA, pp. 73-89.

Wiseman, F.M., 1985. Agriculture and Vegetation Dynamics of the Maya Collapse in Central Petén, Guatemala. In M. Pohl, ed., *Prehistoric lowland Maya environment and subsistence economy.* Peabody Museum Papers 77. Harvard University Press, Cambridge, MA, pp. 63-71.

BIOGRAPHICAL SKETCH

Sarah Davidson Newell was born on 31 March 1980 in Schenectady, NY. She lived her first 22 years in upstate New York and spent most of her childhood years covered in mud. Eventually, she grew out of trudging through the woods and spent her teenage years at Galway High School as a typical teen involved in academics, athletics, drama and student government. She enrolled at Union College in September of 1998 and, after briefly contemplating a classics major, rediscovered her passion for being covered in mud and chose a major in geology. After working with Dr. Don Rodbell for three years in the Core Lab at Union, Sarah graduated *cum laude* from Union College in 2002 with a BS in geology. Sarah continued her education at the University of Florida where she pursued a MS degree in geological sciences under the supervision of Dr. David A. Hodell. At the University of Florida, Sarah spent much of her time developing methods for compound-specific isotopic studies and worked on sediments from northern Guatemala. Sarah will graduate with her MS degree in May 2005 and has already taken a position at Stanford University, beginning work towards her PhD in ocean sciences. Sarah is working with Dr. Robert Dunbar, developing a multi-centennial record of climate variability in the South Pacific using stable isotopes and trace metals from Easter Island corals.